Nansen Environmental and Remote Sensing Center

A non-profit environmental research institute affiliated with the University of Bergen

Edvard Griegsvei 3 a
N-5037 Solheimsviken
Norway

Technical report no. 213

Development of satellite remote sensing for marine monitoring and climate applications

A 3-year project 1999 - 2001

Final Report to Norwegian Space Centre

by

Ola M. Johannessen, Stein Sandven, Torill Hamre, Heidi Espedal, Birgitte R. Furevik, Johnny A. Johannessen, Lasse H. Pettersson, Dominique Durand and Knut A. Lisæter

July 2002

NANSEN ENVIRONMENTAL AND REMOTE SENSING CENTER

Edv. Griegsvei 3a
N-5059 Bergen, NORWAY.
Phone: +47 55 29 72 88
Fax: +47 55 20 00 50
e-mail: admin@nrsc.no
http://www.nersc.no

Nansen Environmental and Remote Sensing Center Technical Report

TITLE	**REPORT IDENTIFICATION**
Development of satellite remote sensing for marine monitoring and climate applications **A 3-year project 1999 2001** **Final Report**	NERSC Technical Report no. 213
CLIENT Norwegian Space Centre	**CONTRACT** Contract no. JOP.8.3.3.06.99.2/ JOP.8.3.3.03.00.2/ JOP.8.3.3.06.01.2
CLIENT REFERENCE Guro Dahle Strøm	**AVAILABILITY** Open
INVESTIGATORS Ola M. Johannessen, Stein Sandven, Torill Hamre Heidi Espedal, Birgitte R. Furevik, Johnny A. Johannessen, Lasse H. Pettersson, Dominique Durand and Knut A. Lisæter	**AUTHORISATION** Bergen, July 2002 DIRECTOR Ola M. Johannessen

Contents

PROJECT SUMMARY (PÅ NORSK) **4**

2. OBJECTIVES **8**

2.1 OVERALL OBJECTIVE 8
2.2 THE MAIN TASKS 8

3. RESULTS OF TASK 1: MARSAS (MARINE SAR ANALYSIS SYSTEM) **8**

3.1 THE MARSAS CONCEPT 8
3.2 VISION AND SCOPE OF MARSAS 9
3.2.1 High-level requirements *9*
3.2.2 Technical requirements to MARSAS *10*
3.2.3 Assumptions about input data *10*
3.3 DESIGN OF MARSAS 11
3.3.1 Overall functionality *12*
3.3.2 Data flow in MARSAS *13*
3.4 SEA ICE MONITORING APPLICATION 14
3.4.1 Overview of algorithms and tools used in MARSAS *14*
3.4.2 Example of SAR ice classification using LDA and BNN methods *15*
3.5 SAR-WIND APPLICATION 21
3.5.1 Wind retrieval in the marginal ice zone *22*
3.5.2 Wind energy mapping for siting wind turbines *23*
3.5.3 Methodology to derive wind from SAR *24*
3.6 SAR OIL SPILL DISCRIMINATION 25
3.7 COMMON FEATURES IN ALL SCENARIOS 26
3.8 OUTLINE OF A SOLUTION INCLUDING USE OF INTERNET AND JAVA TECHNOLOGIES 27
3.9 LINKS TO OTHER PROJECTS 30

4. RESULTS OF TASK 2: SEAWIFS MONITORING OF ALGAL BLOOMS **32**

4.1 THE HABIM BACKGROUND 32
4.1.1 Contribution of EO-derived information *32*
4.1.2 The Applications of ocean colour EO data – Chlorophyll-a and other Pigments *33*
4.1.3 EO applications in coupled bio-physical forecasting models *36*
4.1.4 Validation and Accuracy *37*
4.2 THE HABIM APPROACH 38
4.2.1 Summary of Service capability *39*
Products *40*
Supply chain *40*
Benefit *40*
Customer readiness *41*
4.2.2 The technology behind HABIM *41*
4.2.3 The EO data Information Flow *41*
4.2.4 The HABIM Products and Information Dissemination *46*
4.2.5 Project Interactions with the Existing Service *50*
4.3 SERVICE DEMONSTRATION - EVENTS AND MONITORING 50
4.4 LINKS TO RELATED PROJECTS 52

5. RESULTS FROM TASK 3: ASSIMILATION OF SEA ICE DATA IN A CLIMATE MODEL **53**

5.1 INTRODUCTION TO ARCTIC SEA ICE OBSERVATIONS 53
5.2 MODEL DESCRIPTION 54
5.3 USE OF SATELLITE DATA 56
5.4 SEA-ICE EXTENT AND AREA 56
5.4.1 Monthly averages *56*
5.4.2 Trends from anomalies *58*
5.5 TEMPORAL AND SPATIAL DISTRIBUTION OF THE MODEL ERROR IN ICE CONCENTRATION 61
5.6 MULTI-YEAR ICE AREA 63
5.7 FIRST RESULTS FROM ASSIMILATION OF SATELLITE DATA INTO THE ICE-OCEAN MODEL 65
5.8 LINKS TO RELATED PROJECTS 69

6. SUBCONTRACT TO VLADIMIR N. KUDRYAVTSEV..... 70

6.1 A SEMI-EMPIRICAL MODEL OF THE NORMALIZED RADAR CROSS SECTION OF THE SEA SURFACE..... 70
6.2 AIR-SEA INTERACTION: WIND OVER WAVE COUPLING APPROACH..... 70

7. CONCLUSIONS AND RECOMMENDATION FOR FURTHER WORK..... 71

7.1 THE MARSAS SYSTEM..... 71
7.2 SEAWIFS MONITORING OF ALGAEL BLOOMS..... 73
7.3 ASSIMILATION OF SEA ICE DATA IN A CLIMATE MODEL..... 76
7.4 AIR-SEA INTERACTION AND SAR MODELLING..... 78
7.5 DEVELOPMENT OF SATELLITE DATA PRODUCTS FOR OPERATIONAL OCEANOGRAPHY..... 78

8. ACKOWLEDGEMENT..... 78

9. REFERENCES..... 79

Appendix:

Observing the Ocean from Space: Emerging Capabilities in Europe, review paper by J. A. Johannessen et al., 2001

Project Summary (på norsk)

Det overordnete mål med prosjektet **"Utvikling av satelittfjernmåling innen klima og marin overvåking"** er å utvikle videre bruk av jordobservasjon innen disse anvendelselområdene ved å utnytte nye mikrobølge og optiske satellittsensorer til å fremskaffe geofysiske og biologiske data.

Bakgrunnen for prosjektet er at det innen marin og polar klimaovervåking i de neste tre – fem år vil være tre forhold som har betydning for utvikling av marin satellittfjernmåling:

- økt tilgang på jordobservasjonsdata fra flere nye satelitter hvorav ENVISAT vil være den viktigste
- forbedring av modeller og data-assimilering som simulerer atmosfære, hav og issirkulasjon og som potensielt kan utnytte jordobservasjonsdata mye bedre enn det som gjøres idag.
- etablering av EuroGOOS som vil bli en pådriver for operasjonell oseanografi og hvor særlig satelittdata vil bli viktig

Kort beskrivelse av prosjektet

Prosjektet vil prioritere delmål og tilhørende arbeidsoppgaver som skal føre til at bruken av satelittdata økes innenfor utvalgte områder. Prosjektet tar utgangspunkt i at den økte tilgangen på satellittdata krever at systemer for prosessering, analyse og assimilering i modeller utvikles og tilrettelegges for at brukere skal kunne utnytte dataene i operasjonell sammenheng. Prosjektet skal bidra til at den oppbygde kompetansen kan utvikles og brukes til å skape levedyktige anvendelser av satelittdata innen den marine sektor.

Tre hovedoppgaver inngår i prosjektet:

1. Utvikle et generisk SAR analysesystem (MARSAS) som kan bruke eksisterende algoritmer for vind, oljesøl, virvler/fronter, naturlig slick og is-parametre og gjøre det mulig for brukerne å integrere andre datasett og analyseverktøy for å lage sluttprodukter som vindfelt, iskart, analyserte bilder og varsling av hav og isparametre. Et slikt analysesystem vil bli særlig viktig for ENVISAT hvor samtidige data fra SAR, optisk og infrarøde sensorer inngår, og for at ENVISAT data skal kunne brukes i kombinasjon med andre satelitt data.
2. Utvikle bruk av havfarge data for overvåking av klorofyll i Nordsjøen og Skagerrak. Siden 1999 har det vært utført demonstrasjoner av SeaWiFS data under våroppblomstringenn. Vår og sommer perioden er den viktigste for overvåking av alger i disse områdene og perioden er den mest gunstige med hensyn til skydekke slik at optiske og infrarøde satelittdata kan komme til full utnyttelse. SeaWiFS sammen med MERIS og MODIS data er de viktigste som kan gi synoptisk kartlegging av klorophyll over større havområder i nær sann tidsbruk av satellitt data vil inngå som en del av et integrert system hvor *in situ* data og modelleringsresultater er brukes til overvåking og varsling.
3. Teste hvordan havisparametre fra satellittdata kan anvendes i klimamodeller både som validering og ved assimilering. Iskonstrasjon og is-areal tatt over de siste 20 år er de viktgste dataene som brukes i prosjektet.

Langsiktige målsettinger

Ved bruk av ENVISAT in kombinasjon med andre JO satelitter er de langsiktige målsettinger:

- *øke den praktiske anvendelsen av SAR og optiske satelittdata inne kyst-og polarovervåling*
- *gjøre det mulig å bruke SAR data in synergi med andre data inkludert modell simuleringer*
- *utvikle operasjonelle / kommersielle anvendelser av SAR og andre satelittdata til nytte for industri og forvaltning*

Oppnådde resultater i perioden 1999 - 2001

1 MARSAS arbeidet har fokusert på å lage et strømlinjeformet analyse verktøy for SAR billed data. Verktøyet, som er basert på eksisterende algoritmer og basis-systemer som MatLab og IDL, er nå utviklet til et stadium hvor brukeren kan gjennomføre en prosessering fra input data til ferdig produkt. Verktøyet kan brukes på SAR isalgoritmer (isklassifisering og iskinematikk), vind algoritmen CMOD, og slick deteksjon fra ERS data. Brukeren kan være både forsker,

tjenesteutvikler og opeasjonell enhet, avhengig av institusjoner som leverer produkter fra SAR data. Vi har diskutert SAR produkter og analyseverktøy med MI og NPI som viktige brukere i Norge, og det er et klart behov for å ha slike verktøy på plass for at SAR data skal kunne brukes operasjonelt i marin og polar overvåking. Det har vært møter med Kongsberg Spacetec for å diskutere hvordan MARSAS kan inkluderes som en del av MEOS systemet, men for å kunne gå videre med dette samarbeidet trengs et konkret prosjekt. Den delen av MARSAS som gjelder framstilling av SAR is produkter er overført til NPI gjennom isprosjektet som NRS har hatt med NPI, NERSC og NORUT. Videre utvikling av MARSAS må tilpasses bruk av Internet og Java hvor flere leverandører kan bidra til ulike deler av en mer integrert tjeneste. NERSC har utviklet en algetjenste for SeaWiFS data via Internet (se beskrivelse under) og holder på å lage tilsvarende tjenester for SAR-produkter. SAR-basert informasjon har en klar rolle når det gjelder den type tjenester som prosjektet har fokusert på, nemlig istjeneste, oljesøl deteksjon og vindobservasjon. Men det er flere hindre som må overvinnes før regulær bruk av SAR data kan etableres, spesielt når det gjelder pris på SAR data, data dekning i tid og rom og hvordan SAR informasjon best skal integreres inn i eksisterenede tjenester. Videre arbeid med SAR anvendelser vil fokusere på å lage bedre informasjonsprodukter hvor SAR inngår, som en av flere data kilder.

2 Bruk av SeaWiFS data til overvåking av alger har vært demonstrert med hell de siste årene. Dette er et resultat av at flere ESA og EU-prosjekter, i tillegg til Norsk Romsenters Rammeprogram, har bidratt til å gjøre et løft, slik at bruk av EO data er etablert på et høyere nivå. Dette betyr at det har vært utført regulær overvåking av algoppblomstring med SeaWiFS data de siste tre årene, og at det er brukere utenfor forskningsmiljøene som har gjort seg nytte av informasjonen. En web-basert tjeneste er satt opp hvor brukere kan gå inn og se på SeaWiFS produkter som produseres daglig i perioder hvor algoppblomstring er aktuelt. De viktigste samarbeidspartnere og brukerorganisasjoner er Fiskeridirektoratet og Havforskningsinstituttet. Dermed har tjensteutviklingen hvor EO data inngår også gjort et betydelig fremskritt. Dette betyr ikke at EO-data er fullt utviklet for den norske algeovervåkingstjenesten. Det er flere hindre som må overvinnes i prosessen med å etablere en operasjonell tjeneste, f. eks er dataene fra SeaWiFS ikke offentlig tilgjengelig. Hovedaktiviteten i prosjektet har ligget på algoritme utvikling og validering, og på demonstrasjon av nytteverdien av integrasjon mellom EO data, in situ og modell data. Videre tjenesteutvikling er planlagt for de neste årene hvor bruk av MERIS og MODIS data inngår.

3 Når det gjelder bruk av EO data i klimaovervåking og klimamodellering har vi en langsiktig målsetting om at særlig isdata for Arktis og randområdene kan spille en betydelig rolle til å forbedre og validere klimamodellene. Passive mikrobølge data fra 1978, som er de viktigste EO-baserte klimadata for polarområdne, har vist nedgang i isarealet Arktis og disse dataene er brukt til å validere en koblet hav-is modell. Dette har vært første skritt i utvikling av data assimilering av EO data inn i en slik koblet modell. Assimilering av simulerte istjukkelsesdata ved hjelp av optimal interpolasjon har vært testet med denne modellen. Flere assimileringeksperimenter er planlagt med bruk av isdata fra satelitt. I de neste 3 – 5 år er det særlig ENVISAT data (iskonsentrasjon, isdrift) og CRYOSAT data (istjukkelse) som vil bidra til å gi bedre isdata. Vi har etablert samarbeid med NPI hvor modeller og satelittdata skal brukes i kombinasjon med data fra oseaongrafiske rigger med ULS (Upward-Looking Sonars) som måler isdrift og istjukkelse. Dette er særlig aktuelt in Framstredet hvor NPI har som viktig oppgave å overvåke isfluksene. Modellerings- og assimileringsverktøyet som er utviklet med hovedstøtte fra EU og Norges Forskningsråd, og med delstøtte fra Rammeprogrammet, er nå planlagt brukt til overvåking av Framstredet. Et eget forslag er under forberedelse til NFR hvor et integrert system med modeller, satelittdata og oseanografiske data skal utvikles.

Alge-informasjon på Internet

Nansen Senteret har gjennom en rekke prosjekter bygget opp en satellitt basert Web-tjeneste for overvåkning av algeoppblomstringer (http://www.nersc.no/HAB) i sydlige farvann av norsk interesse (Nordsjøen til Stadt). Aktiviteten startet med støtte fra blant andre NRS, som ga oss muligheten til å by på et ESA ITT og få et prosjekt for å implementer (Decide-HAB) og demonstrere et mer helhetlig konsept ovenfor fiskeriforskning (HI), myndigheter (FD) og til dels oppdrettsindustri (AquaFarm AS). Tjenesten baserer seg på **forskningsbruk** av SeaWiFS data for ikke å komme i konflikt med OrbImage og NASA sin data policy for bruk av SeaWiFS data. Med tilgjengelig finansiering er det ikke mulig å etablere en avtale med OrbImage om ”kommersiell” bruk av SeaWiFS. Som følge av

dette har sanntids tilgang til JO informasjon vært passordbeskyttet og bare tilgjengelig for "planlegging av feltobservasjoner og forskningsbruk".

ALGEINFO (http://algeinfo.imr.no) er en offentlig og privat finansiert tjeneste som regulært utarbeider ukentlige tilstandsrapporter for algesituasjonen i norske kystfarvann. ALGEINFO baserer seg normalt på et stasjonsnett fra 29 lokaliteter langs kysten og på laboratorieanalyse av vannprøver fra disse. Algetype/art, antall (celler/liter) og eventuell skadelighet bestemmes og danner basis for rapporteringen. Ved oppblomstrings situasjoner benyttes også annen informasjon som er tilgjengelig, inkludert JO data. En av utfordringene er **tidlig** bestemmelse av mulige skadelige algeoppblomstringer. Ved de siste års skadelige algeoppblomstringer har en tidlig sett signaler fra disse i JO data. Disse observasjonene har vært en del av grunnlaget for å foreta dedikerte feltobservasjoner for verifisering av alge type, mengde og eventuell skadelighet. Under identifiserte skadelige oppblomstringer I 1998, 2000 og 2001 bidro Nansen Senteret aktivt med informasjon til Fiskeridirektoratets beredskapsgruppe – satellittbilder og tolkninger ble gjort tilgjengelig for og benyttet av feltenheter for prøvetaking (Munin som opererte på Sørlandskysten) og for beredskapsledelsen ved FD/HI i Bergen.

ALGEINFO kan ikke regulært gjøre SeaWiFS data tilgjengelig på eller via sin Web-side, pga. begrensningene mht. opphavrettigheter og ikke-forskningsbruk. Derfor er det bare under "Andre Sider" en referanse til Decide-HAB på ALGEINFO. Informasjonsinnholdet i satellitt dataene alene er også for lite til å kunne arts og mengde bestemme en observert oppblomstring, slik at en effektiv bruk vil kreve integrering med feltobservasjoner. På denne måten har HI og FD benyttet SeaWiFS data under siste års alge oppblomstringer.

Prioriterte oppgaver for perioden 2002 – 2005

Med vellykket oppskyting av ENVISAT 1. Mars iår, vil det naturlig nok bli av prioritert å utvikle marine og polare anvendelser av ENVISAT sensorene, ASAR, MERIS og AATSR. I flere godkjente "Announcement of Opportunity" prosjekter har vi definert aktiviteter som gjelder is- og iskantprosesser, alger, oljesøl, vindobservasjoner, fronter, virvler, strøm og andre prosesser hvor ASAR og MERIS vil ha en sentral rolle, både hver for seg og i kombinasjon. Nansen Senteret er koordinator for to nye EU-prosjekter under GMES programmet: MERSEA (Marine EnviRonment and Security for the European Area) og DISMAR (Data Integration System for Marine Pollution and Water Quality). Begge disse er relatert til utvikling av operasjonelle tjeneseter for det marine miljø hvor EO data inngår. Et annet viktig prosjekt som gjelder tjenestutvikling for et kommersielt marked startet i desember 2001 er EMOFOR (ENVISAT monitoring and forecasting services for the offshore industry) som er delfinansiert av ESA under "Long term earth observation market development of ENVISAT services". Alle disse prosjektene, i tillegg til andre pågående prosjekter knyttet til utvikling av EO anvendelser, vil for en stor del legge føringer på det som Nansen Senteret skal gjøre i de nærmeste årene.

I et videre prosjekt med støtte fra Norsk Romsenter, som fokuserer på operasjonall bruk av ENVISAT data i marin og polar overvåking, anbefaler vi følgende tre hovedarbeidspakker:

Arbeidspakke 1: ENVISAT overvåking av det marine miljø i nordområdene, med fokus på havis, den marginale issone og områder med potensielle miljørisiko. Her vil spesielt bruk av ASAR bli prioritert, men synergi med MERIS og AATSR vil også bli viktig.

Arbeidspakke 2: ENVISAT overv king av kyst og havområder i Sør- og Midt-Norge, hvor både fysiske parametre (vind, strøm, virvler, oljesøl, etc.) og biolgiske parametre (alger) vil bli observert. ASAR, MERIS of AATSR vil alle bli bruke både hver for seg og i synergi.

Arbeidspakke 3: Assimilering av satelittbaserte havisdata i modeller for klimaovervåking og isvarsling. Her vil nye data assimilering og varslingseksperimenter bli utført og bruk av parametre fra ASAR vil bli testet.

Det nye prosjektet vil være i tråd med Handlingsplanen for Operasjonell Jordobservasjon og SatHav prosjektet som er under utarbeidelse av Norsk Romsenter. Prosjektet vil ha samarbeidspartnere både i Norge og i utlandet og være relatert til nasjonale og internasjonale programmer.

1. Background and justification

In marine and polar monitoring there are three factors which will have impact on the development of satellite remote sensing

- increased access to earth observation data from several new satellites in the next few years, where ENVISAT is one of the most important;
- improvement in models and data assimilation for atmosphere, ice and ocean circulation simulations which can potentially use earth observation data much more than what is the case today;
- establishment of EuroGOOS as a driver for operational oceanography where satellite data will be particularly important

To justify EuroGOOS it is stated that operational oceanography will facilitate investments which can lead to significant economic development and return for Europe, especially within environmental management, protection of health and support to monitoring and forecasting of climate change (EuroGOOS, publ. No. 6, 1998). The Nansen Center is founding member of EuroGOOS and has been instrumental in the development of EuroGOOS. Operational users of oceanographical data in Norway are primarily Institute of Marine Research, Norwegian Meteorological Institute (both are members of EuroGOOS) and oil companies. But also industries such as fisheries, aquaculture, shipping and insurance kan become important users of oceanographical information which is presented in a way which is adapted to the needs of the industries. Within EuroGOOS five application modules have been defined and satellite data can play important roles in all of them:

- climate monitoring, assessment and forecasting
- monitoring and assessment of marine living resources
- monitoring of the coastal environment and how it changes
- assessment and monitoring of the health of the ocean
- marine meteorological and oceanographical operational services

The project is relevant for all these modules through activities which will incorporate use of ENVISAT data for monitoring of the marine and polar environment,. The project will demonstrate use of ocean colour data to monitor algaes in the coastal waters of southern Norway. A SeaWiFS demonstration will be part of the preparation for ENVISAT/MERIS and MODIS data. The ongoing modelling activities at the Nansen Center/G. C. Rieber Climate Instiute will use sea ice data from passive microwave satellites to validate model simulations of sea ice extent in the Arctic Ocean and adjacent seas. This validation is very important for assessment of the model performance to predict climate change in the next decades. Sea ice data such as ice concentration and ice area have been observed regularly since 1978 and are among the longest available data records from satellite data. Two decades of data shows that the total ice area in the Arctic has decreased by about 6 % while the multiyear fraction of the ice cover has decreased by about 14 % in this period (Johanessen et al., 1999). One important task is to simulate corresponding changes in the sea ice cover by climate models and to use such models for climate prediction in our ocean areas. The highest global warming is expected in the Arctic, so monitoring and prediction is particularly important in this region.

Use of satellite data in marine and polar monitoring has been an area of heavy investments in Norway during the ERS programme, where considerable national expertise and competence has been built up and resulted in several useful applications of SAR such as ice monitoring, oil spill monitoring, ship detection and wave forecasting. This project is an important contribution to consolidate and develop further this expertise into the period of ENVISAT.

2. Objectives

2.1 Overall objective

The overall objective of the project is to develop further applications of earth observation in marine monitoring and climate by using new microwave and ocean colour satellite data to provide geophysical and biological data

2.2 The main tasks

The project consists of the following three main tasks::

Task 1: Development of a generic SAR analysis system, MARSAS.
The system will use existing algorithms for wind, oil spill, eddies/fronts, natural slicks and ice parameters, and make it possible to integrate other data sets and analysis tools to derive products like wind fields, ice maps, analysed images and forecasting of ocean and ice parameters. SAR data which will be used in MARSAS are ERS, RADARSAT, SeaWiFS and later ENVISAT.

Task 2: Develop use of ocean colour data for monitoring of chlorophyll and primary production in Norwegian waters.
Spring and summer is the most important period for monitoring of algaes in these waters and also the most favourable concerning cloud cover which makes it possible to use optical and infrared satellite data on several consecutive days. Data from SeaWiFS, MERIS and MODIS are the only data which can give synoptic mapping of chlorophyll over larger ocean areas in near real time.

Task 3: Assimilation of passive microwave satellite data in climate models.
Ice concentration and ice area taken over the last 20 years are used to improve global climate models used at the Nansen Center/G. C. Rieber Climate Institute for simulation and forecasting of climate change.

3. Results of Task 1: MARSAS (MARine SAR analysis System)

3.1 The MARSAS concept

One of the factors which limits use of satellite data is the lack of good, flexible and user-friendly analysis tools which makes it easy to extract parameters from satellite data, analyse meteorological, oceanographical and other ancillary data, and use satellite data in geophysical-biological ocean and climate models. The idea of MARSAS is to develop a set of user-friendly analysis tools, including adaption of existing software packages, which facilitates the analysis of satellite data. The MARSAS concept is illustrated in Fig. 1.

MARSAS should be an “end-to-end” system, which enables the user to ingest different types of SAR data, perform calibration and geolocation, apply SAR algorithms, integrate meteorological and oceanographical data, perform analysis with existing tools (i.e. Matlab) and combine SAR with other satellite data (optical and infrared images, scatterometer, altimeter data, etc.). The users should not only be scientists but also operational entities and other professional users with background in oceanography and/or meteorology who are active users of marine data. MARSAS should function as an overall coordinating tool where use of SAR algorithms is a central element. To use SAR algorithms it is often required to use temperature, wind, currents and other metocean data either as input to the algorithms or for validation of the algorithm output. With ENVISAT data it will be possible to observe the ocean surface with SAR, infrared radiometer and optical imager at the same time. This requires tools for synergetic use and analysis of data from several sensors. MARSAS will facilitate such synergetic analysis of ENVISAT data. MARSAS will have a user interface that makes it possible to access other tools (image processing software, GIS, statistical analysis packages) as well as ocean and

ice simulation models. Thereby, MARSAS can be further developed into an operational monitoring and forecasting system.

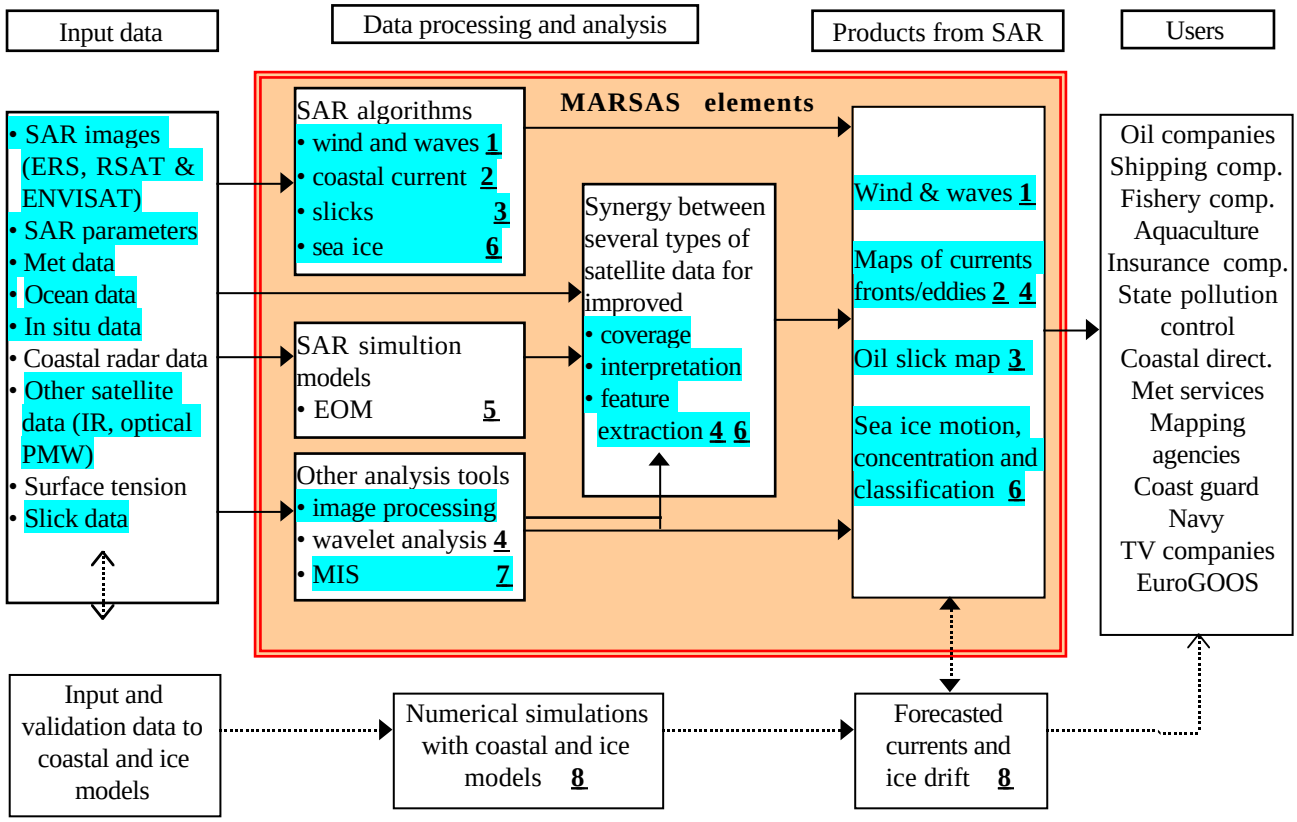

*Figure 1. The MARSAS concept. The core of MARSAS is defined by the red rectangle. The numbers (**1** to **8**) show the modules of the system. Module **7** is the implementation of the software system which integrates the other modules including the user interface. The parts which are shaded in blue will be investigated in this project.*

3.2 Vision and scope of MARSAS

3.2.1 High-level requirements

The development of a Marine SAR Analysis System (MARSAS) is driven by several factors. The most important are:

A need for integration and streamlining of processing and analysis tools in order to extract information from satellite and other data in a cost-efficient manner. In addition to providing a smoother processing line, there is a need for MARSAS to archive and manage both the measured and simulated data. In this way, a wider group of users would benefit from satellite data, especially if the system can provide access to algorithms and models for obtaining geophysical or biological/chemical data from SAR and other satellite data without having to learn low-level details about specific analysis methodologies or computer programs. The users do not need to experts in satellite data analysis, and can employ the derived parameters in their work, e.g. in algae bloom monitoring or site planning of wind mills.

For a professional user there are several specific problems that need to be solved before EO data can be used efficiently. Professional users include operational institutions, value-adding companies, service providers, industry and others who are not necessarily experts in remote sensing, but have professional

tasks to perform monitoring or develop monitoring systems for the marine environment. MARSAS will help to the users in the following way:

- The amount of time required to analyse a single data set (i.e. a single SAR image) in many cases prohibits analysis of all interesting data sets. MARSAS will therefore supply both archiving and retrieval functions for previously analysed images as well as tools for processing new data.

- It is difficult to find which algorithms and models are available, and how to use them due to outdated or incomplete descriptions. MARSAS will help the user to select suitable algorithms or models.

- Scientists and students have to learn different analysis systems for different projects, which reduces the time available for analysis, method development and validation. MARSAS offers a standardised procedure which can be used in several applications.

- Increased application of EO data is hindered by lack of suitable tools for integration, automated algorithms for delivering a demonstration or pre-operational service to specific customers. MARSAS will help to develop EO – applications by facilitating integration with other data.

3.2.2 Technical requirements to MARSAS

The technical requirements are defined with the scope of delivering EO-products for users in value-adding companies, operational services, industry, etc. User investigations in other projects have provided the following list of requirements:

- MARSAS must be able to handle all important data set types for marine apllications: 1) EO data (SAR, SSM/I, optical data, altimeter and scatterometer); 2) in situ data (such as buoy data, CTD data, wind measurements, etc.), and 3) model data from ocean and ice models (such as ice concentration, motion and thickness). Data handling includes pre-processing, storage and retrieval in the marine database, analysis, prediction and presentation.
- MARSAS must provide a common Graphical User Interface (GUI) from which all available data sets and associated tools can be accessed.
- The common GUI must also include an instruction module (tutorial), which explains the terminology used, the types of data sets that are supported, and the analysis and prediction methods included in MARSAS.
- MARSAS must run on both Unix workstations and PCs. (Operating systems and versions to be defined by NERSC personnel and end-users.)
- MARSAS must support distributed computing so that CPU-intensive tasks can be performed by powerful Unix workstations or parallel computers, while simpler analysis and presentation tasks can be done locally on the user's PC.
- MARSAS must adhere to international and industry standards for data exchange via Internet.
- Standard map projections, such as UTM and polar stereographic projections must be supported.
- MARSAS must maintain metadata for each data set, and enable queries on these.
- MARSAS must provide facilities for import/export of data sets in standard formats, such as HDF, netCDF, TIFF, etc.
- It must be easy to include new types of data and their associated pre-processing, analysis and presentation tools.
- MARSAS must be designed and implemented for use on Internet, allowing several providers to contribute to the service chain.

3.2.3 Assumptions about input data

There will be specific requirements to the input data to MARSAS. For example, MARSAS will not include some of the pre-processing. For example, SAR data must be pre-processed to images, oceanographical data must be calibrated, etc. However, the system can accommodate recalibration data or other necessary processing for a specific application.

3.3 Design of MARSAS

The overall MARSAS system, as described in Figs, 1,2 and 3, is larger and more extensive that the actual system which has been implemented within this project from 1999 to 2001. The work performed in the 3-year period has focused on the Analysis and Prediction Module (Fig. 2), while the other four modules (Data Exchange, Data Storage and Retrieval, Presentation and Monitoring/Forecasting Service) are not specifically addressed and are therefore not implemented yet. In the three-level diagram of a marine monitoring and forecasting system (Fig. 3) the work in this project has concentrated on level 2, where where specific input data are run through processing chains which deliver SAR-derived information products. Work in level 1 and level 3 are done with support from other projects.

The first step in the development of MARSAS is to design the system based on the requirements for input data, analysis tools, algorithms, and how the output of the analysis should be presented for the users.

The objectives of the design study is to

(a) Identify input data, main processing steps and desired products
(b) Discuss common problems, and
(c) Outline technological solutions

The design study focused on three scenarios where use of SAR data is a central part:

1. Sea ice classification and kinematics
2. Wind speed and energy estimation
3. Oil spill and natural film detection

The main modules of MARSAS are shown in Fig. 2.

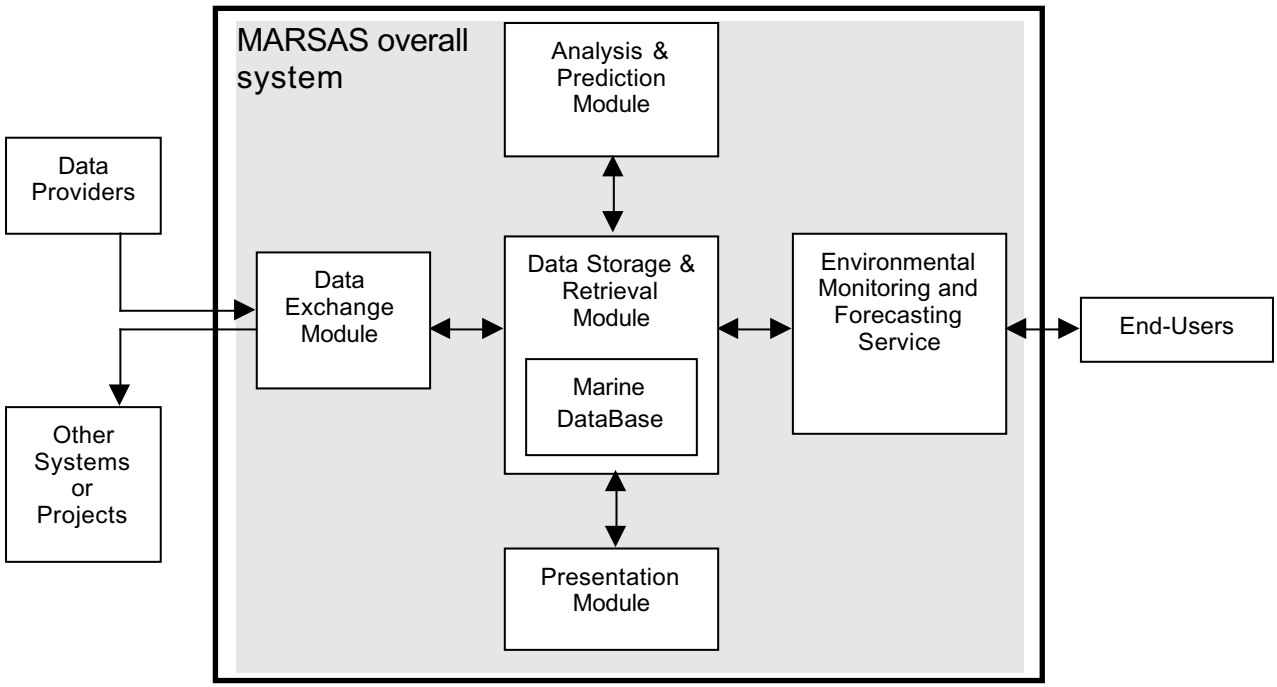

Figure 2 The main modules of MARSAS.

A Data Exchange Module is needed for ingestion of new data sets from various data providers, and for exporting data in digital form to other information systems or project repositories. The Data Storage &

Retrieval Module, including a Marine DataBase, will be the central module in MARSAS. Its main responsibility is to structure observations and estimates of marine environmental parameters in a way that facilitates integration of data from different sources. In addition, it must provide the other modules with capabilities for permanent storage and selection of data based on user-defined criteria.

The Analysis & Prediction Module, which is the core of the MARSAS system developed in this project, contains a suite of algorithms and models that process, extract or forecast a marine parameter using data from the Marine DataBase. This module will include tools for format conversion, resampling, etc., that are needed to harmonise the legacy algorithms and models within the MARSAS data structure. Likewise, data tranformations tools will be needed in the Presentation Module, which will offer presentation and visualisation facilities needed to assist the operator in interpreting and quality controlling observations and estimates.

The Environmental Monitoring and Forecasting Service will be important part of a pre-operational MARSAS system, offering data and information products tailored to specific end-user groups. This module will provide access to products through a user-friendly web interface, and include educational and promotional material for existing and potential new users.

3.3.1 Overall functionality

The overall functionality for a marine monitoring and forecasting system can be defined at three different levels as shown in Fig. 3.

The three levels can be characterized as follows:

Level 1: Total system
• high level description of the total system where level 2 and 3 include the subsystems
• links all required elements: data, models, analysis tools, presentation methods, etc.
• fully operational system which includes monitoring and prediction
• example of pre-operational services: ocean forecasting in the DIADEM/TOPAZ projects
• example of fullt operational services: weather forecasting

Level 2: From observations to geophysical parameters
• includes use of all available data sources
• methodology to derive parameters from several data types
• processing and interpretation of data
• synergetic use of several data sources
• example: sea ice monitoring
• the level where MARSAS core system is under development

Level 3: Algorithm level
• methodolgy to derive one parameter from one type of data
• clusters of algorithms are usually needed at level 2
• examples: SAR wind algorithm, scatterometer wind algorithm, wind speed from altimeter, etc.

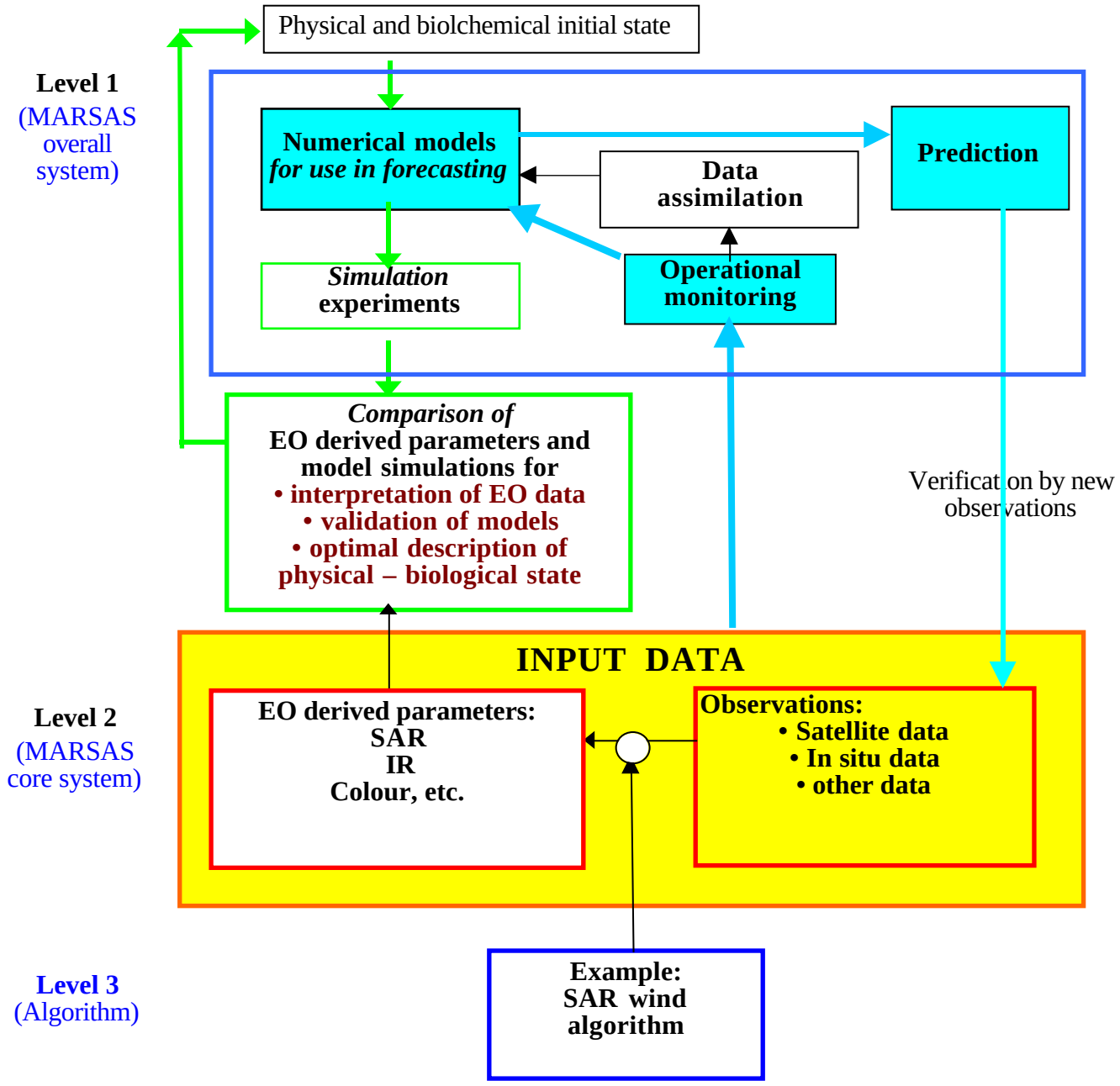

Figure 3. A three-level perspective on marine monitoring and forecasting system. Level 1 is the total system with all elements needed to carry out operational services. Level 2 is focused on the derivation of geophysial and biological parameters observed by remote sensing or other methods. The MARSAS system will developed on this level. Level 3 is the lowest level where algorithms are developed which translates raw satellite data into a higher level data product. Several data types and algorithms are often required to obtain the geophysical/biological parameter to be used in the model simulations.

3.3.2 Data flow in MARSAS

A logical flow of data in MARSAS is shown in Fig. 4. For a given problem, specific types of satellite data are processed in a sensor dependent manner, and analysed in conjunction with other types of data, such as meteorological data, in order to generate a user defined product. A wide range of input data, processing and analysis techniques are used to derive different products, as described below.

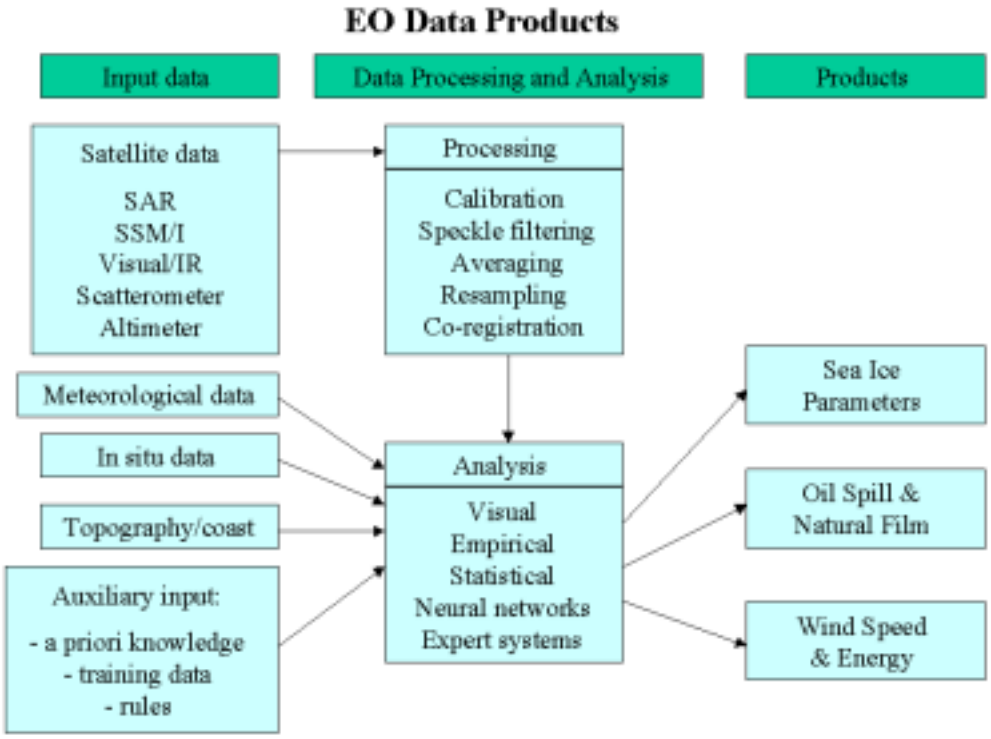

Figure 4. Logical structure of MARSAS

In order to develop the MARSAS system for some of the most important applications, several scenarios are described where the input data, analysis procedures including algorithms and output formats are specified. The first scenario that was implemented in MARSAS was the SAR wind speed algorithm. Other algorithms were then implemented.

3.4 Sea Ice Monitoring Application

3.4.1 Overview of algorithms and tools used in MARSAS

Several sea ice parameters can be retrieved from SAR images, as shown in previous studies (ie.e Sandven et al., 1999). In this project we have focused on two sea ice products from SAR data: ice type classification and ice movement for which several algorithms exist. In previous projects, sea ice classification has mainly been done using ERS LRI images from TSS, and for these images only relative calibration could be performed. Thus, software for general purpose processing tasks were implemented in C. From 1999, TSS also provides ERS PRI data. With PRI as input data, this scenario can also employ ESA's ERS SAR Toolbox, which is used in the other scenarios. For future pre-processing of LRI data, the existing software can be used.

Ice classification by means of texture parameters and elements has been implemented in Fortran (Wackerman and Miller, 1996), and ice concentration derived from SSM/I data (by another Fortran program) can be used to aid the operator. Where available, in situ data from ships in the area and wind derived from SAR-scatterometer can provide additional information for the classification process. The current texture algorithm cosists of three main steps. First, a set of training areas are defined and labeled as instances of a particular ice type.For each area, a set of texture parameters is computed and stored in a file called a 'database file'. Secondly, the 'database' generated in step 1 is used to computed a set of classification vectors using either eigenvector analysis or the arithmetic mean. The output from this step is a so-called classification vector file, which is then used in the third and final step, where an entire image is classified using the vectors generated from the selected training areas. Images are stored in 'flat files', i.e. no header, and the database and vector files are stored in ASCII format.

The program does not have a graphical user interface (GUI), and especially the first step requires a significant amount of manual input of data, making the process quite time consuming. It is therefore proposed to re-organise the program to make it more user friendly, especially with respect to definition of training areas and graphical display of intermediate results after each main step. A GUI must be developed, while the computational parts of the algorithm may remain in Fortran or be replaced with more efficient code in another programming language, e.g. C or C++. The GUI will be implemented in Java. For the computation of texture parameters, existing code may be taken from public domain libraries, such as NETPBM or PBMPLUS, or from a commercial software package, such as Matlab.

For the ice movement application, the pre-processing steps are the same as for ice classification, and hence the software can be shared. PRI data may also be used for motion estimates, in which case the ERS SAR Toolbox can replace the in-house developed C programs.

The ice motion is estimated by a maximum cross-correlation (MCC) method, which is implemented in C (Kloster et al., 1992). This method takes two 8-bit images as input and produces a set of ice motion vectors as output. Each such vector is assumed to be the mean displacement for a block of N by N pixels, and has associated a correlation factor that indicates its quality, i.e. a confidence level. The MCC method is efficient and provides good results for relatively small and uniform ice movement, but often requires an initial displacement defined by the user to obtain a set of motion vectors with high correlation factors. Thus, improvements can be made by developing and testing techniques for automating the process of computing the initial estimate, which will reduce the need for operator input to get a good result. A GUI enabling the user to specify input parameters such as search window size, and for display of intermediate and final results will also be implemented. As an aid to the operator, the GUI will also provide display of meteorological data and wind derived from SAR imagery, if these data are available. The new parts of the MCC method will be written in C, while the GUI will be written in Java.

The data and processing steps for the two sea ice applications using MARSAS are shown in Fig. 5 a and b

3.4.2 Example of SAR ice classification using LDA and BNN methods

The project does not aim to assess the quality or accuracy of given SAR algorithms, but to facilitate use and validation of different algorithms, compare different SAR systems, etc. The example of ice classification with two algorithms (LDA and BNN), which are described below, is included to illustrate this point. From a user point of view, the MARSAS system should have a menue of algorithms where the user can select the algorithm which is most suitable for a given problem. When a new algorithm is available, it should be included in MARSAS, allowing the user to test it or use it instead of older algorithms.

For ice type classification the LDA (Least Discriminant Analysis) and BNN (Backpropagation Neural Network) algorithms have been applied and trained for sea ice SAR images in the Kara Sea region (Bogdanov et al., 1999; Hamre et al., 2001). The LDA algorithm uses a set of texture parameters to distinguish between different ice classes, based on a set of training data provided by the operator. The process of construction of linear discriminants does not rely on any assumption of the form of probability density function and the estimation of its parameters, but uses instead the estimation of between and within class variability in the data set. The decision boundaries separating regions in feature space corresponding to sea ice types are hyper planes, and the performance of the algorithm depends to a large degree on the separation between clusters provided by the given set of texture and local statistical parameters. If the classes are well separated, the linear separation can produce satisfactory results. Non-linear separation may be required if the data clusters have a complex form and are interlocked. Multi-layer neural model with hidden layers is one of the methods that provide nonlinear discrimination between classes.

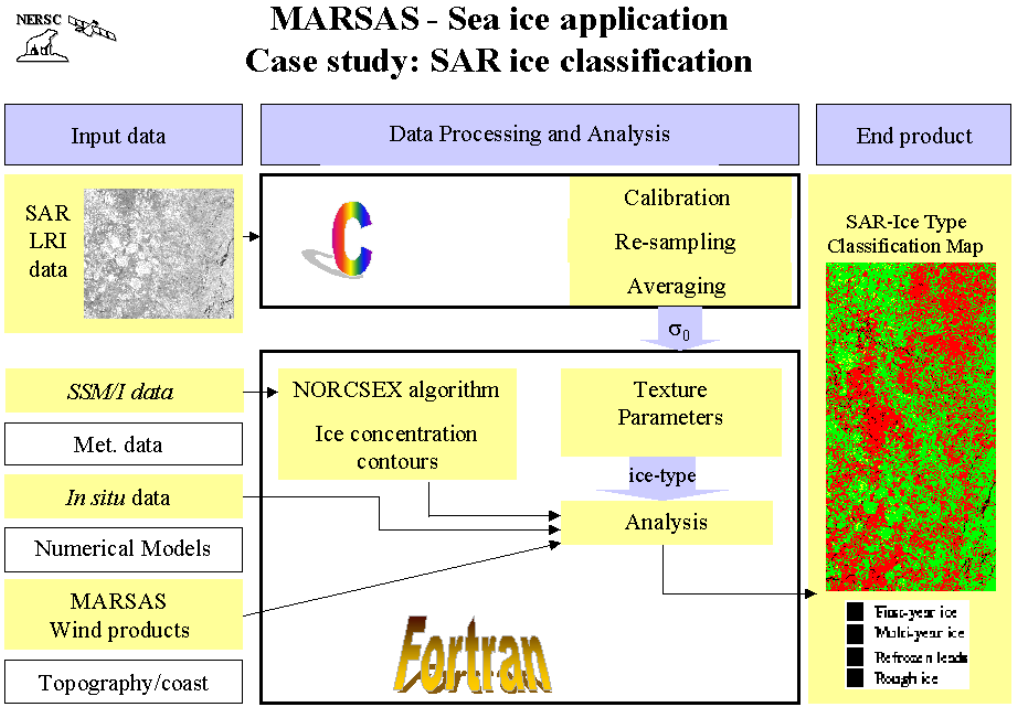

a)

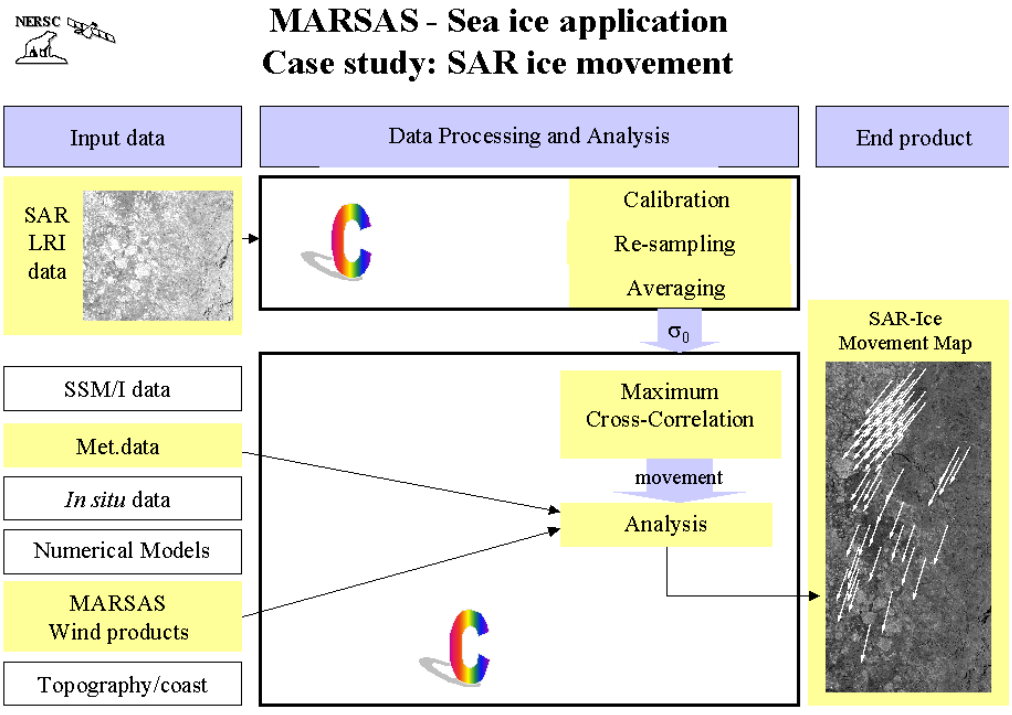

b)

Figure 5. Procedure for SAR ice classification (a) and ice motion estimation (b).

For the SAR ice applications, it will be useful to have a tutorial, and the Sea Ice Interpretation Guide, presently in preparation for access via Internet, is the first step to develop such tutorial. This should both explain the methods used, as well as provide examples of input data and resulting products. The development of a tutorial should be coordinated with the other scenarios, which will also benefit from having training material.

Our approach uses a fully connected, multi-layer, feed forward BNN (Bishop, 1995). The information propagates in one direction from input processing units to output processing units. Statistical and texture parameters from the SAR images are fed into the neural network. The input to a processing unit is the weighted sum of the outputs from the previous layer. During the iterative training procedure, the weights between processing units are adjusted. The result is a classification of each pixel, assigned a probability of inclusion in each class. The backpropagation neural network used for sea ice classification consists of four layers of processing units or nodes.

A RADARSAT ScanSAR image acquired on April 30, 1998 covering the southern part of the Kara Sea, Ob and Enisey estuaries has been classified with the LDA and BNN methods. The results are shown in Fig. 6 (a) and (b), respectively. The visual analysis of the sea ice maps reveals that BNN algorithm overestimates the young ice in upper left-hand corner of the image, where young ice exists in mixture with rough first-year ice. The BNN algorithm, on the other hand, has an advantage of better classification of open water and new ice, which is evident in classification of flaw polynyas in the upper right-hand corner of the image.

Separation of open water areas (low wind speed) and new ice (grease ice) from the surrounding ice is usually not difficult due to their low backscatter values and can be done by simple thresholding. In the selected SAR image some other sea ice types such as strips of small ice cakes exist, leading to variations of sigma zero values and thereby complicating the classification task. Application of texture and local statistical parameters with a neural network leads to better results in this case than using LDA algorithm with the same input parameters. The latter can be explained by better generalisation of the neural network on the data that the algorithm was not trained on.

The image was acquired nearly at the same time as the ship entered the area covered by the image so it was possible to identify sea ice types along the route very accurately. For quantitative assessment of the classification results homogeneous regions along the ship route were delineated and assigned manually to the sea ice classes according ship observations.

When assessing the presented results it should be taken into account that they are obtained using only one SAR image and therefore may not represent the overall performance of the algorithms when other geographical regions and seasons are considered. It also should be also mentioned here that sea ice conditions along the ship route are easiest for navigation and resemble those observed in the Marginal Ice Zone (MIZ). For automatic classification such regions represent more difficulties than the interior regions of sea ice massifs. The obtained results reflect "real life" results of automatic classification to be used for tactical navigation.

Application of the NN algorithm improved the classification accuracy of young ice by 42 % with a slight decrease in accuracy of classification of deformed first-year (FY) ice. Some image pixels were misclassified as level FY ice that was not observed in the testing region. Classification accuracy of open water (OW) and nilas class is low for both algorithms, but this can be improved by incorporating additional data sources such as radar data obtained at different polarisation and wavelength, passive and active microwave images.

Three ERS-2 SAR images were acquired on April 30, 1998 near simultaneously with acquisition of the RADARSAT SAR image. The ERS-2 SAR images cover the same region as the fragment of the RADARSAT image (Fig. 7). Both algorithms were applied separately to the ERS and RADARSAT SAR images to see the differences in algorithm performance entailed by the differences of radar parameters (polarisation, spatial resolution, range of incidence angles).

a)

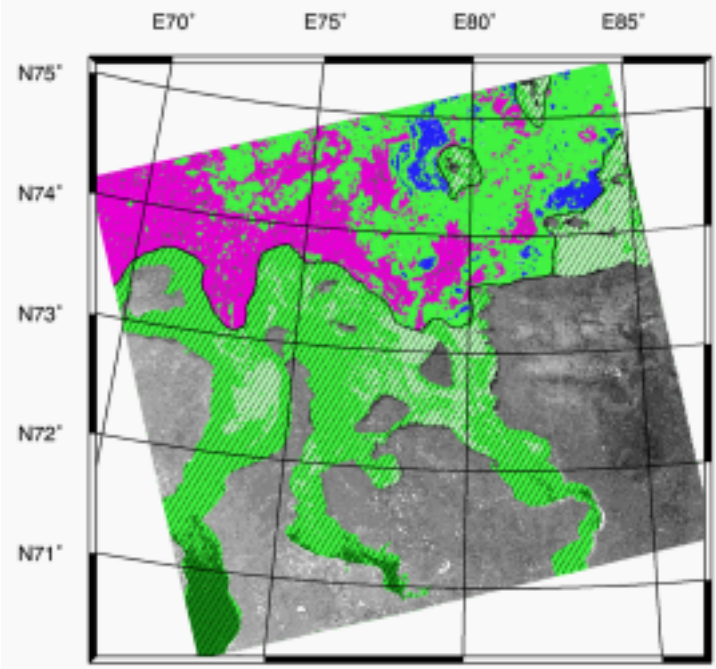

b)

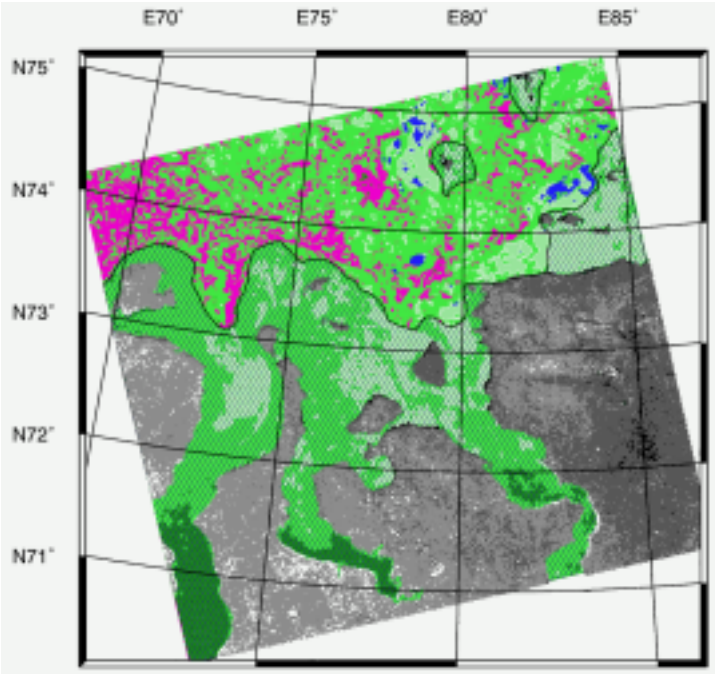

Drifting ice types

Smooth first-year ice

Deformed first-year ice

Very deformed first-year ice

Young ice

OW and new ice

Grease ice and nilas

Fast ice types

Smooth fast ice

Deformed fast ice

River ice

Figure 6. RADARSAT ScanSAR image from 30 April 1998 classified with the NN (a) and LDA (b) algorithms

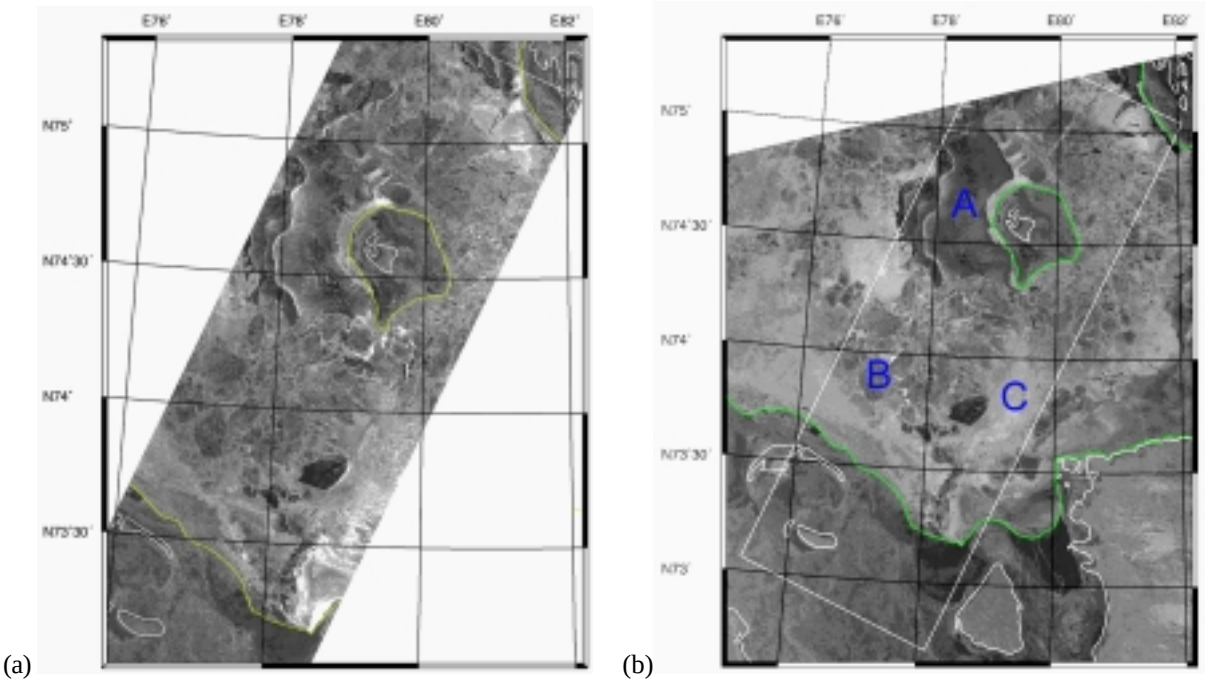

Figure 7. Mosaic of ERS-2 SAR images (a) and part of RADARSAT SAR image (b) acquired on 30 April, 1998, at 06:38 GMT and 11:58 GMT, respectively. A: Grease ice and nilas; B: Deformed firstyear ice; C: Young ice

The quantitative comparison of the obtained sea ice maps was based on the results of manual interpretation by NERSC and NIERSC sea ice experts. The percentage of correctly classified pixels for each sea ice class is shown in Table 3.1 and 3.2 for RADARSAT and ERS SAR images, respectively. It can be seen that accuracy of LDA algorithm applied to the two different test sites is not very different while for the BNN algorithm the discrepancies are quite big. The latter can be explained not only by the differences in sea ice conditions in two different test sites but also by two different approaches used for gaining truth data and subjectivity of the expert knowledge.

Table 3.2 shows that classification of young ice using ERS SAR images is better than using RADARSAT SAR images for both test sites. OW and nilas class is better recognized in RADARSAT SAR than in ERS SAR images. The neural network algorithm is also better at classifying OW and nilas in RADARSAT SAR images, for both test sites. These differences can be explained by differences of sigma zero values for different sea ice types at HH and VV polarisation and also by differences of texture features for different polarisations.

The conducted studies showed that application of the NN algorithm with texture and local statistical parameters improved the classification accuracy of young ice (5-42%) and OW (low wind speed)/nilas class (4-35%), while yielding a decrease in classification accuray of FY ice (5-11%) for different sensors and test sites. Application of the classification algorithms to the ERS and RADARSAT SAR images showed that classification accuracy of young ice is higher when ERS SAR images are used, while OW and nilas are better separated from the other sea ice types using RADARSAT SAR images. Merging of these two data sources in a single classification procedure based on BNN algorithm is expected to improve sea ice classification results.

Texture and local statistical features applied in this study were found useful for sea ice discrimination. Especially for classes with overlapping ranges of backscatter coefficients, such as FY deformed ice and young ice. This experience will be drawn upon in a future sea ice classification algorithm.

Table 3.1 Classification accuracy for RADARSAT SAR image

	Deformed FY ice	Young ice	OW & nilas
LDA	89.7	36.6	15.9
BNN	83.3	63.3	50.8

Table 3.2 Classification accuracy for ERS SAR images

	Deformed FY ice	Young ice	OW & nilas
LDA	81.0	83.0	5.3
BNN	70.3	83.0	8.9

3.5 SAR-Wind Application

Wind retrieval from SAR imagery in Norwegian waters has been investigated by Korsbakken et al. (1998) who carried out a systematic analysis of the mesoscale coastal wind field conditions expressed in a series of ERS-1 and -2 SAR images obtained during the COASTWATCH'95 experiment. Quantitative estimates of wind speed and direction are based on examination of both the SAR backscatter and the spectral properties. In another investigation, the wind speed retrieval from ERS SAR has been compared with Scatterometer wind from the ERS-1 & -2 tandem phase. The wind retrieval algorithm CMOD IFR2 (Quilfen, 1995) used on both SAR and scatterometer data has been implemented in a prototype of MARSAS as shown in Fig. 8.

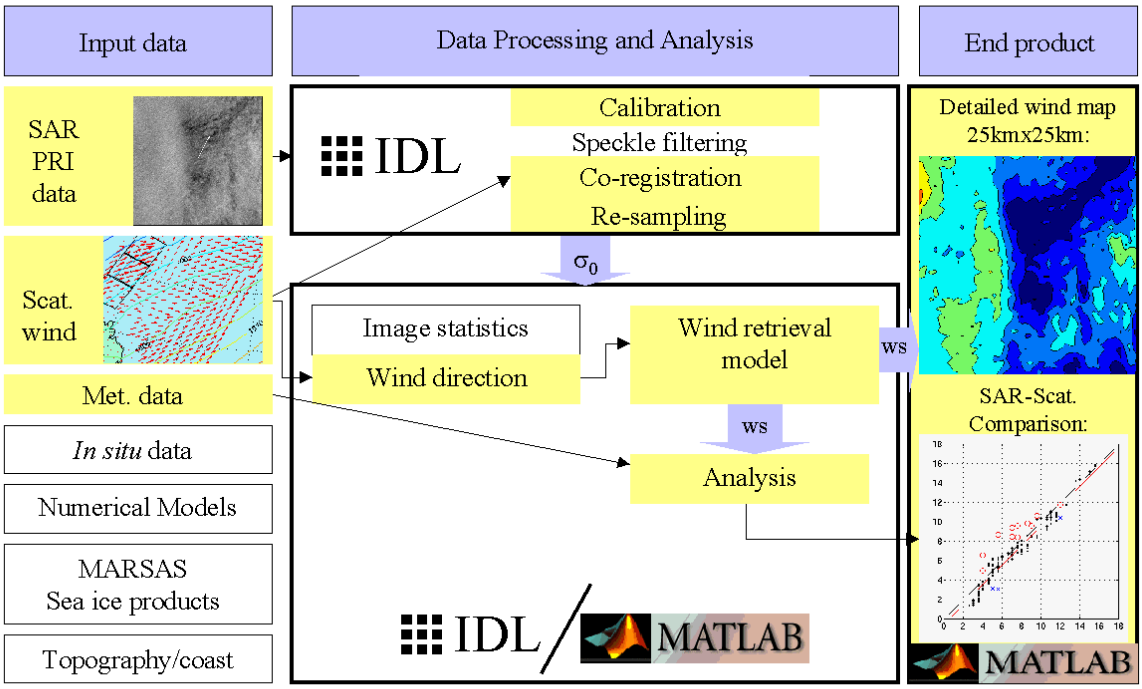

Figure 8. Flow chart of the analysis procedure of the SAR-Scatterometer synergy data from ERS Tandem Phase.

A validation of wind retrieval from Synthetic Aperture Radar (SAR) images has been performed by comparing wind speed estimated from ERS-2 SAR with ERS-1 Wind Scatterometer (WSC) measurements, both using the CMOD-IFR2 algorithm (Furevik and Korsbakken, 2000). This was made possible by using data from the open ocean and north of 63° N during the Tandem Phase of the ERS satellites. Here the WSC and SAR coverage overlapped with a time difference in the data acquisition of only 30 minutes. The SAR-derived wind speed values from subimages centred around the WSC window agreed to within ±2m/s, but underestimated the WSC wind speed values by approximately 0.4 m/s. Studying the spatial variability of the high resolution wind speed values leads us to conclude that the SAR wind field seems useful at least down to a spatial resolution of 500m, provided that external information on the wind direction is available.

SAR PRI data was calibrated using programs written in the IDL language. The two data types were co-registered to each other and the SAR image was re-sampled to 100m pixel size. Analysis of the SAR and Scatterometer data was done using some IDL and some Matlab programs. The end products such as plots and maps were created using Matlab.

3.5.1 Wind retrieval in the marginal ice zone

Validation and application of SAR wind retrieval has been done in the marginal ice zone (Furevik et al., 2001). The wind stress in the MIZ is the driving force for upwelling along the ice edge and important for the ice drift. Upwelling is an important factor for the bio-mass production, as it brings deeper water containing nutrients up to the near surface productive waters. Offshore winds can act to keep large coastal areas open during periods in winter, resulting in large heat fluxes and the possibility of subsequent deep-water formation along the shelves. Renewal of the deep and bottom water in the Arctic is important for the global ocean circulation, therefore meso-scale wind-driven phenomena are important to monitor in order to make the correct parameterization in the global ocean circulation models.

Today's monitoring of the wind field in the Arctic mainly consists of the output from weather prediction models. The results from these models suffer from a fairly limited number of observations in the polar regions, thus giving less accurate output than for more densely populated regions. In addition, the output is very coarse with a grid cell spacing of 50-75 km. With SAR it is possible to much more detailed wind information as shown in Fig. 9.

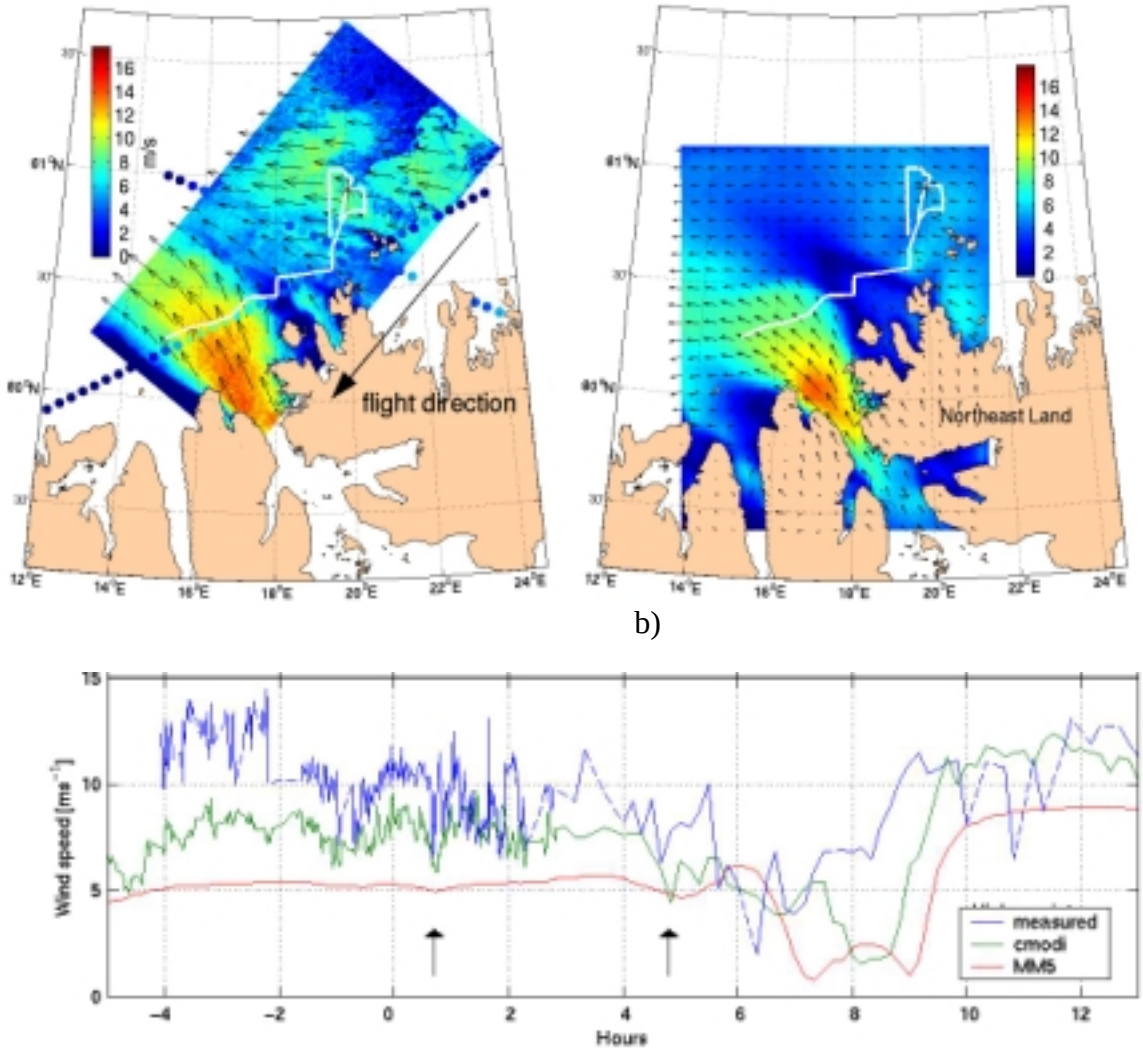

Figure 9: a) Wind field retrieved from ERS-2 SAR, and altimeter wind speed (dots) North of Spitsbergen, August 14, 1996. Ship track of R/V Håkon Mosby from 5 hours before SAR passage to 13 hours after, is shown as the white line. b) Wind field at 2km grid as modeled by the MM5 with a nested model run. c) Comparison of wind speed from ship (blue), SAR (green) and model (red) along the ship track. The x-axis denotes the difference to the SAR passage time. The ship moves into the jet in the end of the track at 9 hours after SAR passage.

Wind retrieval from SAR has a potential to provide the needed routine measurements in the MIZ. In a resent study, analysis have been made of data from two oceanographically expeditions consisting of SAR.PRI scenes, altimeter wind speed and wind measurements from ship (Furevik et al 2001). In addition, a non-hydrostatic numerical atmosphere model was used to investigate the atmospheric conditions and validate the retrieved wind field from SAR. An example of derived wind field from SAR and wind speed from ERS Altimeter is found in Figure 9 a. The spatial variations are reproduced well by the atmospheric model (MM5), of which the wind field from the 2 km grid is shown in Figure 9 b. The good correlation is also seen from the comparison of wind speed from SAR, model and ship along the ship track (white track in Figure 9 a, b) that is shown in Figure 9 c.

3.5.2 Wind energy mapping for siting wind turbines

In coastal regions, large variations in the wind conditions may occur due to interaction of the airflow with topography. Such variations are impossible to model using the coarse weather forecast models. Wind field retrieval from SAR in coastal regions has been done in particular for studying the potential of remote sensing in siting wind turbines. The utilization of wind energy is of growing interest, as this type of power production is free from pollution and thus is able to help reduce the release of CO_2. Also in developing countries and remote areas where a local source of energy is needed, wind power can be used. However, in these areas the local wind conditions may not be well known and available maps are often not precise. In order to ease the task of optimally position a wind farm under such conditions, the use of satellite wind measurements is expected to be an advantage.

In the WEMSAR project (EU-funded 2000 – 2002) wind speed will be retrieved from a series of ERS SAR scenes from the west coast of Norway near Bergen (Johannessen et al., 1999, 2000). An example with moderate northwesterly winds is shown in Fig. 10 together with the wind rose from observations at Hellesøy lighthouse. The wind roses gives a statistical distribution of wind direction and speed at a given location. In the WEMSAR project these data will be compared with model runs for the prevailing wind directions. This requires that MARSAS can include other wind data in addition to the SAR data. It is noteworthy that Fig. 10 shows many details of the wind speed in the fjords and near land which is not available from the synoptic weather data. The superposition of a detailed land mask on top of the SAR image masks out artificial wind speeds over land.

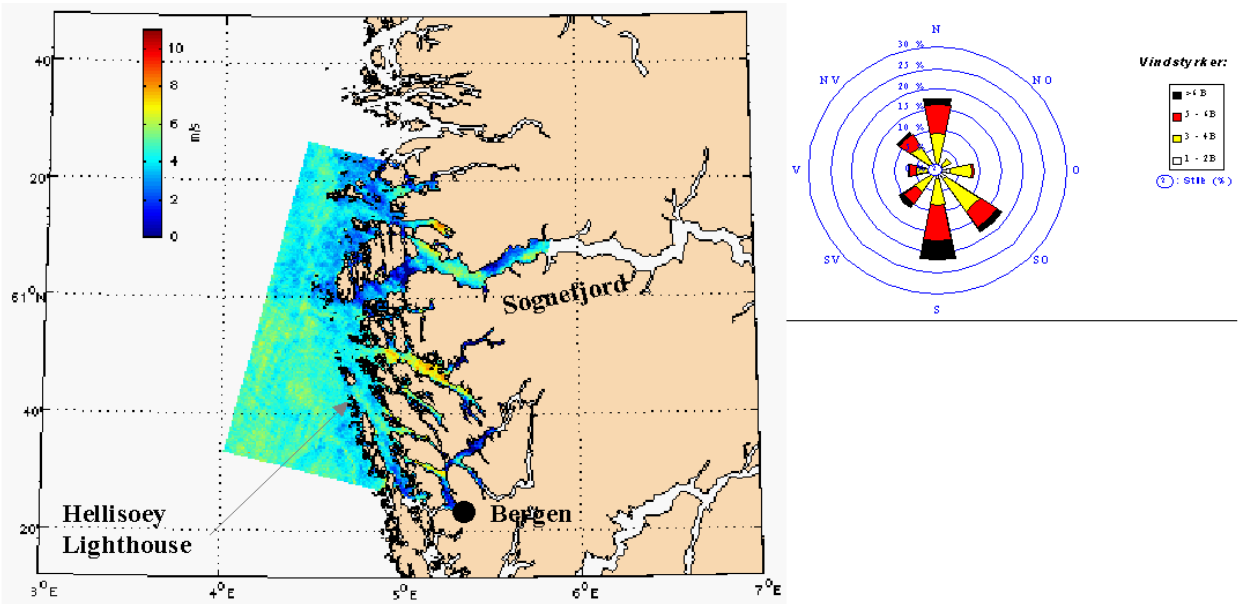

Figure 10. Example of a SAR-derived wind speed map at the Norwegian coast (left figure) and the wind rose from Hellisøy lighthouse (right figure). Data from the SatWind and WEMSAR projects (Furevik and Espedal, 2001)

3.5.3 Methodology to derive wind from SAR

The SAR.PRI data are calibrated using the SAR toolbox provided by ESA/ESRIN. This software is based on IDL and it is therefore very convenient to use this programming language to read the output and reduce the image size. Processing of a SAR.PRI scene from CD-ROM to output wind information using a C-band model as shown in Figure 11 is done in 4 steps:

1) Calibration of SAR scene using SAR toolbox.
2) Output file containing normalised radar cross section values is reduced to lower resolution matrices using IDL.
3) Lower resolution matrices are giving wind direction and speed using MATLAB.
4) Analysis, comparison, visualisation, etc.

The input to step 1 is the SAR.PRI data from CD-ROM provided by ESA. The calibration of the data done in this step gives an accurate estimate of the normalised radar cross section, which is necessary for the use of the C-band models. The output is a backscatter matrix with 12.5 m - by - 12.5m pixel size, together with header file and corner co-ordinates used for geo-localisation. The backscatter matrix is read in step 2 and reduced to a lower spatial resolution in order to save space and reduce speckle noise. Wind direction in an 8-by-8 matrix over the scene is estimated from 2-dimensional FFT derived image spectra in step 3. This wind direction field is used as input to the CMOD algorithm. Output from step 3 is thus a SAR derived wind field. The programmes for analysis in step 4 are naturally dependent upon the purpose of the study. Presently it contains different programmes giving plots of the derived wind field on a map, programmes collecting data from a large number of scenes from the same area and comparing with in situ data, programmes for comparing with wind field from non-hydrostatic numerical models, and so on.

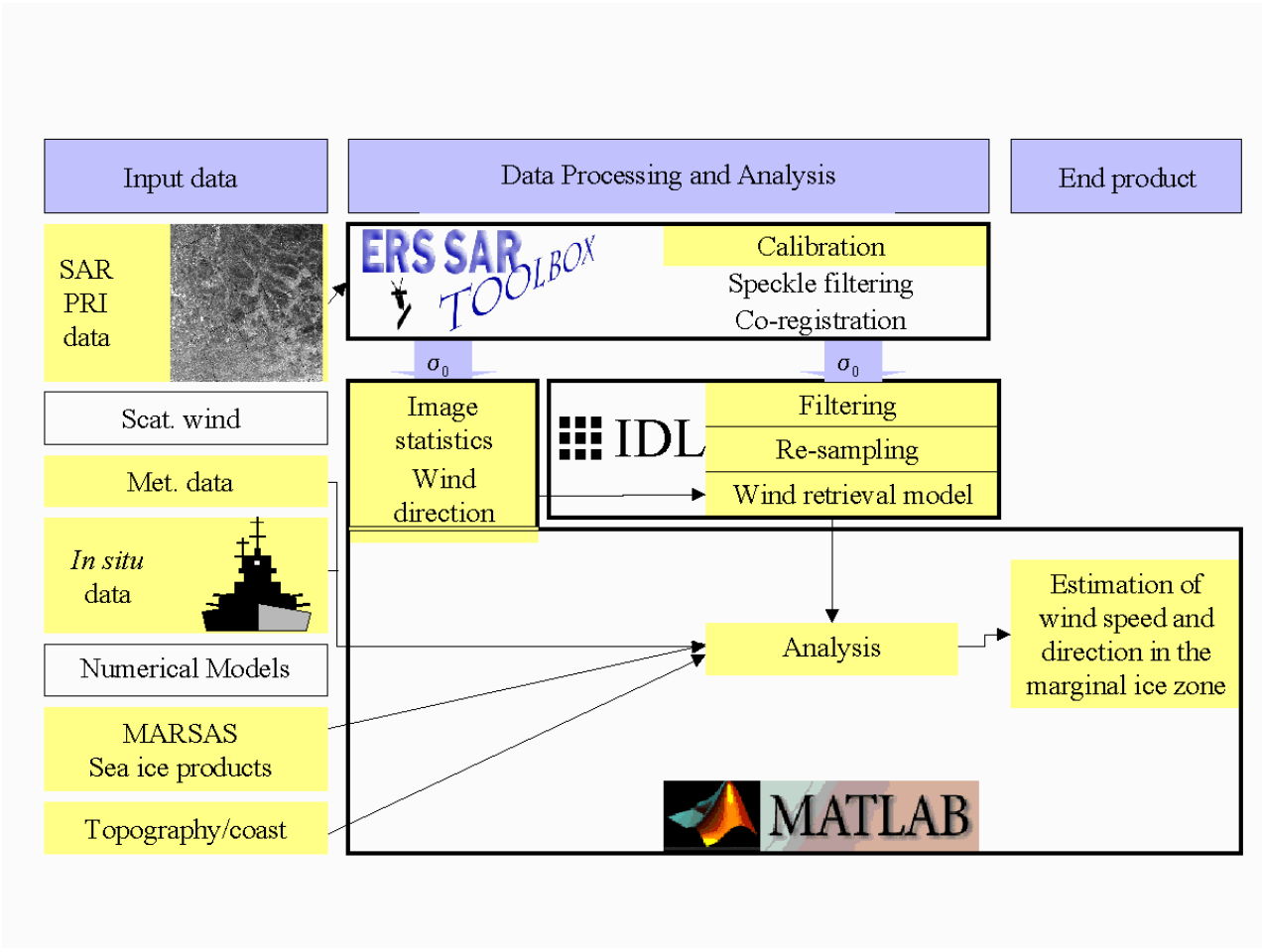

Figure11. Example of flow chart for SAR wind field retrieval in the marginal ice zone.

The calibration is done using SAR toolbox giving the normalised radar backscatter value. Median filtering and re-sampling of the SAR data to 100 m pixel size is done in IDL. These programs will be written as functions that can be called by all users. Also in the case of using CMOD-4 or CMOD-IFR2 as wind retrieval models IDL programs will be used. If other wind retrieval models are used it is also possible to switch to another programming language for this module. Image statistics such as spectral analysis leading to estimation of the wind direction will be done on sub-images imported into Matlab. Programs for this and other central programs in analysing of SAR images and visualisation of results is to be written as functions that can be use in other applications of MARSAS. In this way we intend to create a Matlab library of SAR analysis tools.

The MARSAS system is designed to accommodate different types of wind algorithms. The reason why we use the CMOD algorithm is practical, because this algorithm has been well studied and validated by NERSC. Other algorithms can be included as needed.

3.6 SAR oil spill discrimination

The superviced SAR oil spill discrimination algorithm developed by Heidi A. Espedal (Espedal, 1998, 2000) can be adapted to the MARSAS concept as shown in Fig. 11. The algorithm was developed to supply standard procedures, including tools to aid in a SAR slick discrimination process.

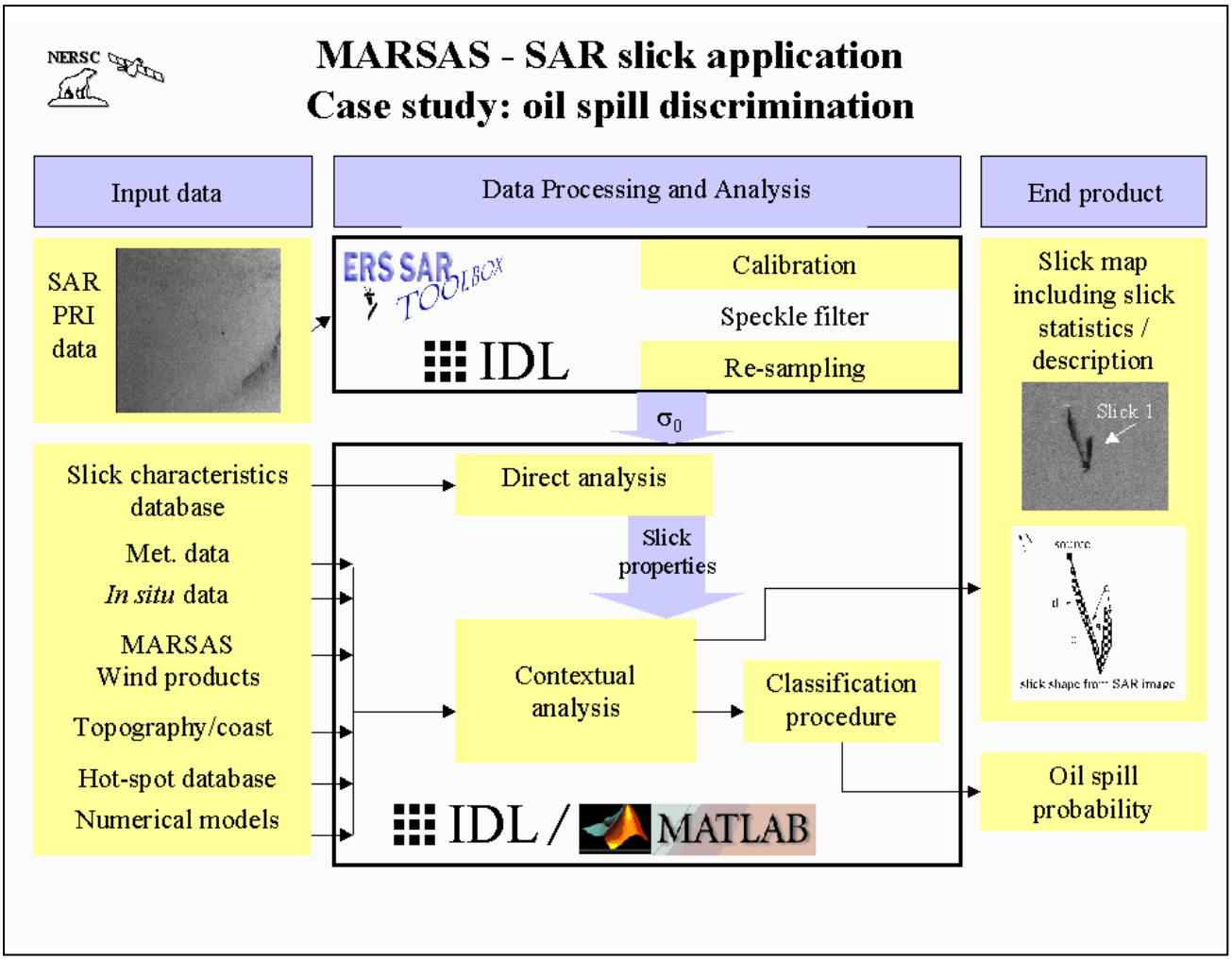

Figure 11. The MARSAS system applied to oil spill discrimination. Note that the whole spectrum of input data is required for this analysis.

There is no new analysis of oil slicks in this project.The work has focused on adapting the SAR analysis part of the slick algorithm by Espedal (1998, 2000) to the MARSAS concept as shown in Fig. 11. The SAR processing steps are impemented, while the contextual analysis remains to be done. The steps in the algorithm have been analysed and are described in this section.

The algorithm was originally developed using low resolution ERS imagery (LRI) from Tromsø Satellite Station (TSS). The images were calibrated using a procedure developed at the Nansen Center, and included range normalization, linear scaling from 16 to 8 bit pixels, resampling to square 100 m pixels, and absolute calibration.

During the first phase of this project in 1999, the calibration procedures have been implemented using ESA's ERS SAR Toolbox and IDL. These are based on input data in the form of full resolution ERS imagery (PRI format). All the slick analysis is then based on imagery averaged to100m resolution, exept for detection of slick sources/startion point. These are sometimes more easily seen in the full resolution imagery.

The direct analysis encompass all information that may be derivated from the slick itself (shape, size, length, texture, damping, and gradients). These parameters were originally extracted using a Khoros program package, based on viff-formatted imagery, and also some simple IDL procedures. These parameters are then compared against a slick characteristics database.

The first efforts have been made to extract the parameters in the initial analysis using the IDL and MATLAB program packages.

The contextual analysis is based on information from the region surrounding the slick (local winds, currents, rain, temperature, season, bathymetry, and locations of possible pollution sources). Most of this information is already available using IDL procedures. However, more work is required to streamline the procedures, and also to test whether MATLAB proves a better package for this part in the discrimination procedure.

The analysis will also include numerical models, such as the ERIM SAR Ocean Model (EOM) and an oil drift model. The EOM model is available at NERSC, and is written in FORTRAN code. An oil drift model is not currently available at NERSC, but can fairly easily be developed using FORTRAN or C code. The need for such models should be further evaluated in the future work on the slick discrimination package.

The output of the slick analysis procedure is a SAR image indicating the relevant slick, a slick map and a slick statistics/description. After a manual classification procedure, the information from the direct and contextual analysis can be used together with the data base of slick characteristics, to give an oil spill probability estimate.

3.7 Common features in all scenarios

There are several common problems in all scenarios described in this report, which justify the development of the MARSAS concept. The first category of problems are related to providing common requirements for functionality in an efficient manner. The second category consists of problems related to software system development and maintenance. Selected problems from these two categories are discussed below.

Certain auxilary data, like topography and bathymetry, are needed in all scenarios. These data should be shared, along with the tools to process and display them. If these data are available at different spatial resolutions the MARSAS tool should select the most appropriate resolution for the given case, based on the size of the geographic area selected by the user or the product type that is chosen. The user should not need to know the physical location or storage format of the data (transparent access).

Some types of EO data, e.g. SAR imagery, are used in all the scenarios, and pre-processing tools should be shared to reduce both time for learning to use the system and for software development and

maintenance. Other types of 'common' tools, such as image processing and display facilities are also needed in many applications, and should therefore be harmonised too.

Another problem related to the use of the system, is keeping track of the processing a data set has gone through. For instance, there are several tools available for calibration of SAR data, and a description of the program used and parameters applied will be useful in subsequent analyses. The format used by the in-house developed processing packages does not store the history as part of the data set. Instead it is written to a separate file, and usually printed on paper for later use. Other processing packages may provide information about processing history as part of the data set.

Perhaps the biggest problem is that there is no homogeneous user interface for the different types of products, and documentation of how to use a particular algorithm is often incomplete or outdated. With a common GUI, the learning curve will be substantially reduced. This interface should also include a tutorial so that novice users can quickly get familiar with the system. It should provide access to all relevant types of data and tools, and hide details of physical location and internal data formats that are of no interest to the user.

Different users may have access to different types of computers, typically PCs and Unix workstations. Hence, the MARSAS system should be available on the major computer platforms, under operating systems such as Windows, Unix and Linux. It should also provide the same functionality, although CPU-demanding operations will take longer time on a simple PC compared to a more powerful workstation.

It must be possible to link to existing software, written in either Fortran, C or some other standard programming language, including commercial packages such as Matlab. The MARSAS system should not behave differently if a new version of a program is installed, as long as the input parameters and output data are the same.

From a pure software development and maintenance point of view, there are also common characteristics for all three scenarios. For instance, the issue of supporting the system on several computer platforms. Apart from automating the installation process, the most time saving process is to develop the system by means of standard (and portable) development tools to avoid re-implementing parts of it for each new platform. In addition, keeping the number of different development tools to a minimum will reduce time and effort in system development. Tools for linking programs must be included, since both application dependent algorithms and general purpose software need to be integrated. Each algorithm must be implemented as a standalone program with a well defined interface (i.e. a specification of input and output data). This enables the implementation of it to be changed, if a more accurate or faster technique is developed at a later stage.

Organisation of data sets is another important issue. The MARSAS system can: (1) keep all data in a database and provide customised search and retrieval facitilites for the different scenarios, (2) store all data in files and enforce the user to keep track of data and products, or (3) provide a solution with some data in a database and some data in files. In either case a suite of format conversion tools will be needed, and these can either be taken from existing software (if the available format is a standard format) or be developed in the project (if data are collected on ad-hoc basis or become available in a new format).

Yet another problem is related to the intended use and distribution of the system. For non-commercial systems, public domain packages and methods can be freely included, as can any available COTS tool installed at NERSC. On the other hand, a operational version of MARSAS must be developed by means of purchased software development tools and algorithms developed by NERSC personnel.

3.8 Outline of a Solution including use of Internet and Java technologies

A proposed solution is to build MARSAS from a set of common modules which can be used in all applications (for example ERS SAR Toolbox, Matlab, Oracle, etc.) and a set of specific modules which are only used for a given application (for example ice motion algorithm, ice classification algorithms, wind algorithms, etc.), as shown in Fig. 13.

The MARSAS system can be seen as the End-User System in a larger Service Chain illustrated in Fig.14 (a), distributing marine SAR products via Internet. The MARSAS system would then run on the user's desktop (or laptop) computer, and connect to the WWW to obtain the latest data sets and derived products. Each data set and product will be accompanied by standardised metadata, enabling users to search for items of interest before downloading full data sets and products. All metadata will be handled by a Broker, that will act as a mediator between the user's client system (MARSAS) and the various service producers. Each service provider can then set up a production chain that prepares data and products in standardised metadata and data formats. Metadata will be published via the Broker, while full data sets and products reside on an inhouse web server that delivers them directly to the users, upon request.

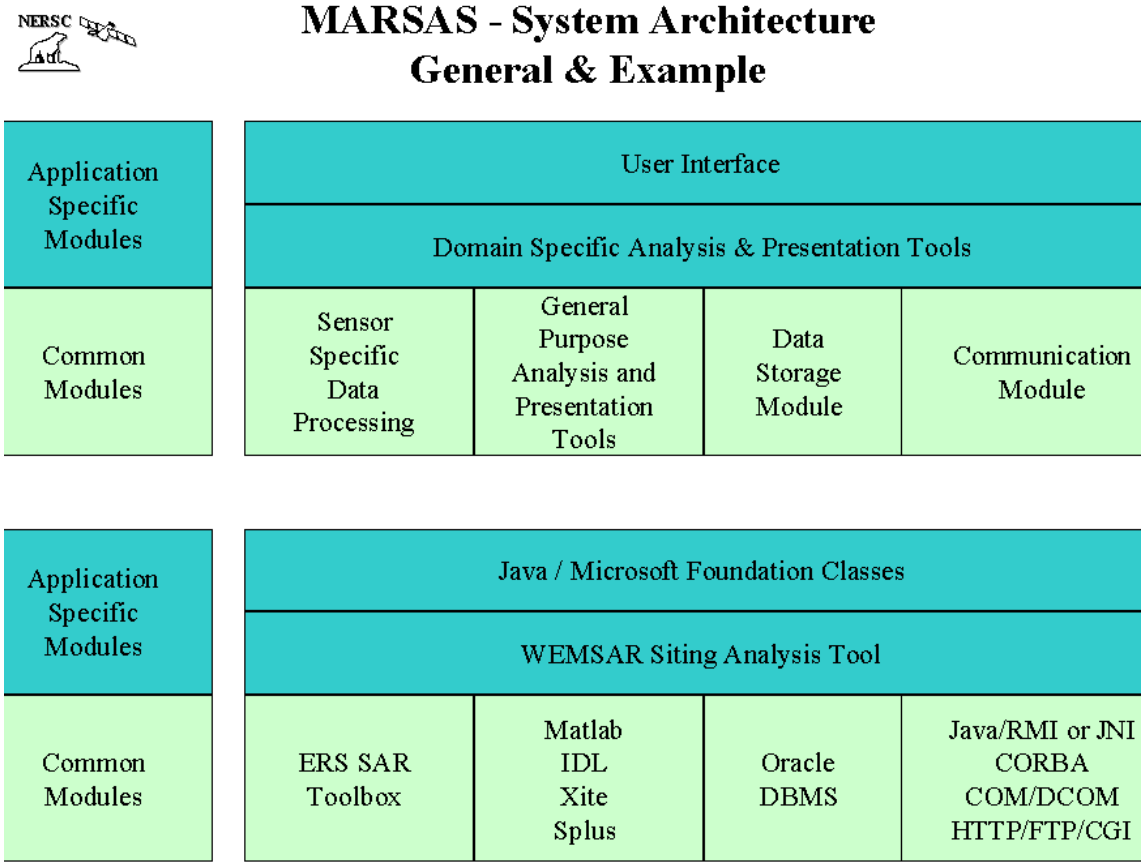

Figure 13. Modules of the MARSAS system architecture illustrated in general (upper graph) and for a specific application, SAR wind analysis for wind energy planning (lower graph)

A modular system architecture based on standard formats and communication protocols, offers a high degree of flexibility in terms of setting up dedicated services for specific user groups. Users can connect to the system (Broker) via Internet, a facility which is already in place at most workplaces today. This means low development and maintenance costs for service providers, and low entry-costs for the users (only cost of connecting to Internet). The increased use of web services in other business areas is foreseen to spread also to the field of environmental monitoring and management. Hence, basing the MARSAS system on Java and other web technologies is timely, and will ensure viable solutions that can be further extended in years to come.

A prototype of such an Internet-based service chain has been implemented in the EC funded IWICOS project (Sandven, Hamre, et al., 2001). The Producer Server links the producer's existing production chain to the common Broker. It communicates with the Broker using specific small stub programs designed for the messaging between these components.

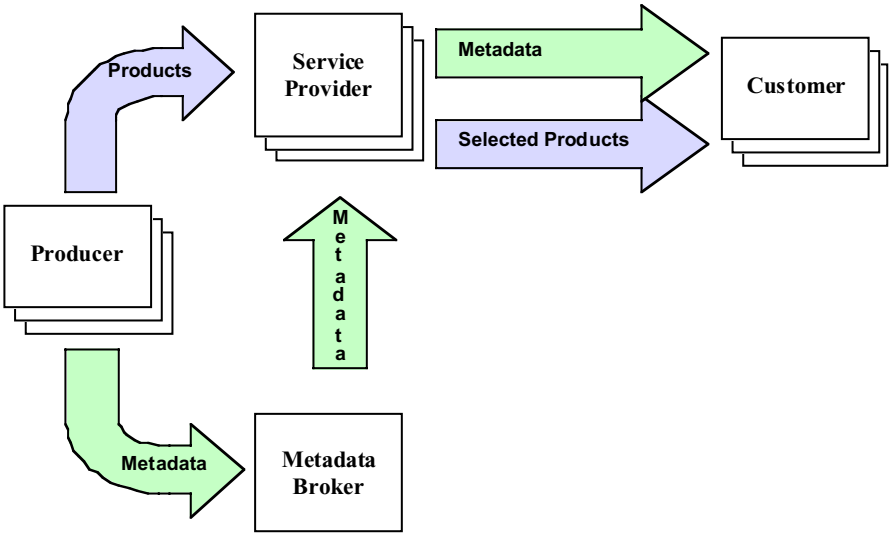

a) Service chain for marine SAR products

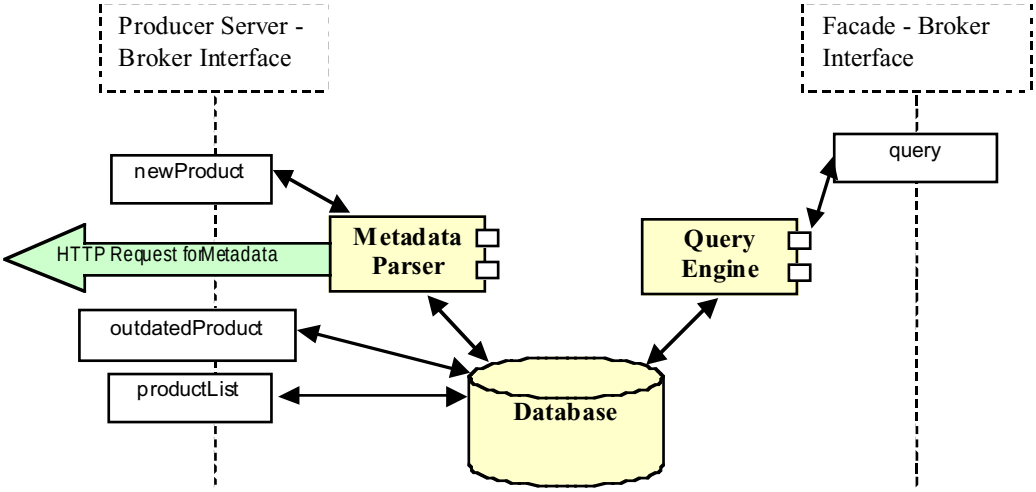

b) Broker internal structure.

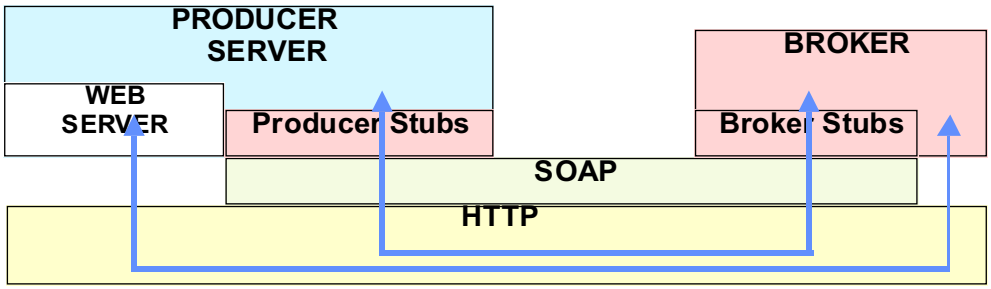

c) Producer Server and Broker stubs.

Figure 14. Overview of Internet-based system for delivery of marine SAR products.

The Producer Server consists of two parts:

- An active part, that informs the Broker of the events, such as a new product becoming available or an old product getting outdated, that occur in the production process.
- A passive part, that is basically a web server where the active part places it's output for the Broker (the metadata) and the Facades (the product data) to retrieve.

The set of data formats for the communication between the Producer Servers and the Facades was limited to Binary Sequential Files (BSQ), GRIB (GRIdded Binary), Shapefile, and XML for reducing the complexity of the implementation. Within the End-User Systems (Facade and Client Software pair) there are no such limitations. The Facades can use the base types listed above to generate products in any format. Basically the End-User System is a black box - the subsystems outside should and shall not be interested in what happens there.

The Broker provides two interfaces for metadata operations. One is intended for the Producer Servers for managing the Broker's metadata content. The other one is the query interface for the End-User Systems through which they can access the Broker's metadata content. The Broker was developed using freely available elements: the Apache Tomcat web-server, the Apache SOAP 2.0 implementation, the MySQL database, and Linux OS (RedHat). The service programs were written in Java.

The Broker is divided into three main components: the Database, a storage for metadata; the Metadata Parser, that will process the metadata descriptions of the new products and store them to DB for later access by queries; and the Query Engine that will interpret the queries posed in an XML format to SQL and execute them on the DB and return the results for the caller (see Fig14 b). The Broker communication is implemented with the Remote Procedure Calls (RPC) implemented over the Simple Object Access Protocol (SOAP). The RPC uses a small program called a *stub* in both ends of the communication, which will marshal the required parameters and return values of the call. Example of stubs is shown in Fig.14(c).

The Facade implementations can vary a lot. For a simple web-browser based client it will be closely integrated to the Client Software and it is hard to say where one begins and the other one ends. On the other hand it may be very complicated element containing reasoning of user needs based on a profile, product generation based on the products provided by the Producer Servers, and filtering of unnecessary components of products (e.g. layers with unnecessary data content). The Client Software is intended for presenting the acquired data and the implementations have a range from thin to thick clients. All types of clients (thin, balanced and thick) will probably be tested in the demonstrations during the project.

3.9 Links to other projects

The development of MARSAS system is linked to three EU-funded projects which are coordinated by NERSC: IWICOS (Integrated Weather, Ice and Ocean Service System) under the IST programme, MARSAIS (Develoment and Implementation of a Generic Marine SAR Analysis and Interpretation System for Applications to the Coastal Zones) and WEMSAR (Wind Energy Mapping by SAR) under the Energy, Environment and Sustainable Development programme. All projects have contrinuted to the definition of user requirements and system specification for SAR-based services. IWICOS is focused on developing a single-entry service for different monitoring and data products delivered by several service providers via Internet and by use of a common broker. IWICOS supports different end user systems, called clients. MARSAIS is focusing on algorithms and model development for marine SAR applications, including testing and validation. Parts of the MARSAS system will be further developed in MARSAIS. However, there are planned activities in this project which need additional funding, for example to develop a system where service providers allows users to run SAR algorithms via Internet. WEMSAR is developing use of SAR for wind resource mapping for wind energy companies. Focus of this project up to now has been to test and validate the CMOD wind algorithm in different regions of Europe.

Relevant reports:

MARSAIS Consortium: MARSAIS First Annual Consolidated Report – Scientific-technical Part, January 2002, 39 pp (see http://www.nersc.no/~marsais/).

Sandven, S, T. Hamre, et al., Integrated Weather, Sea Ice and Ocean Service System (IWICOS). Baseline System Report, NERSC Technical Report no. 204, 67 pp, December 2001 (see http://www.nrsc.no/~iwicos)

WEMSAR Consortium: WEMSAR Second Annual report - Scientific-technical Part, March 2002, 31 pp (see http://www.nrsc.no/~wemsar)

4. Results of Task 2: SeaWiFS monitoring of Algal Blooms

Task 2 aimed at the development of a capacity to monitor marine phytoplankton abundance and production from ocean colour and other satellite data. During the period 1999 – 2001, The Nansen Center has developed a system for near real-time processing, analysing and dissemination of information products derived from ocean colour and TIR data for the purpose of monitoring marine biological activity along the coast of Norway, with emphasis on possibly harmful algal bloom – (H)AB – identification and early warning.

This system HABIM, Near Real-time Harmful Algal Bloom Investigation and Monitoring System, is composed of two main modules: (1) a data processing modules, which aims at atomising the processing of EO data from level 1 (raw data) to level 2 (geophysical parameters), and (2) Dissemination and archiving module, which aims at posting and dynamically updating information products and related interpretation on the internet. The strategic institutional development of HABIM at the Nansen Center has been undertaken under various past and on-going project activities, starting with funding from the Norwegian Space Centre in 1998 and significant developments in the operational scheme under the ESA project "**DeciDe for near real-time use of ocean colour data in management of harmful algae blooms (**Decide-HAB), contract no. 13662/99/I-DC in 1999-2001 (Pettersson et al, 2001), as well as this project with the current project with the Norwegian Space Centre.

4.1 The HABIM background

The goal of HAB actions is *effective management of fisheries/aquaculture, public health, and ecosystem problems related to algae blooms*, including specific tasks such as:

1. Improvement of *in situ* sampling strategy.
2. Development of early warning and forecasting capabilities for the occurrence and impacts of harmful marine algae blooms.
3. Development of management and mitigation strategies to minimise the impacts of harmful algae.
4. Provision for rapid response to toxic and otherwise harmful marine algae blooms.
5. Identification and improvement of access to databases for bloom incidence, toxin occurrence in shellfish, mass mortality events, and epidemiology.

In this context, the HABIM system aimed to prototype an EO-based AB monitoring application with public user involvement. The application would be complementary to existing monitoring activities, and would contribute to the efficiency of the ongoing HAB monitoring activities.

4.1.1 Contribution of EO-derived information

Earth Observation (EO) data have proved valuable for early warning of some categories of algae blooms, and through use of information about ocean fronts, eddies and gradient zones, a more efficient field sampling strategy can be implemented. A remote sensing system designed to monitor and track the formation and decay of HABs may improve an eventual forecast capability that is necessary for the development of management and mitigation strategies for rapid response to algae blooms. In addition, routine monitoring data required for a forecast system would provide a database containing information about the algae species, location, frequency, and duration of HAB events. These data would support studies on the impacts of HAB on the fisheries/aquaculture industries, on public health, and for basic algae and oceanographic research. Information would be displayed through the World Wide Web to allow authorities, aquaculture industry, coastal managers, research community, educators and the general public easy access to the most recent information.
In order to improve understanding of the temporal and spatial distribution of blooms and ocean front zones, remotely sensed imagery is an important source of frequent, synoptic information of the surface layer conditions. Near real-time (NRT) extraction of this information may be put to practical use in monitoring procedures for algae blooms and other oceanographic processes. In this respect EO techniques are identified to support the current command chain through:

- *detection and monitoring of the distribution of photosynthetic pigment concentration, which is an estimate of phytoplankton biomass, using time-series ocean colour EO data sources;*
- *detection and monitoring of ocean fronts through use of sea-surface temperature (SST) imagery;*
- *contribute to an earlier warning of algae blooms (harmful or not) and to the understanding of the factors that influence the initiation of a bloom;*
- *identify, to a very limited extent, the phytoplankton categories, e.g., discrimination of coccolithophorid blooms (not harmful) from areas with other algae blooms.*

Although multi-spectral Earth observation sensors can be used to detect the optical characteristics of chlorophyll *a* and other pigments that characterise algae, efforts have been constrained by the limited ability of the present sensors to discriminate phytoplankton populations at the or even family level. This is, of course, a fundamental requirement of a HAB monitoring program [Anderson *et al.*, 1995]. However, integrated use of EO with other sources of information on HAB species (primarily field observations) and their exact concentration will increase the value of the complementary information sources.

Due to the limited active movement of phytoplankton, most blooms are passively advected with the water masses. The main progress has been made first linking specific water masses to a bloom event, and then to identify and track these water masses with an appropriate remote sensing technique. In particular, remotely sensed sea surface temperatures (SST) have been used to follow the movement/advection of fronts, currents, water masses or other physical ocean features where phytoplankton accumulate. Pettersson *et al.* [1992] used SST data from the NOAA AVHRR weather satellite to monitor the advection of the harmful *Chrysochromulina polylepis* bloom in the waters of southern Norway, in 1988 [Dundas *et al*, 1989].

In August 1997 Orbital Sciences Corporation (OSC) launched the OrbView-2 satellite, carrying the Sea-viewing Wide Field-of-view Sensor (SeaWiFS). The SeaWiFS sensor was designed to measure ocean colour in eight spectral bands, covering the spectral variation of water-leaving radiance related to concentrations of phytoplankton pigments, coloured dissolved organic material, and suspended particulate material [Hooker et al., 1992]. NASA funded the instrument development and purchased the right to use SeaWiFS data for academic research. Scientific investigators wishing to use imagery must register with NASA (http://seawifs.gsfc.nasa.gov/ SEAWIFS/LICENSE/checklist.html). NASA licenses permit SeaWiFS data to be supplied in "near-real time" to support oceanographic research cruises for sampling of validation data. For all other research use there is a two weeks embargo on the scientific use of the data. For commercial and other regular near real-time applications SeaWiFS data are distributed on commercial terms by Orbimage Corp.

This type of visual/optical and IR satellite EO sensor typically covers a swath width of some hundred to thousand kilometres. The swath width covered is a trade-off of the spatial resolution of the data, which typically are between some hundred meters to approximately one kilometre. For SeaWiFS the swath width is 2800 km and the spatial resolution 1.1 kilometre. The orbital repeat coverage of the same location is usually several times per day, but for EO data in the visible spectral range, which are dependent on solar illumination conditions, one or two potential useful orbits per day may be available at high latitudes. Thermal infrared EO data are also applicable during night passes and typically four passes are acquired per day. These spatial and temporal scales for coverage of information are warranted because oceanographic features that initiate blooms and the blooms themselves occur at such scales. However, cloud cover and haze prevents the use of optical and infrared satellite sensors to observe the surface of the earth.

4.1.2 The Applications of ocean colour EO data – Chlorophyll-a and other Pigments

The photosynthetic pigment in phytoplankton cells, chlorophyll *a*, alters the ocean colour from that of pure water. Multi-spectral ocean colour EO instruments can detect these colour changes from their orbit in space. However, deriving the chlorophyll concentration is not a straight forward task, with common validated solutions. The parameter retrieval requires complex atmospheric correction algorithms, particularly in order to retrieve with acceptable accuracy the water-leaving signal, which accounts for less than 10% of the total signal reaching the satellite sensor. Moreover, determination of the phytoplankton species and their harmfulness requires additional laboratory analysis of water samples.

According to the requirements to HAB information the most relevant EO information is related to the so-called "water quality" parameters. This includes information on the physical, biological, ecological and chemical conditions of the ocean water (Table 4.1). These water quality parameters are usually derived via intermediate parameters, which are directly measured by ocean-colour remote sensing instruments. Retrieval models and other *a priori* information are needed to derive water quality parameters.

Table 4.1: Basic physical, biological, ecological and chemical parameters observable by multi-spectral satellite earth observation sensors.

Parameters	Intermediate parameter	a priori information required
water transparency	*a, b, c,* K_d	hydro-optical model(1) or statistically-significant correlation between an up-welling radiance ratio and K_d
water colour	*R*, colour co-ordinates, dominant wavelength, colour purity	hydro-optical model
Chlorophyllous pigments	a	hydro-optical model
Auxiliary pigments	a	hydro-optical model
Primary production rate	C_{chl}	vertical profiles of major optically active components, area specific primary production model parameters
Suspended sediments	C_{sm}	hydro-optical model
Dissolved organic carbon	C_y	hydro-optical model

(1): hydro-optical model is defined as *a priori* information as it is based on *a priori* knowledge of the inherent and apparent optical properties of the water.

The basic technical terms for some of the key ocean optical parameters (used in Table 4.1) include:

a, b, c	are the coefficients of absorption, scattering and attenuation of light by bulk water
K_d	is the coefficient of down-welling irradiance diffuse attenuation
R	is the water volume reflectance
C_{chl}, C_{sm}, C_y	are the concentrations of chlorophyll, suspended minerals and coloured dissolved organic matter (yellow substance), respectively

Atmospherically corrected SeaWiFS data provide normalised water-leaving radiance at five key wavelengths in the visible region of the spectrum. These basic measurements are used to derive products including chlorophyll *a* concentration as a proxy of phytoplankton biomass parameter (Fig. 15) the diffuse attenuation coefficient at 490 nm as an indicator of water transparency, and water reflectance.

Advantages:

SeaWiFS images provide data with a horizontal swath width in the order of 2800 km with spatial ground resolution of 1.1 km; nominal repeat coverage of an area occurs approximately every day at high latitudes (60°).

Limitations:

(a) Useful data are dependent on cloud-free conditions to detect the ocean surface signal.
(b) Algorithms to derive phytoplankton pigments from the ocean colour signal are still a field of significant research, requiring improvements in accuracy particularly for coastal waters.
(c) Spatial resolution (1.1 km) of currently available sensors is too coarse for near coast and fjord observations.
(d) High chlorophyll *a* concentrations do not necessarily indicate a harmful bloom and currently no species-specific algorithm to determine harmful algae blooms from water-leaving radiance

has been developed, however identification of Coccolithophorid blooms have been successfully performed [Pettersson *et al.*, 1995].

(e) Only surface layer characteristics are visible to satellite sensors, and a deeper sub-surface bloom may be hidden.

Currently, SeaWiFS has a two-week embargo on data availability that limits near-real-time access to data unless commercial prices are paid for the data.

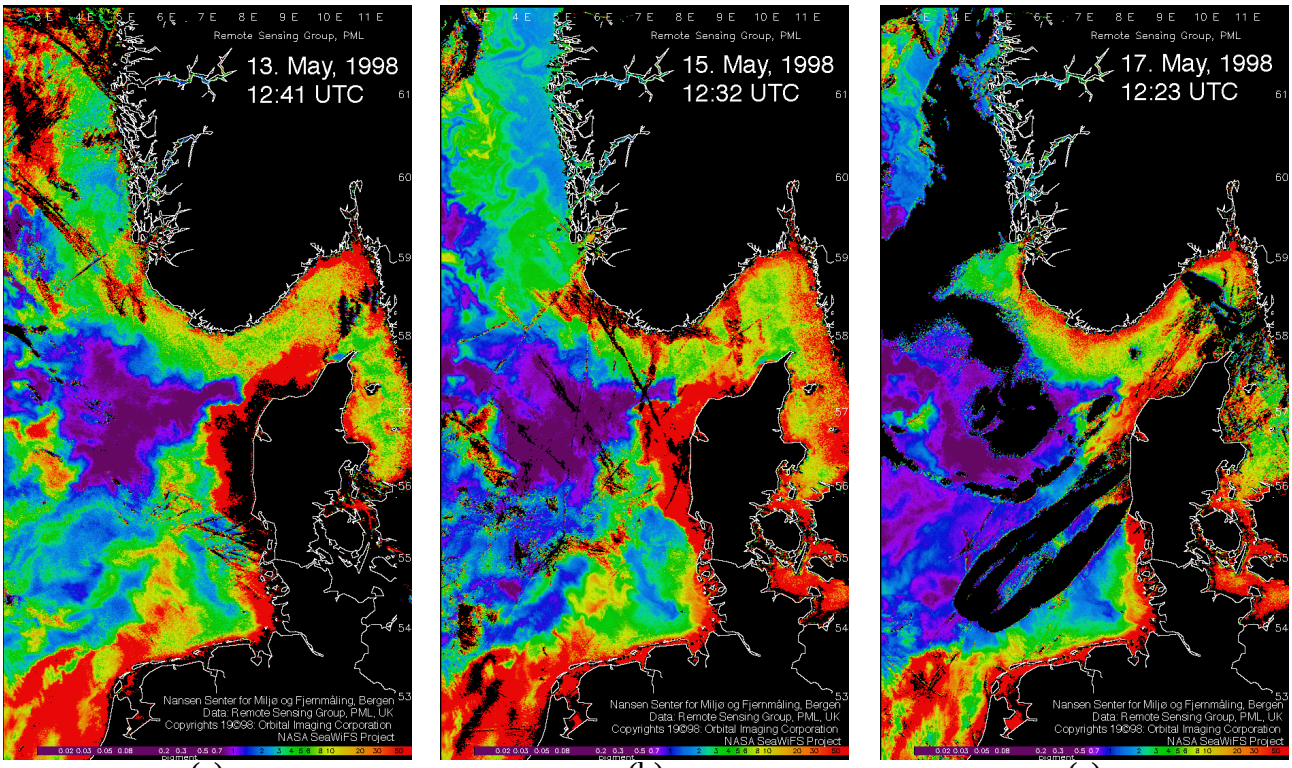

(a) (b) (c)

Figure 15. Chlorophyll pigment concentration product from SeaWiFS over the North Sea and the Skagerrak, on (a) May 13, (b) May 15 and (c) May 17, 1998. © Orbital Imaging Corps and NASA SeaWiFS project. The time series shows the increases and demise of a Chattonella spp. bloom, along the Danish coast. Blue indicates low pigment; red indicates high pigment. Data courtesy: Remote Sensing Group, Centre for Coastal and Marine Sciences – Plymouth Marine Laboratory.

4.1.3 EO applications in coupled bio-physical forecasting models

The use of coupled 3-dimensional biogeochemical and physical models in algae bloom monitoring systems is still at a research stage, and routine use of such models is not implemented operationally. However, during HAB alert events, research models in combination with regular ocean forecasting models of the meteorological service have been used to predict HAB development.

Since the algae can be considered as a "passive tracer", a good physical model simulation the advection of the water masses will provide useful short-term transport predictions of the movement of an algae bloom. Most biogeochemical models include only a few functional groups of algae and the model developed and used by Institute of Marine Research (IMR), the NORWegian Ecological Model system (NORWECOM) (Aksnes *et al.*, 1995; Skogen *et al.*, 1995; Skogen and Søiland, 1998), includes two such functional algae groups - diatoms and flagellates. Most harmful algae species belong to the flagellate group and thus the modelled flagellate concentrations may be used as a proxy for the harmful algae species during HAB events. However, due to insufficient knowledge of the bloom triggering factors, the NORWECOM model (as is the case with most other numerical models of this kind) is not able to predict the occurrence in time and space of a bloom of a specific species. Thus, the interpretation of the model predictions is strongly dependent on other observations, which can be used to initiate the occurrence and extent of the bloom in the model system. This was the case during the *Chattonella* bloom in the North Sea and Skagerrak in May 1998. During the bloom event the NORWECOM model was run in real-time and used as one of several tools, including satellite EO data, in monitoring of the bloom development and decay. The model results were very useful in combination with *in situ* observations and satellite data of the bloom region. Importantly, the model was able to forecast bloom development including the growth and movement of this large harmful algae bloom to the threatened region 48 hours into the future.

IMR performs model simulations and forecasting of algae bloom spreading and advection during emergency bloom situations, using their "Norwegian Ecological Model (NORWECOM)" tool. Due to insufficient knowledge of the mechanisms that triggers the initiation and development of algae blooms, the current model is not able to predict the initiation of new bloom developments. The forcing and interpretation of the model results is thus strongly dependent on other observations from *in situ* or EO sources to initiate the bloom situation in the model.

Integration of satellite-derived bio-physical parameters, such as sea surface temperature and chlorophyll pigment concentration, with the numerical model is a way to improve its forecasting capability. In particular, a recent study reports that even if NORWECOM was able to qualitatively reproduce the *Chattonella* bloom in 1998 [Lekve, 1998], the quantitative estimates were far from the *in situ* observations of the bloom [Durand *et al.*, 1999b].

Integration of chlorophyll *a* distribution map based on EO and *in situ* information sources, as a biological field after the physical model spin-up could constrain the model with unbiased data, and thus improve the quantification of the model variables. More advanced coupling between EO data and model can be achieved through a data assimilation scheme, which performs a dynamical and controlled adjustment of the model variable as a function of time [Evensen *et al.*, 1997].

4.1.4 Validation and Accuracy

Naturally EO-derived parameters need to be validated against *in situ* high-accuracy measurements used by the current service. Practical realisation of this is a scientific challenge, due to the different observation characteristics of the two types of data sources. The various algorithms developed for retrieval of in-water parameters from ocean colour data have been validated. A general summary of the quantitative achievements of EO techniques regarding the geophysical parameters of relevance of AB monitoring is given in Table 4.2. The values indicated in the table correspond to the best results expected under favourable observation conditions.

Table 4.2. Quantitative achievements of state-of-the-art ocean-colour algorithms relevant to use in ALGEINFO. The values reported in the table result of a compilation of various algorithms, and are representative of the best achievement that can be expected for EO [revised from Durand et al., 1999a].

Remotely sensed derived parameters		Algorithms		Satellite / sensor		
	Units	Range of value	Relative/ absolute accuracy	Spatial resolution (km)	Frequency of sampling (days)	Delay* (days)
Water constituents						
C_{chl} [Chl-a]	$mg.m^{-3}$	0.01 - 60	30 - 40 %	1.1	1	NRT
Primary production	$gC.m^{-2}.d^{-1}$	0.5 - 3.0	40 %	1.1	1	NRT
C_{sm}	$mg.l^{-1}$	0.1 - 30	30 - 50 %	1.1	1	NRT
C_y / a_y(380 or 440 nm)	$mgC.m^{-3}$	0.1 - 20	50 %	1.1	1	NRT
Optical properties						
Absorption coef.: a	m^{-1}	all	NS	1.1	1	NRT
Scattering coef.: b	m^{-1}	all	NS	1.1	1	NRT
Diffuse attenuation: K_d	m^{-1}	0- 6.5	0.1	1.1	1	NRT
Turbidity/Secchi depth	m	0.25 - 5.0	50 %	1.1	1	NRT
Surface Temperature						
SST	℃	all	Rel. 0.2°C	1.1	<0.5	NRT

***Delay**: Time delay of availability of products, **NS**: not specified, **NRT**: Near real-time

4.2 The HABIM Approach

Within HABIM, a pre-operational system for integrated use of EO information products in the existing operational AB-monitoring command chain was specified, designed and implemented. A demonstration period was carried out from the middle of April to the end of June 2000, followed by a pre-operational phase during spring 2001. Near-real time EO imagery and information have been made available on a daily basis (dependant on the cloud cover conditions) for use in the monitoring of AB events in the waters of Norwegian interest – including the up stream Danish and Swedish waters surrounding the North Sea and Skagerrak/Kattegatt area. Value-added information products were provided for regular scientific users in support of their decision making process and field data sampling during eventual HAB situations.

In this section we describe the design structure and the main products and tools for the HABIM service support to the existing Norwegian ALGEINFO system.

The general outline of the scheme (Fig. 16) adopted for the EO data implementation and the associated overall information flow, was developed in terms of four main modules:

1. EO Data provision
2. Value-adding
3. Distribution and dissemination of service products and information
4. Interaction with and within the decision support system

In the regular ALGEINFO Service, phytoplankton cell counts and algae taxonomy are adopted as suitable parameters for characterisation of (harmful) algae blooms. Both regular and dedicated cruises are carried out under the general IMR monitoring programs, for *in situ* measurements of a number of biogeochemical parameters relevant for HAB monitoring. Sampling and analysis for chlorophyll concentration depth-profiles, phytoplankton cell counts, nutrient concentration, suspended sediment, numeration and identification of algae species are performed both during these cruises and from near shore station locations. The near real-time availability of this information is however limited to certain parameters, since other parameters require further analysis in the laboratory (e.g. algae cell counts and pigment concentrations). Regular monitoring cruises are organised along the southern coast of Norway and across the Skagerrak between Norway and Denmark during the bloom period from April to July, each year. The data sets collected during these campaigns will be delivered to NERSC for use in the validation and tuning of EO-derived parameters, used in the analysis performed within this project.

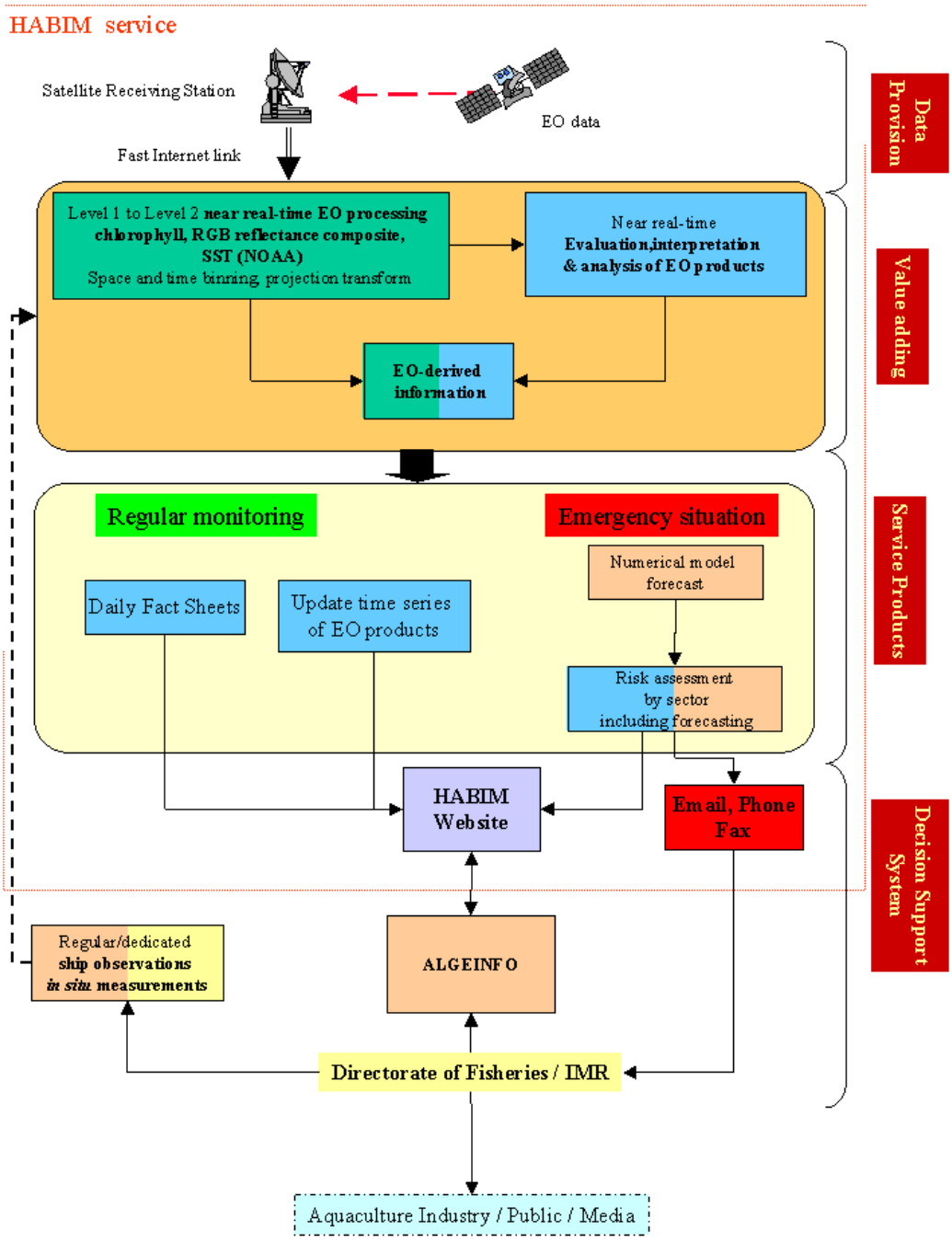

Figure 16. Information flow and principal modules of the HABIM service (red dotted area).

4.2.1 Summary of Service capability

We give in Table 4.3 a synoptic summary of the maturity and current status of the support service as by the end of the project period.

Table 4.3. Current status of the HABIM service

Service component	Status and Performance
Products	
Information content	Maps of sea surface temperature and chlorophyll-a concentration from r4spectively AVHRR and SeaWiFS imagery. Additional derived products (RGB ocean colour composite, Diffuse attenuation – K490) may be used to help in interpreting algal bloom events and ocean surface features. Daily report on algal bloom events based on analysis of time series of satellite data and possibly additional *in situ* information (currents, wind, *in situ* measurements of chlorophyll concentration and cell count.
Accuracy	SST maps accuracy: 0.5 °C Chlorophyll-a maps: 30 to 100 % depending on applied algorithm and ecosystem status.
Algorithms	SST maps split-window method. Chlorophyll-a maps in near real-time: black pixel assumption for atmospheric correction and NASA OC-2 algorithm for in-water processing. Re-analysed chlorophyll-a maps: Atmospheric correction: either black pixel assumption with iterative approach for determination of aerosol parameter or bright pixel assumption (MUMM algorithm – Ruddick *et al.*, 2000) In-water processing: OC-2 algorithm or Levenberg-Marquardt inverse approach.
Functioning	
Availability	Access to SST maps and short report opened to anyone Access to SeaWiFS-derived products and detailed analysis restricted to NASA authorised SeaWiFS data users. In case of identified risk, direct contact with authorities through phone, fax and/or email.
Timeliness	The service has proven timely with regards to the *Chattonella* blooms in 2000 and 2001.
Reliability	*Identification of new algal bloom event*: The HABIM system has proven to be quite reliable for identifying high-biomass algal bloom. Although no information is provided on the possible harmfulness of the bloom, and limited accuracy on algal concentration is obtained. *Monitoring of identified bloom and HAB*: efficient monitoring of the development, propagation and decay of bloom has been demonstrated.
Service component	**Status and Performance**
Supply chain	
Distribution performance	Information is provided on a daily basis. A delay of 6-hr or better is routinely ensured between data acquisition and information provision on the web site.
Automation level	The entire acquisition and processing chain and web-site updating are automated. Analysis may be performed online using image visualisation and navigation tools available through the web-site. Reporting may be performed online through the web-site by authorised persons.
Packaging of information	Daily information is provided through two main web-pages for SST and SeaWiFS-derived maps respectively. Links to additional information, such as outputs of model simulation and forecasting is provided when appropriate and/or available.
Benefit	
Cost effectiveness	So far, cost effectiveness has been ensured by free-of-charge provision of satellite data to the project. Service operation and maintenance requires a half-time appointment. The level of automation that has been reached, ensure now the work to be focused on analysis and information provision, instead of administration and web-site development routines

Table 4.3 follow-on

Competitiveness	The service has no competitors in its category (remote sensing based information provision), A number of other HAB-related "services" and information suppliers exists indeed. The information provided is either based on *in situ* sampling, ship-of-opportunity, remote sensing or modelling. However none of them has up to now reached the level of HABIM in terms of automation and near real-time access to the information.
Customer readiness	
Awareness	The HABIM service has received a good echo in the local and national press with a couple of articles published during the *Chattonella* bloom in March 2001. The project was first restricted to Norwegian authorities in charge of HAB monitoring (Directorate of Fisheries and Institute of Marine Research). The restricted area is now accessible to twenty operational and science users originated from 6 European counties. The web-site receives 10 daily connections in average, with peaks to more than 200 connections during HAB events.
Acceptance	Based on the demonstrations provided by the HABIM project the Directorate of Fisheries view the satellite EO imagery and the modelling results received as an essential part of the monitoring and emergency handling of algae blooms in coastal Norwegian waters. Since NERSC takes part of the daily steering and advisory meetings during crisis monitoring.
Practices	Registered users seeks for information on the web site every two weeks in period of regular monitoring and in average every two days during HAB events.
Customers	National Authorities in charge of HAB monitoring, Research centers in environmental study, Civil-engineer school, Defence Department, Space Centers.

4.2.2 The technology behind HABIM

HABIM makes used of several software solutions in order to achieve its goals and constraints (see Table 4.2 above).

A scheme presenting these solutions is given in Fig. 17. Processing of satellite ocean colour data is performed using SeaDAS, the NASA processing package. This package has been developed on IDL advance programming language. It gives the main advantage to enable the automation of the processing through simple scripts and small programmes. A number of such programmes have been elaborate during the project in order to ensure the near real-time processing of SeaWiFS data. More details on applied algorithms are given in the following sections.

The management (creation, update, archive, links) of web-pages is controlled by shell scripts, CGI applications and javascripts. More advanced dynamical solutions will be implemented in the future (Perl and java scripts).

4.2.3 The EO data Information Flow

A main requirement on the EO based information and service implemented under the HABIM project was the time delay of accessibility to user friendly information products. According to the HAB user authorities a delay of up to two days from the data acquisition to the delivery of information was acceptable under regular monitoring conditions, however earlier delivery will improve the current time lag in the provision of information. Value-added and aggregated EO information products is also essential in order to match the requirements of easy use and analysis within the existing monitoring activities. The personnel involved in these operations have limited experience and time available to analyse and digest the additional information from the satellite EO data sources. Hence, easy access and availability as well as information delivery within 24 hours could bring a significant improvement of the existing system in term of its early warning capabilities for HAB events.

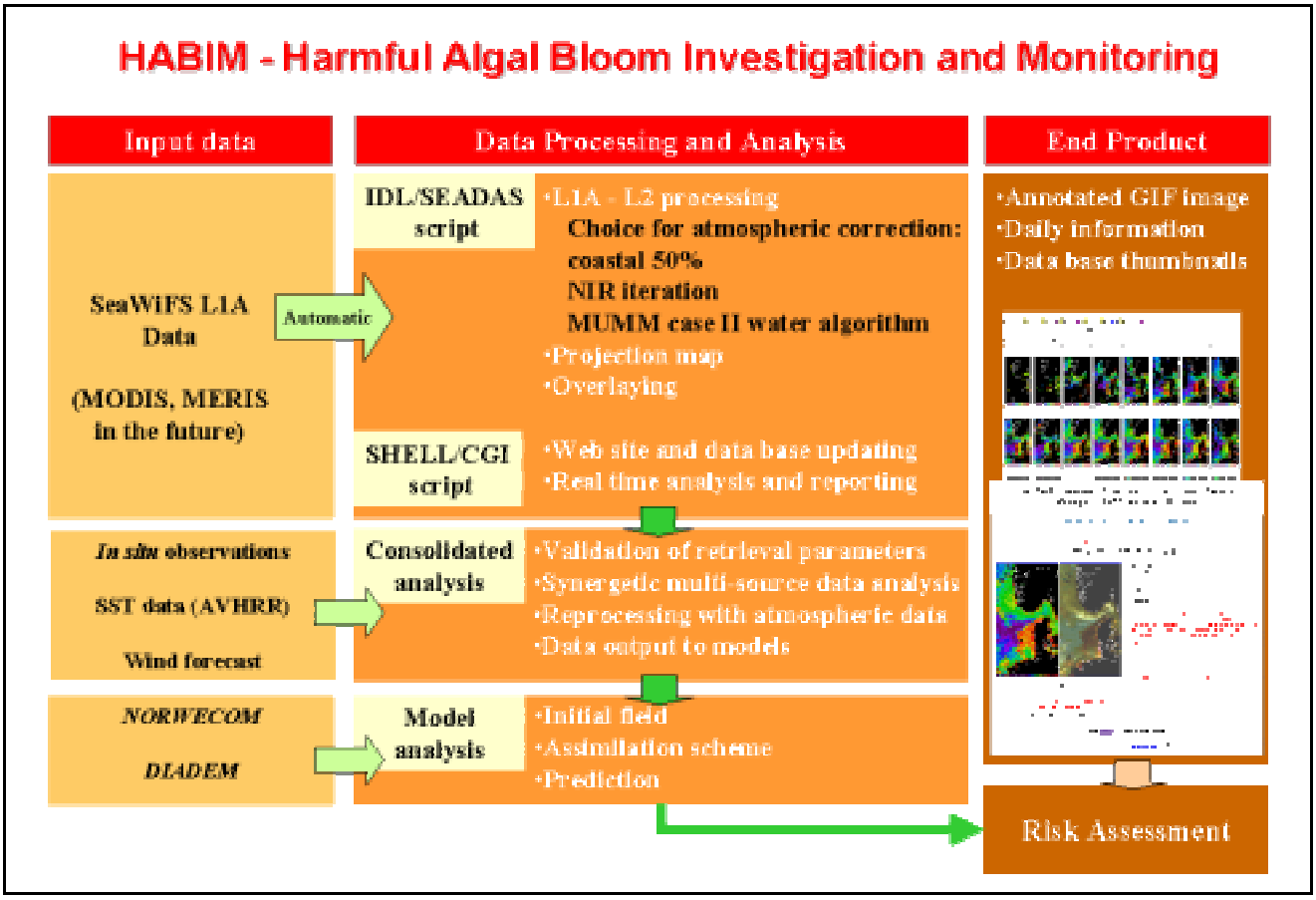

Figure 17 Data flow and technology adopted in the frame of the implementation of the HABIM service.

The success evaluation criteria for the implementation of HABIM depends on four main components:

1. Availability of EO data, i.e. acquisition and transmission of the data by the satellite system; real-time pre-processing and transmission of validated information products by the receiving station to the HABIM project team.
2. Efficiency of the system implemented within HABIM project.
3. Appropriate definition and dissemination of the project concept, implementation and main information provided.
4. Feedback from HAB Management authorities to the HABIM Project in terms of service evaluation and provision of *in situ* validation data.

The key elements and modules of the HABIM service include (Fig. 17):

- Provision of various EO data products through the existing UK infrastructure for near real-time satellite data acquisition at the University of Dundee.
- Value-adding processing of information products, including standard SeaWiFS and AVHRR data products, dedicated product generation and expert analysis and interpretation of integrated information from EO and other data sources.
- Service provision and information products. This part of the service has been operated in various modes according to the level of operations (regular service or the two levels of emergency HAB situations). The various products and information sources are updated regularly during the period of the services operations.
- Information dissemination and interactive contact with the decision support system (ALGEINFO). In order to assure introduction and use of value-added EO products and information the dissemination links has been based on a web-site distribution as well as direct interaction and contacts with the personnel (from IMR and Fishery Directorate) involved in the support system for HAB events.

Real-time data transmission

The demonstration service relies on an existing operational satellite data acquisition service performed by the National Environment Research Council (NERC) funded Dundee Satellite Receiving Station (DSRS) at the University of Dundee, and the Plymouth Marine Laboratory (PML). The ocean-colour service is based on the daily acquisition of SeaWiFS data from the US Orbview-2 satellite. The receiving station of the University of Dundee provides an operational service and real-time dissemination of various satellite based EO data to specific value-adding entities, including PML.

DSRS receives and archives SeaWiFS and AVHRR imagery over the UK and European shelf seas and north-east Atlantic Ocean. The Remote Sensing Group at the PML undertakes the processing for the UK research user community, and for foreign customers under special agreement and contracts. SeaWiFS images are converted into level 1 HDF format while AVHRR remain in the raw HRPT format and are then transferred automatically at 2 Mbit/s over the UK academic network. L1 and L2 products are sent to NERSC for further processing and interpretation. At NERSC an automated data processing system checks for the arrival of an image and starts processing usually within five minutes of pass reception. Most of the processing is automated in order to ensure an operational provision of data seven days a week and twenty-four hours a day.

The EO data preprocessing

Ocean colour processing

The ocean colour is governed by the optical properties of seawater together with suspended particles (organic and inorganic) and coloured dissolved organic matter (CDOM). Phytoplankton absorb sunlight, required for photosynthesis, through pigments with 95% of the light absorbed by chlorophyll-a, b, c, photosynthetic carotenoids (PSC) and photoprotectant carotenoids (PPC) which are grouped together as the total pigments (Aiken *et al.*, 1995). As the phytoplankton concentration increases the reflectance in the blue decreases (due to the absorption of chlorophyll-like pigments over a broad wavelength band) and the green increases slightly, and a ratio of blue to green water reflectance can be used to derive quantitative estimates of pigment concentration (Clarke *et al.*, 1970). CDOM reduces the reflectance as it causes significant absorption in the ultraviolet and blue wavelengths relative to those in the red. Suspended particulate matter (SPM) enhances reflectance because of the particle backscattering that is inversely related to wavelength, is strong in the blue and then decreasing in influence through the spectrum.

The IOCCG Working Group (1998) recommended that a chlorophyll retrieval algorithm for satellite EO data should utilise wavebands at 555 or 560 nm and 443 nm and an additional waveband at 410 nm to account for CDOM absorption. SeaWiFS uses an algorithm based on the 490/555 band ratio and a cubic polynomial fit based on the SeaWiFS Bio-optical Algorithm Mini-workshop (O'Reilly *et al.*, 1998). The 490/555 ratio is used, rather than the 443/555 ratio, as it is more linear in log-log space when compared to chlorophyll-a. This is because the CDOM absorption is lower at 490 compared to 443 and there is usually a strong correlation between the chlorophyll-a and carotenoids, which are the main absorbing pigments at 490 nm, (Aiken *et al.*, 1995). The coefficients have since been updated, due to the addition of data sets, and the algorithm used at the start of the project was Ocean Chlorophyll 2 version 2 (OC2-v2). This was replaced by OC2-v3, see equation 3, which has additional data from chlorophyll-rich (greater than 10 $mg.m^{-3}$) waters (O'Reilly *et al.*, 1999). In 2000 a new 4-band algorithm (OC4) was implemented in SeaDAS.

For SeaWiFS data, the processing uses a combination of the NASA SeaWiFS Data Analysis System (SeaDAS) and additional IDL code developed at NERSC (Fig. 18). The average processing time for a SeaWiFS image is approximately 120 minutes (on a dual processor Sun Ultra-2), and includes placing the final products on the World Wide Web (http://www.nersc.no/HAB) for immediate browsing. SeaDAS is primarily designed for processing data of the so-called Case I waters (mainly open-ocean conditions), where the optical properties are dominated by phytoplankton and associated by-products. Many European coastal waters are of the so-called Case II, where the optical properties are determined by either SPM or CDOM, and frequently by a combination of SPM, CDOM and phytoplankton. HABIM has additional atmospheric correction algorithms, specifically designed for SPM dominated "bright pixel" waters where the near-infra red water-leaving radiance can no longer be taken as negligible and the Case I atmospheric correction (dark pixel) method fails (Ruddick, *et al.*, 2000)

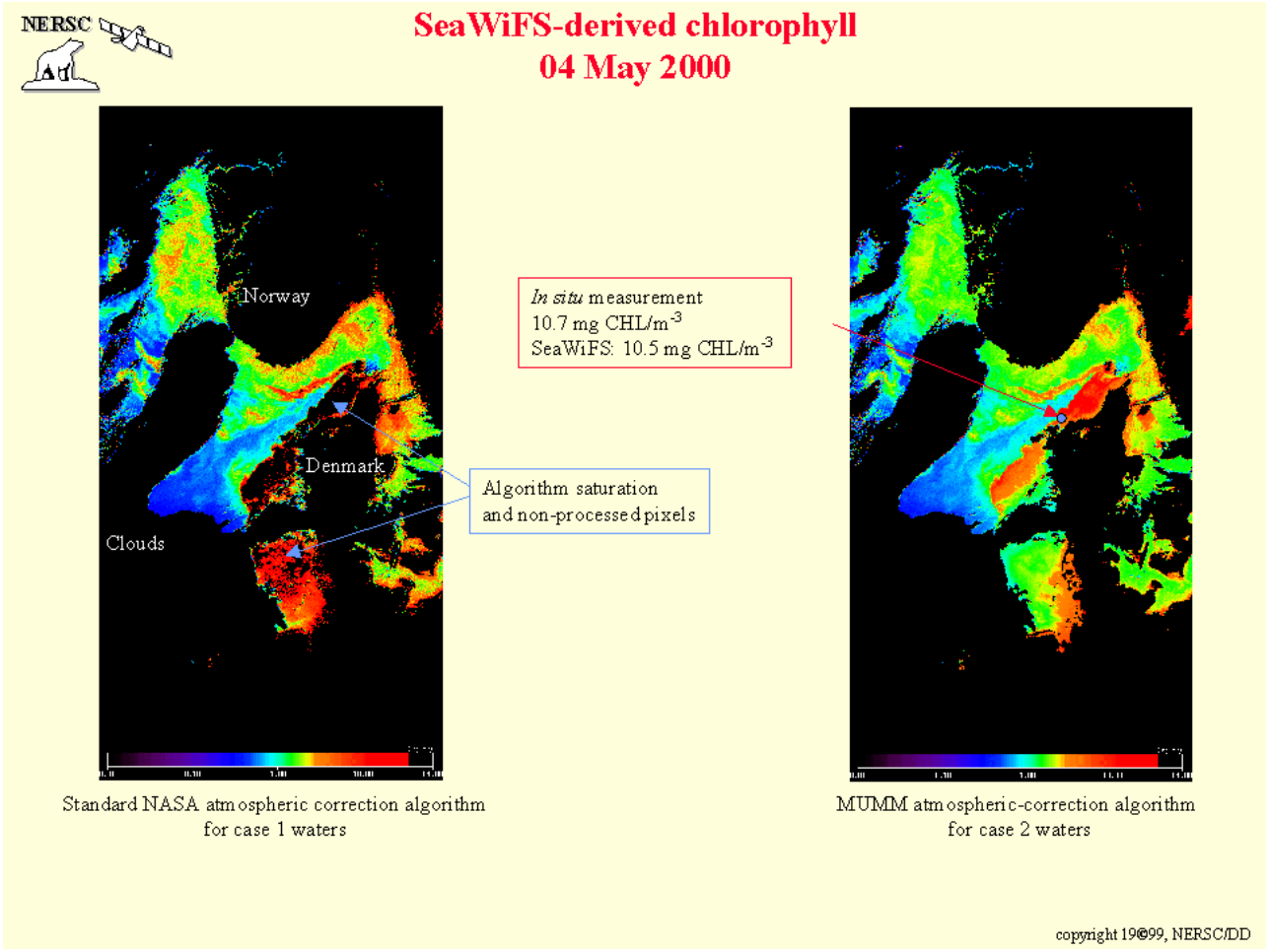

Figure 18 Chlorophyll-a concentration as retrieved from SeaWiFS data (04 May 2000) by (left) the standard NASA algorithm, (right) Ruddick, et al. (2000) case II atmospheric correction algorithm.

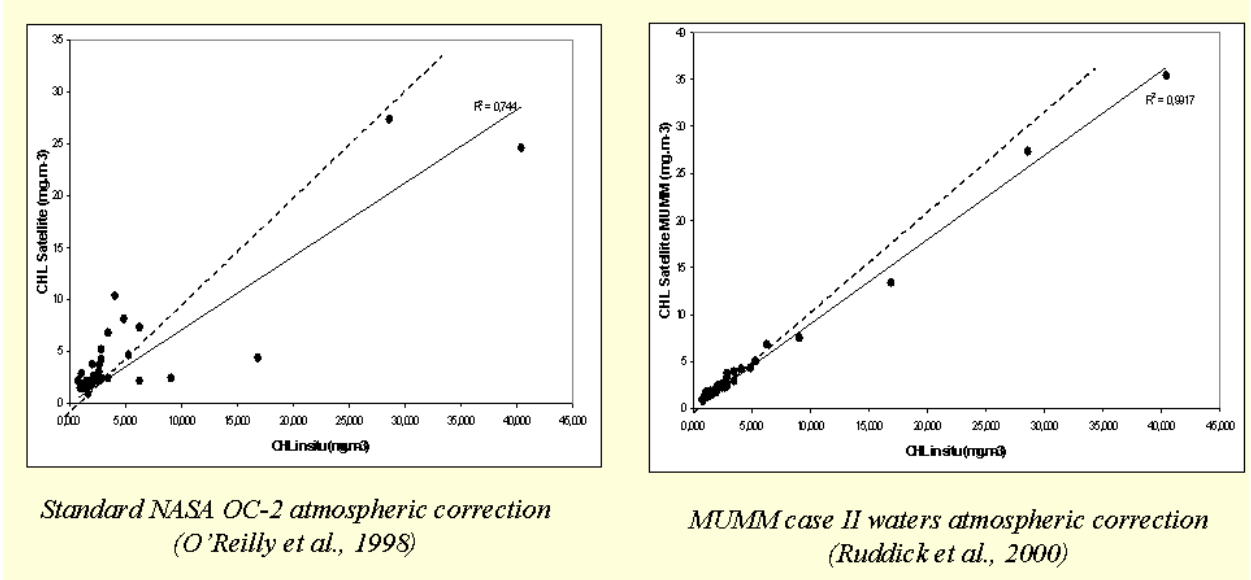

Figure 19 Validation of retrieved chlorophyll against in situ data (data courtesy of Institute of Marine Research, Bergen). (Left) standard NASA algorithm, (right) Ruddick, et al. (2000) algorithm.

Atmospherically corrected level 1 data are used to produce level-2 biological and geophysical products: water-leaving radiance at five visible wavebands (412, 443, 490, 510 and 555 nm); derived products including chlorophyll *a* concentration, diffuse attenuation coefficient at 490 nm, several atmospheric parameters determined during the atmospheric correction procedure.
In summary, the HABIM SeaWiFS processing follows the following pathway:

- Data extraction of individual bands.
- Geolocation using an orbital model and GPS data from the on-board GPS system.
- Calibration of visible bands followed by calculation of water leaving radiance and biological or physical quantities, such as chlorophyll concentration or attenuation at 490nm
- Mapping of images to pre-selected geographical areas specified in a database with added latitude/longitude marks, annotation, temperature scale etc.
- Production of images in GIF or TIF format and storage on the WWW server.

The HABIM system produce both colour GIF file for easy and quick visual interpretation of algae bloom situation, as well as Black-and-white 8bits GIF files from which numerical values of chlorophyll concentration can be retrieved from further numerical analysis and evaluation.

For the HABIM project the geographical area extended initially from 02°E to 12°E, and from 52°N to 62°N and were in 2001 extended eastward to 13.5°E in order to cover the entire Kattegat region. At this latitude the optimal SeaWiFS over-flight occurs between 11.00 AM and 14.00, with respect to the orbiting cycle. Therefore, a first analysis of daily acquisition is made available in the evening of the day of acquisition. The entire processing chain has been automated for operational purpose.

EO Data Value-adding
The GIF maps and L1 data are automatically down-linked using the FTP protocol from PML to NERSC in order to disseminate the value-added information through official HABIM web site (www.nersc.no/HAB). The EO data acquisition and automatic processing is nominally performed within less than six hours after data transmission by the satellite, allowing for analysis of the data during the evening of the day of acquisition.

A two-level analysis process has been implemented at NERSC. The first stage comprises near real-time visual analysis of the SeaWiFS level-2 data products and includes:

1. an overall evaluation of the data quality, including cloud cover detection and rejected pixels;
2. interpretation of algae bloom situation in term of chlorophyll-a pigment concentration from individual pass images and time-series of change detection;
3. in case of detection of high chlorophyll values, analysis of RGB composite and SST images in order to reduce ambiguity on the nature of the high pigment concentration (necessary in case II waters);
4. Generation of a short analysis report of the bloom situation that summarises the bloom situation as interpreted from EO and other information sources. This report also takes into account the historic development of the situations from the previous observations. The report should include identification of water masses of different origin, ocean fronts and features and the actual pigment distribution, using both SeaWiFS, AVHRR and other information sources.
5. Eventually, inform the users and the HAB command chain directly, via dedicated e-mail or telephone messages, of the detection of extensive (potentially harmful) algae blooms or other significant changes of features of importance.

A second-level analysis is undertaken in case of identified harmful algae bloom situations. This level of investigations will then include a more detailed analysis of the satellite-derived pigment concentration, synergetic analysis with other source of information (*in situ* observations, meteorological conditions, EO data reprocessing with Case II water algorithms, model simulations, user reports, other source of EO data, etc.). The goal of this detailed analysis is to generate an overall risk assessment map for the investigation area as well as providing direct advises for further *in situ* acquisition of information (e.g. planning of dedicated cruise activities).

4.2.4 The HABIM Products and Information Dissemination

The service products depend upon the environmental situation, i.e. regular monitoring or emergency situation (algae bloom alert) efforts. Different types of existing and modified products have been evaluated, which are targeted toward different group of potential users, e.g. HAB information users: HAB management authorities, aquaculture industry, monitoring scientists and public media. However, in the context of HABIM and of the command-chain for decision making in management of HAB in Norway, the users of the system are primarily the Directorate of Fisheries and the Institute of Marine Research, located in both Bergen and Flødevigen. The personnel involved in HAB management at these institutions are generally scientists and/or staff with good knowledge on environmental monitoring and data sample analysis, mainly marine biologists and oceanographers.

EO products during regular monitoring

The regular monitoring system, the direct user access and the dissemination of the standard EO products has been performed through the dedicated HABIM web-site established at http://www.nersc.no/HAB. The WWW interface provides easy access to daily AVHRR-SST and selected SeaWiFS products, and interpretation reports of the situation related to HAB. Potential users must register with the system (via a WWW page) and their details are entered into a database, which is configured to provided access to only certain areas and products.

During the project demonstration phase, the Nansen Center performed interpretation and analysis of the EO data, and derive information products for access via the HABIM web-site. All remote sensing products, i.e. SeaWiFS level 2 and AVHRR-SST files are split into standard Mercator-projected areas. The following EO based information products has been implemented for use:

- SeaWiFS data with a nadir spatial resolution of 1.1 km and so higher resolution satellite or airborne imagery may be useful if the bloom is relatively small or close to shore. Standard level-2 products such as:
- chlorophyll concentration (see Fig 20, left panel),
- diffuse attenuation coefficient, and
- project-specific products such as RGB colour composite of water leaving radiance at 443, 520 and 550 nm (see Fig. 20, right panel).
- AVHRR sea surface temperature images, possibly completed with ATSR data, can provide high frequency coverage, several passes per day, when these situations occur. The analysis of SST data gives insight on the main circulation patterns and water masses. This type of indirect information is valuable while giving additional environmental parameters to the interpretation of the current situation.

Generally, the expert analysis requires the use of information from both the AVHRR and SeaWiFS sensors. The main product is the chlorophyll-a concentration map derived from SeaWiFS using the standard NASA SeaWiFS algorithm. However, because of the inadequacy of this algorithm for case 2 coastal water, computed high values are not necessarily the mark of an algae bloom, but may be due to the presence of other optically-active substances in the water-column. The ambiguity of high chlorophyll-concentration values may, in favourable cases, be reduced by the analysis of the water-leaving radiance spectra.
Within the HABIM project, PML provided colour composite of the water-leaving radiances at 443, 510 and 555 nm. This specific product may be of high value to discriminate algae bloom from suspended sediment, and even different family of algae (e.g. for coccolithophorid blooms).

Use of EO products during HAB emergency situations

During the demonstration periods of the HABIM project two major harmful algae blooms were detected and monitored by use of integrated EO, in situ and modelling tools. These were two major blooms of *Chattonella* in respectively the west Danish (Jutland) waters in April-May 2000 and in the coastal Skagerrak waters during March-April 2001.

During emergency bloom situations of *Chattonella* the project ran a regular operational monitoring mode delivering daily images (or as frequent as they were useful/cloud free). This information was supplemented by additional data sets, which came from other environmental observations and/or model sources. Auxiliary to the project information from dedicated ship observations/cruises and airborne reconnaissance, including visual observations, were also initiated by the Directorate of Fisheries. The

Nansen Center and IMR participated in the day to day advisory efforts with up-dates of the satellite EO information and model forecasts.

During emergency bloom situations, IMR also performed real-time model simulations and forecasting of algae bloom development, using their combined physical ocean and marine ecosystem model (NORWECOM). For the 1998 HAB event, the model was able to forecast bloom development including the growth and movement of this large harmful algae bloom in the threatened region, up to 48 hours into the future. However, due to insufficient knowledge of the mechanisms that triggers the initiation and development of blooms, NORWECOM (as is the case with most other numerical models of this kind) is not able to predict the occurrence of a new bloom of a specific species. The interpretation of the model results is thus strongly dependent on other observations from *in situ* or EO sources to identify blooming situations.

Integration of satellite-derived bio-physical parameters, such as sea surface temperature and chlorophyll pigment concentration, with the numerical model is a way to improve the forecasting capability. Specific integrated EO information products must then be elaborate for integration within the model. In particular, HABIM enabled the delivery of derived chlorophyll distribution at model grid scale and projection. Since EO data have a much better resolution (about 1 km at nadir) than the model (20 km), optimal data smoothing may be undertaken.

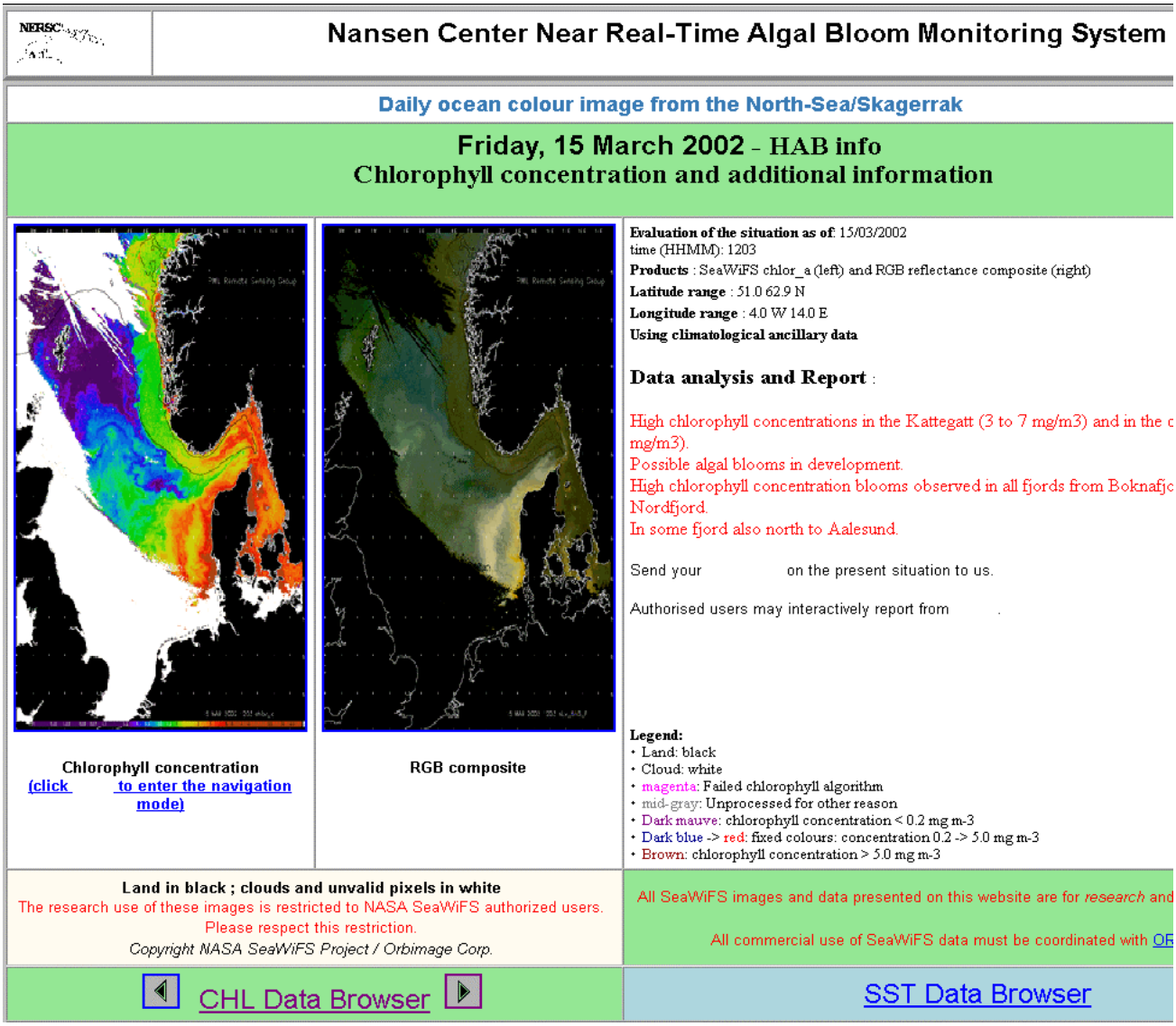

Figure 20 Restricted-to-project web-area, displaying daily SeaWiFS level 2 products (chlorophyll concentration on the left and reflectance RGB composite on the right), and descriptive analysis report of the algae bloom situation.

Evaluation, interpretation and analysis

The region of the HABIM monitoring has been geographically divided into seven sub-regions: Kattegatt, East Skagerrak, West Skagerrak, West Jutland, Hordaland, North Sea, and south-west Norway. For each zone, a brief description of the algae bloom situation is given, taking into account the information gained from the images of the day, as well as the recent history of processes and events in the area and the information from *in situ* field data and observations. The daily analysis required SeaWiFS chlorophyll-a concentration maps complemented by the analysis of water-leaving radiance spectra in order to reduce the false-alarm rate in case II waters. The analysis of SST data provided information about the main ocean circulation pattern and the water masses of various origin. In case of regular monitoring, conclusions of the analysis of the various EO and non-EO data sources are also provided in a short descriptive text, which in wording summarises the bloom situation in the region and facilitate the own interpretation of the non-experts.

The User Interface

The HABIM project implemented a web-based browser system for the dissemination of information on algae bloom situation in near real-time (typically four to ten hours after the acquisition of the satellite data).

The web-site (http://www.nersc.no/HAB) is the main user interface to the information provided by the HABIM service. In case of detection of potential harmful bloom events active and direct communication initialised, following the structure implemented in the national contingency plan for handling of emergency situations in the coastal zone.

The web-site includes five main areas, which can be access through the web-site front-page. Some areas have open availability and some are password protected and available for project accredited users:

- The general project description area, including the project objectives, partnership, promotional information, press releases, project funding, etc.
- The public daily information on oceanographic situation in the monitored area. This information includes selected AVHRR-SST images of the day and a short text analysis of the situation, based on all available information. A link to the SST image time series archive is implemented, as well as a link to the SeaWiFS daily report page (restricted access).
- The project-restricted area for daily information on the algae bloom situation (Fig. 20). The daily updated web-page includes a selection of SeaWiFS image products relevant for algae bloom analysis, i.e., chlorophyll-a concentration and RGB colour composite of water-leaving radiances. A report analysis of the bloom situation is included in text format. Information on previous situations can be browsed through a link to the SeaWiFS image archive organised in monthly batches. A java-script allows the user to navigate the images and point out geographic locations and feature of interest, including the actual value of the concentration parameters within the image.
- The project-restricted area for archive, time series and dynamical analysis of bloom events. The archive area gives access to daily AVHRR-SST, and SeaWiFS chlorophyll and RGB images acquired during the project period (March to July, 2001) and for the three last years (1998 to 2000). A system of graphical links through an intuitive design allows the user to navigate through the time series of products and then to retrieve the information pertaining to a specific day
- The modelling area (Fig. 21) gathers the main results of simulations and prediction of HAB development, performed by IMR using the 3-D coupled physical-ecosystem model for the North Sea region (NORWECOM). The model used to produce these images was initialised from data on 18 and 19 April and indicate that on 8 May the highest concentration of flaggelates (dominated by Chatonella sp.) at a depth of 3 m are still located primarily along the coast of Denmark. A high-concentration band extends also from the northern tip of Denmark westward through the Skagerrak. The overall distribution of the HAB corresponds well with satellite observations of distributions of sea surface temperature and chlorophyll. The simulation also indicates that nitrate in the surface waters may be strongly depleted by the growth of the bloom. Based on the weather forecast for the area, the forecast for HAB development indicates that the bloom will be in a phase of decline by 16 May and will not represent an immediate threat to acquaculture installations along the southern coast of Norway.

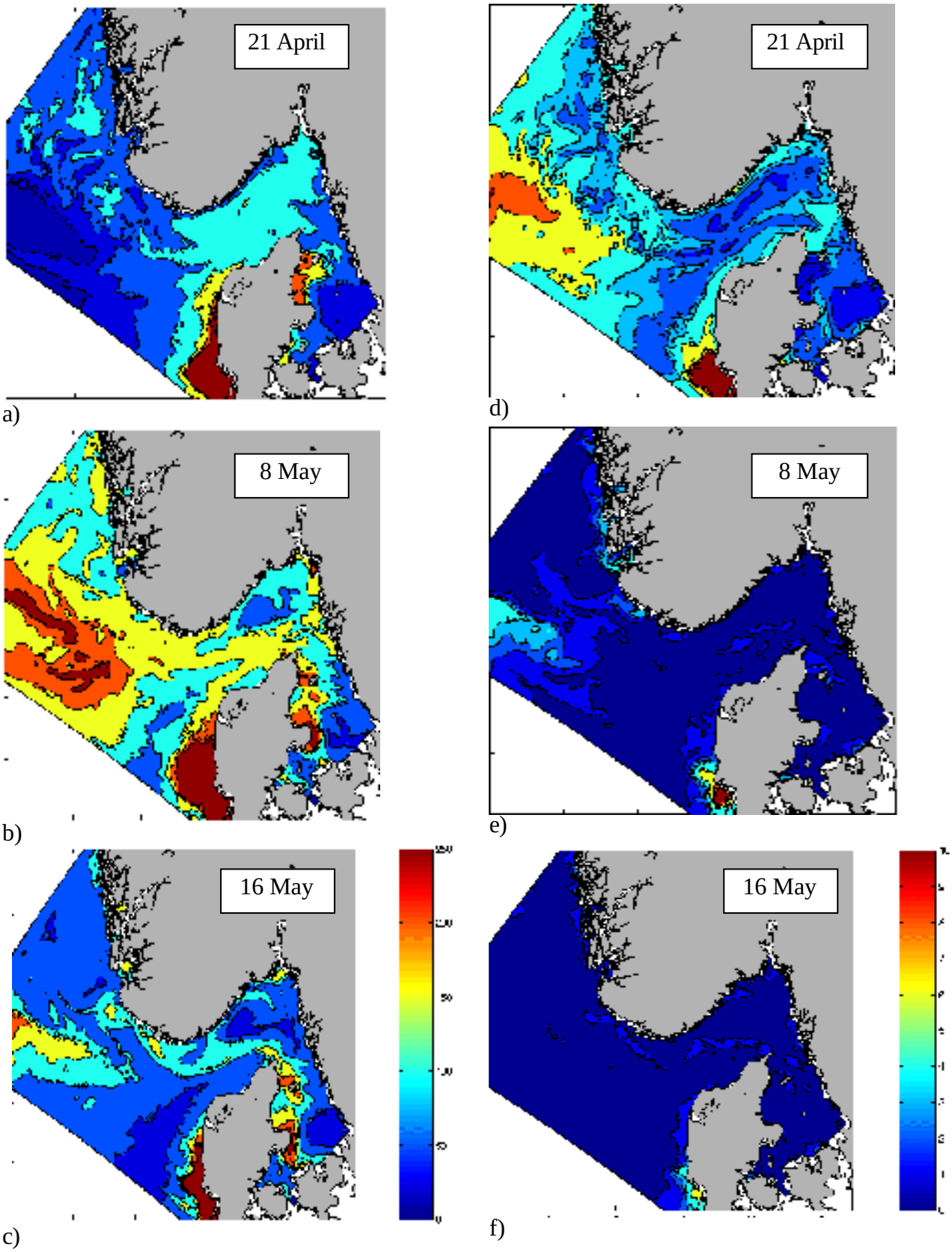

Figure 21. First results from modelling simulations of a harmful algae bloom (HAB) in the Skagerrak – North Sea area in April – May 2002. Figs a), b) and c) show flagellate biomass in mgC per m^3 Figs d), e) and f) show inorganic nitrogen in µmol/L

4.2.5 Project Interactions with the Existing Service

The role of ALGEINFO with respect to the distribution of information is instrumental. It is particularly noteworthy that in an emergency situation, ALGEINFO represents a hub for the rapid dissemination of support-related information. For example, EO products and derived information in the form of graphic, numerical and text presentations of actual bloom distribution is made available by Internet link to HABIM web-site at NERSC. Furthermore, forecasting of HAB development may be graphically illustrated and made available to the public and/or authorities via a link to separate web-site at IMR and/or NERSC. The ALGEINFO web-site has a link to the HABIM project web site at NERSC, as well as to another IMR server (in Bergen) to access views of model simulations of the development of harmful algae blooms. Thus, end users of the web-site may view actual EO images of algae bloom development and prognoses of the extent and development of identified HAB event.

The Directorate of Fisheries in Norway has the primary responsibility for monitoring harmful algal blooms and providing warning and advice during HABs along the Norwegian coast. The Directorate of Fisheries has developed an emergency-response plan with three-level action according to the HAB situation. The plan defines operational responses and lines of command and communication (on internal, national and international levels, and to the marine aquaculture industry, fisheries authorities, the press, etc.), for each level of response.

4.3 Service Demonstration - Events and monitoring

Both in the spring of 2000 and 2001 extensive harmful algae blooms were observed in the geographical area monitored by the ESA HABIM project. The bloom timing and extent were however quite different, as were the monitoring responses initiated by the Directorate of Fisheries.

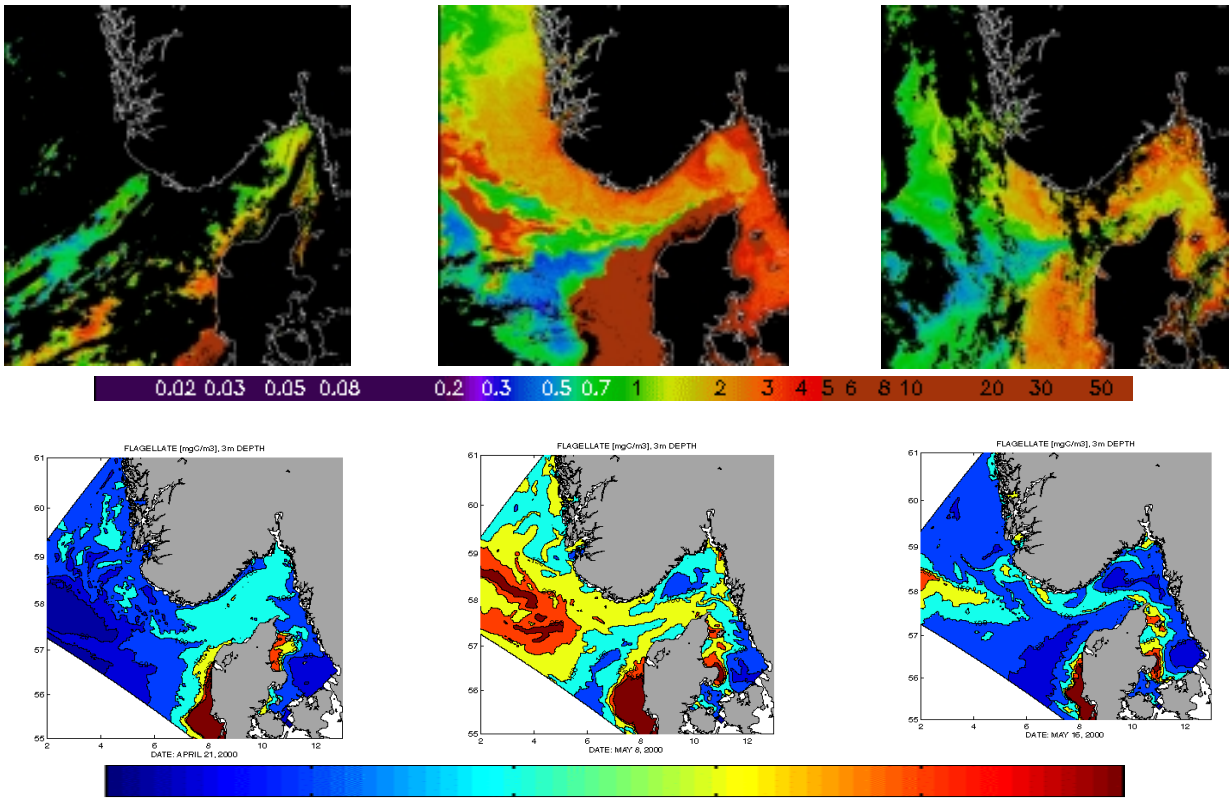

Figure 22 Comparison of the SeaWiFS based chlorophyll pigment distribution (in mg chlorophyll/m^3) and the flagellate concentrations as resolved in the NORWECOM model (in mg Carbon/m^3, range 0-250 mgC/m^3) for respectively 18. April, 8. and 16. May, 2000 during the Chattonella bloom west of Jutland and in Skagerrak.

Late in April 2000 an extensive algal bloom was detected by the project team in the satellite images in the area west of Denmark (Jutland). *In situ* observations confirmed that the algae bloom consisted mainly of *Chattonella spp*. It was feared that the bloom would follow the prevailing cyclonic circulation through the Skagerrak region and eventually affect the fish farms along the coast of southern Norway. At the Institute of Marine Research the NORWECOM model was initialised and predictions of the behaviour of the bloom were produced (Fig. 22).

The Directorate of Fisheries received the information from the HABIM project based on satellite imagery and modelling, but the bloom was not considered an emergency situation. Dedicated *in situ* sampling for algae analysis was carried out, but based on the information from the HABIM project it did not initiate any emergency measures, however the situation was carefully monitored. The modelling results showed that it was unlikely that the bloom would reach the fish farms on the Norwegian coast and the satellite imagery also showed that the bloom remained on the western coast of Denmark. Thus the information from the HABIM project obviated establishment of an emergency situation with extensive dedicated *in situ* sampling and analysis. During a similar bloom event in May 1998 in the same area dedicated field observations were initiated using two research vessels and causing additional costs for the field data sampling and analysis amounting to about NOK 600.000.

The *Chattonella* bloom in the spring of 2001 was quite different. The bloom was first detected through loss of fish in fish farms on the south-east coast of Norway on March 16. The Directorate of Fisheries then contacted the Nansen Center and the HABIM project service was made fully operational with daily updates of satellite imagery on the project web-site. Already prior to this the site was functioning automatically with image updates: however no daily analysis had yet started. Analysis of daily images and retrospective data was very useful in the first assessment and overview of bloom extent as well as the later monitoring of the extent and development. At the Institute of Marine Research, NORWECOM, was initiated and predictions of the development of the algae bloom were produced. An emergency monitoring and advisory group was established by FD. This group had daily meetings to co-ordinate the field data sampling and prepare advice and public information dissemination. Staff from the Nansen Center and IMR participated in daily steering and advisory meetings and the HABIM project provided valuable information on the extent and development of the algae bloom, based on satellite information and images as well as model predictions. This information was of great value in the daily planning of emergency and mitigation measures as well as defining *in situ* data sampling strategy.

These two HAB events illustrate clearly the important roles that EO information can play in the algae monitoring. In the spring of 2000 the satellite images provided an early warning of the bloom, and together with modelling the imagery was used to monitor a situation that had the potential to become a more critical emergency situation. Partially based on the available EO information it was decided to not establish an emergency group at FD, with the resources and cost implications of such initiatives. In this respect resources and money for monitoring efforts was saved.

In 2001 the EO was not able to give an early warning and the bloom was first detected through loss of fish in fish farms. The situation in 2001 was exceptional compared to earlier harmful algae blooms. The bloom caused problems in mid March as compared to earlier spring blooms that have occurred in late April and May. Thus even if a bloom was detected at that early stage it would not have expected to be harmful. The EO information and modelling results, however, proved to be valuable in the handling of the emergency situation and illustrates that this type information often can provide valuable information to complement the monitoring of algae, possibly harmful, blooms (hereafter (H)AB) events.

Based on the demonstrations provided by the Nansen Center and later the HABIM project the Directorate of Fisheries view the satellite EO imagery and the modelling results received as an essential part of the monitoring and emergency handling of algae blooms in coastal Norwegian waters. In the past (in 1998 and 1999) the “service” has been provided on good will from institutions (Nansen Center, PML, IMR), and lately (in 2000 and 2001) by the HABIM demonstration project. The Directorate of Fisheries has taken steps toward the Ministry of Fishery to establish a service of this type on a permanent basis, but funds are not yet available to establish a more permanent access to EO based information in the monitoring of (H)AB events in waters of Norwegian interest. The political debate concerning the future of the aquaculture industry has been raised lately in Norway and includes

the fact that this industry is a very profitable activity. The debate centre on whether the responsibility for such algae monitoring actions should be funded by the industry itself instead of governmental resources as to a large extent is the situation to day.

4.4 Links to related projects

The work in Task 2 is closely linked to the following projects:

DECIDE: The ESA-funded project DECIDE, together with projects supported by Norwegian Space Centre, started to monitor harmful algae blooms in the spring of 2000 with SeaWiFS data. The first demonstration of SeaWiFS data for algae monitong started in 1998. The results of the project are presented in the Final Report by Pettersson et al., 2001.

PROOF: Estimation of Primary Production for Fisheries Management, EU-funded project 2000 – 2002. Use of satellite data, validation of algorithms and comparison with ecosystem models are the main activities in this project.

HABIL: EU-funded project (2001 – 2004) which continued and developed further the use of optical satellite images for algae monitoring which was started in DECIDE. (see http://www.nersc.no/HAB)

Relevant reports

Pettersson, Lasse H., Dominique D. Durand, Einar Svendsen, Thomas Noji, Henrik Søiland, Steve Groom and Samantha Lavender: DECIDE for near-real-time use of ocean colour data in management of toxic algae blooms - Definition and Design document. NERSC Technical report No. 186 to European Space Agency, September, 2000.

Pettersson, L. H., et al., DeciDe for near real time use of ocean colour data in management of harmful algael blooms. ESA Contract no. 13662/99/I-DC, Final Report. NERSC Technical Report no. 200, September 2001, 79 pp.

5. Results from Task 3: Assimilation of sea ice data in a climate model

5.1 Introduction to Arctic sea ice observations

Sea ice is an important component of the Arctic climate system. Its presence modifies heat and momentum exchanges between the atmosphere and the ocean, and snow and ice reflects 70%-80% of the incoming solar radiation. Results from nearly all coupled atmosphere-ice- ocean numerical modeling studies of greenhouse gas scenarios indicate that global warming will be enhanced in the polar regions, especially in the northern hemisphere (Manabe et al., 1992), with a predicted warming of about 3-4 degrees Celsius in the next half-century (Mitchell et al., 1995), and a drastic decrease of the sea ice in the Arctic Ocean (Cattle and Crossley (1995), Vinnikov et al. (1999).

Recent analyses of the ice cover in the Arctic Ocean have established that significant changes have occurred in the latter part of the 20th century. Analysis of upward looking sonar observations from US nuclear submarines indicates that the average ice thickness has decreased from 3.1 m in the 1958-1976 period to 1.8 m in the 1990s, in average 4 cm per year, or totally 40% of the total ice volume (Rothrock et al., 1999). However, these measurements are in contrast to spatially averaged ice thickness estimates obtained from surface elastic- gravity wave measurements carried out by the Russian "North Pole" drifting stations during the period 1970{1991 (Nagurnyi et al., 1999). The average ice thickness during this 21 year period is 2.85 m with a reduction of 0.5 cm/yr, or a factor 8 less than the trend observed by Rothrock et al. (1999) over a 10 year longer period.

Furthermore, analysis of microwave satellite observations has established that the total sea ice area has decreased by 6% over the last two decades (Johannessen et al. (1995), Bj¯rgo et al. (1997), Parkinson et al. (1999)), while the multi-year ice area has decreased by 14% over the same period (Johannessen et al., 1999). Comparison of observations (in situ and satellite) since 1900 with trends seen in two coarse resolution global climate models, incorporating the effects of observed greenhouse gases and tropospheric sulphate aerosols correlates very well. As stated in Vinnikov et al. (1999), this is "suggesting strongly" that the observed decrease in sea ice extent since 1950 is related to the anthropogenic global warming. Prediction by these two coarse resolution global climate models furthermore suggest a substantial decrease of the sea ice extent in the 21st century (Vinnikov et al., 1999). However, the elevated indices of the North Atlantic Oscillation (NAO) (Hurrell, 1995) and the Arctic Oscillation (AO) (Thompson and Wallace, 1998), indicate a pumping of warm air and water masses into the Arctic from the North Atlantic region causing ice melt as well as a mechanism for exporting multi-year ice through the Fram Strait (Hurrell (1995), Thompson and Wallace (1998), Rothrock et al. (1999)). Even some effects on the variability of the sea ice from El Nino has been reported (Gloersen, 1995). Therefore, the decreasing ice cover is probably caused by a combined effect of greenhouse warming (century time scale), high indices of the AO/NAO index (decadal time scale) and even the Atlantic Multidecadal Oscillation (AMO) (Kerr, 2000). For a review of the state of art regarding the Arctic ice cover see e.g. Johannessen and Miles (2000).

The melting and freezing of sea ice leads to changes in the density of the underlying water, and these changes can have a negative or positive effect on convection. Sea ice formation in the Arctic Ocean and the shelf seas around it leads to increased water density and contributes to the formation of Arctic intermediate and deep waters (Midttun (1985), Anderson and Dyrssen (1989), Aagaard and Carmack (1989), Yang and Neelin (1993)), whereas a melting ice cover can prohibit deep water formation by stabilizing the water column and by advecting fresh water into neighboring regions. Advection of fresh water from the Arctic Ocean into the Greenland Sea and the North Atlantic is an example of the latter. The Arctic Ocean and its peripheral seas are therefore of importance for the global thermohaline circulation (the Global conveyor belt, (Broecker et al., 1985)), and make Arctic sea ice a climate component also in a global perspective.

The role sea ice plays in the climate system suggests that sea ice models should be eval- uated and compared before they are included in coupled climate models. Currently such an effort is being carried out in the Sea Ice Model Intercomparison Project (SIMIP) (Lemke et al., 1997), which attempts to determine the best currently available sea ice model when it comes to dynamic realism, thermodynamic

realism and computational efficiency. The major objective of our paper is to validate ice variables from a coupled sea ice and ocean model using sea ice concentrations derived from passive microwave satellite sensors, Validation data for the sea ice concentration were acquired from the Scanning Multimeter Microwave Radiometer (SMMR) carried on board the NASA Nimbus 7 satellite and the Special Sensor Microwave/Imager (SSMI) carried on board satellites F8, F11 and F13 of the US Defense Meteorological Satellite Program (DMSP). The combined data set now spans two decades and represents a reliable day-to-day description of the sea ice concentration in the polar regions. Compared to data sets of other parameters of sea ice, for instance ice thickness, the data set of sea ice concentration is superior when it comes to the spatial coverage and the length of the time series. This makes it well suited for validation of sea ice models. The sea ice concentration has a significant effect upon the thermodynamic part of the sea ice model, but sea ice concentration is also important for the dynamic part since the strength/pressure parameterization in sea ice rheologies depends upon it. The validation with sea ice concentration is carried out over the time period 1978-1998, and a special emphasis has been put on checking whether trends in the passive microwave data sets are recreated. In the validation with sea ice concentration it is also presented statistical methods that are well suited for an objective quantification of the skill of a sea ice model.

The coupled ice-ocean model used here is an Atlantic-Arctic version (Drange, 1999) of the Miami Isopycnic Coordinate Ocean Model (MICOM) (Bleck et al., 1992), coupled with the dynamic sea ice model of Harder (1996) and the thermodynamical module of Drange and Simonsen (1996).

The ocean model was chosen as it has proven to do well in modeling studies of the Atlantic Ocean, e.g. Bleck et al. (1992) and New et al. (1995). A favorable aspect of isopycnic models is their ability to provide high vertical resolution in regions with strong vertical density gradients and to suppress numerical diffusion across isopycnals. A drawback is low vertical resolution in weakly stratified regions, such as in the central Arctic ocean and on the Arctic shelves. However, an isopycnic model by used in the Arctic and the Nordic seas (Holland et al. (1996), Aukrust and Oberhuber (1995)), has shown that this type of ocean model has the capability of doing well in these regions. The dynamic ice model uses the Viscous-Plastic rheology, which was pioneered by Hibler [1979]. Results from the SIMIP and other similar studies indicate that variants of plastic rheologies give the most realistic large scale flow of sea ice Arbetter et al. (1999), Kreyscher et al. (2000).

For validation of the model system it is of utmost importance that the atmospheric forcing fields are of reliable quality. For the model simulation we had the choice between forcing from 1) the National Centers for Environmental Prediction (NCEP)/National Center for Atmospheric Research (NCAR) Reanalysis project for 1958-1998 and, 2) the European Center for Medium range Weather Forecasting (ECMWF) reanalysis project (ERA-15) for the period December 1978 - February 1994. To ensure minimal effects of model spin-up on our results, and because of the greater overlap with the time span of SSMI{SMMR data, we used the NCEP/NCAR reanalysis in the simulation reported here.

The chapter is organized as follows: In section 5.2 and 5.3 the coupled ice-ocean model and the satellite data set are presented. In section 5.4, the total sea ice extent and area are examined, and it is demonstrated that trends in the satellite data are generally well reproduced by the model. The spatial and temporal differences between the data sets are studied in section 5.5, with the aim to locate the majority of the model error. The correspondence between observed and simulated multi-year ice area and ice thickness are given in section 5.6, and section 5.7 describes results of the first data assimilation experiments with the ice-ocean model.

5.2 Model description

As already stated, the model used is an Atlantic-Arctic version of MICOM (Drange, 1999). Atmospheric forcing, provided by NCEP (Kalnay et al., 1996), was applied at the marine interface, and the model was integrated from 1958 until 1998 after a 30 year spinup integration initialized with salinity and temperature climatologies from Levitus et al. (1994) and Levitus and Boyer (1994), respectively. The dynamic part of the sea ice model is based upon the viscous-plastic rheology of Hibler (1979), where sea ice is considered as a two-dimensional continuum. The dynamic ice model used in this study has been further modified by Harder [1996] to include description of sea ice roughness and the age of sea ice, and utilizing the advection scheme of Smolarkiewicz [1984]. The

parameterization of internal stress in ice is usually what distinguishes the dynamics of sea ice models. The internal stress is based upon the mechanical properties of ice, and represents a parameterization of contact forces between individual ice floes.

The thermodynamic part of the ice model balances heat fluxes at the water-ice-air in- terfaces and deduces the freezing and melting rates. The conductive fluxes are linear in ice and snow, so no thermal inertia occurs in the ice. A lead parameterization is included by keeping the total ice concentration less than Fmax = 0.99. Details of ice thermodynamics and lead parameterization are found in Drange and Simonsen (1996).

The ocean model MICOM is a layer model using potential density as the vertical coor- dinate, and the uppermost layer is a mixed layer with freely evolving density. The model is hydrostatic in each layer and has prognostic equations for horizontal momentum and layer thicknesses. Interior layer temperatures are determined prognostically, and salinities are de- termined diagnostically by the equation of state, given potential density and temperature. In the mixed layer, temperature and salinity are both determined prognostically. The mixed- layer thickness is determined from an energy equation where turbulence is maintained against viscous dissipation, buoyancy fluxes and wind stress (Gaspar et al., 1990). In addition to en- trainment/detrainment between the mixed-layer and interior layers a diapycnal mixing is prescribed between the interior layers (Gargett, 1984).

The model equations are discretized on a C-grid constructed with a mapping similar to the conformal mapping of Bentsen et al. (1999), and the momentum equations are solved with a split-explicit numerical scheme (Bleck and Smith, 1990). If we examine the model grid for the same area as that of the SMMR/SSMI data (Figure 23), we see that the model has highest resolution at about 67 N with

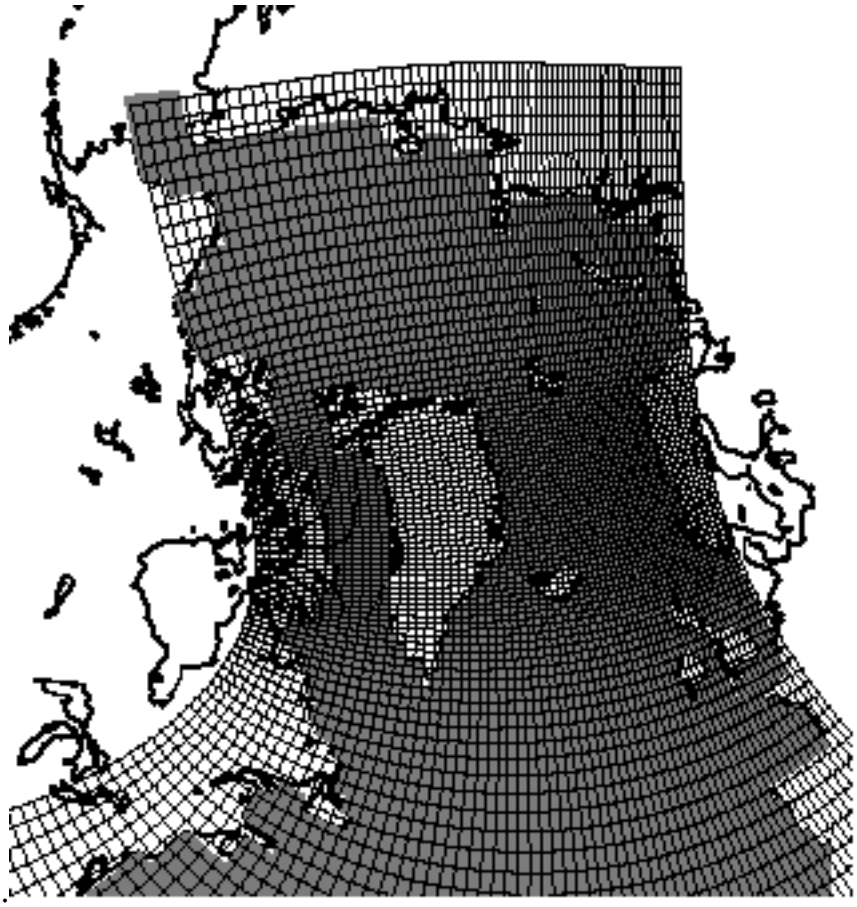

Figure 23: Projection of the numerical grid from the coupled ocean-sea ice model upon the same map as used with SMMR/SSMI data. The model sea mask (grey) has an artificially wide channel that connects Baffin Bay with the central Arctic Ocean.

The model domain includes the Arctic Ocean and extends to 20 S latitude. The domain is considered as a closed basin with relaxation towards monthly climatological values of salinity and temperature at the boundaries (Levitus et al. (1994), Levitus and Boyer (1994)). Vertically the model has 23 layers, with potential density ranging from 24.04 to 28.11. The time step used in the computations was 20 minutes for ocean model and sea ice thermodynamics, the sea ice dynamics was updated every 24 hours, whereas the atmospheric forcing was updated every 12 grid sizes down to 45 km. hours

5.3 Use of satellite data

The National Snow and Ice Data Center (NSIDC) provides the SSMI/SMMR brightness temperatures necessary to calculate sea ice concentrations. They are distributed on 304x448 pixel grids where the Earth is projected onto the grids using a polar stereographic projection true at 70 N. Due to satellite orbits and swath widths a circular region near the Arctic pole is out of sensor range. For the SMMR sensor this is the region poleward of 84.6 Δ N and for the SSMI sensors it is the region poleward of 87.6 N. The NORSEX algorithm Svendsen et al. (1983) was used to calculate sea ice concentration from brightness temperatures, and the resulting data sets from the SSMI and SMMR sensors were merged as in Bjørgo et al. (1997). When we created the combined time series from November 1978 to July 1998 the entire region poleward of 84.6 Δ N was excluded from the SSMI data set, as in the SMMR data set. Additionally the sensors can be used to discern between Multi-Year Ice (MYI) and First- Year Ice (FYI) because these ice types have different emissivity characteristics. During sum- mer the melting snow layer on the ice becomes the dominant emitter and therefore it is not possible to distinguish FYI and MYI by microwave characteristics at this time of year Comiso (1990). A merged data set describing MYI in the winter months November - March from 1978-1998 was created as in Johannessen et al. (1999).

5.4 Sea-ice extent and area

The parameters examined in this section are ice extent, the area within the ice-ocean margin limited by the 15 % ice concentration contour; and ice area, the area of ocean covered by ice within the 15% ice concentration contour. To properly compare the model data with the satellite sensor data the comparison was done over a region that was common to both. This was achieved in three steps, first by projecting the model land mask onto the satellite land mask so that areas seen as land in the model were not included in the satellite-derived data. This region still contained some land areas, so if a model grid cell contained islands or shore lines, this area was subtracted from the grid cell area when calculating model sea ice area and extent. Finally, the area poleward of 84.6° N not included in the satellite data was excluded from the model data. In the following the model and satellite-derived sea ice concentrations will be compared over this common
region.

5.4.1 Monthly averages

The time series of monthly averaged sea ice extent from the satellite and model data are shown in Figure 24 a. The period covered is November 1978-July 1998, and the inset shows the average seasonal cycles for this time period. A corresponding figure for sea ice area is shown in Figure 24 b. From the two figures we see that the model consequently underestimates the sea ice extent and area. From the inset in Figure 24 a we observe that, on average, the model error in sea ice extent lies between 1-2.000.000 km^2 for most of the year, and is largest in winter and summer. The model error in sea ice area (Figure 24 b) is somewhat smaller during winter (1.000.000 km^2.), but increases to about 2.000.000 km^2 in summer. The seasonal variation in sea ice area and extent is reasonably well described by the model, although the values are too low.

Having obtained sea ice area and extent we can examine the quantity

$$A_p = \text{Sea-ice area} / \text{Sea-ice extent}$$

which is a measure of the average sea ice concentration within the 15% ice concentration contour.

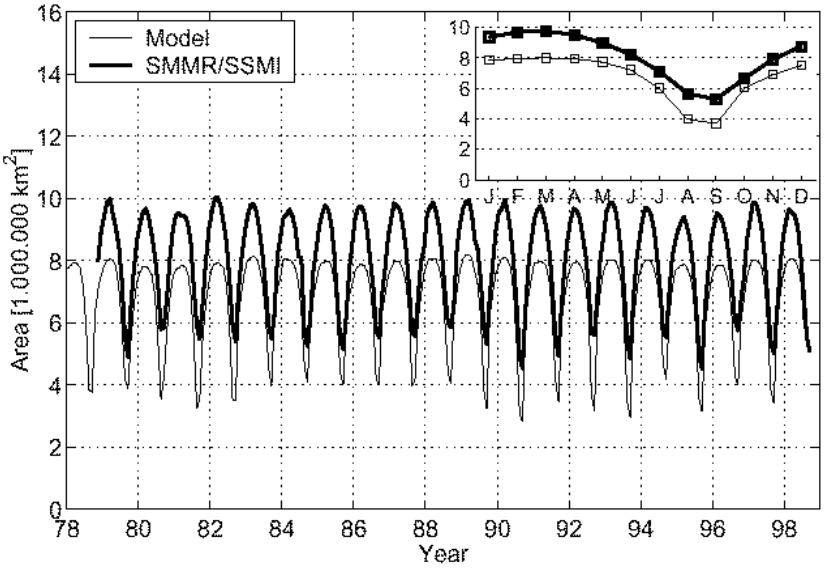

a)

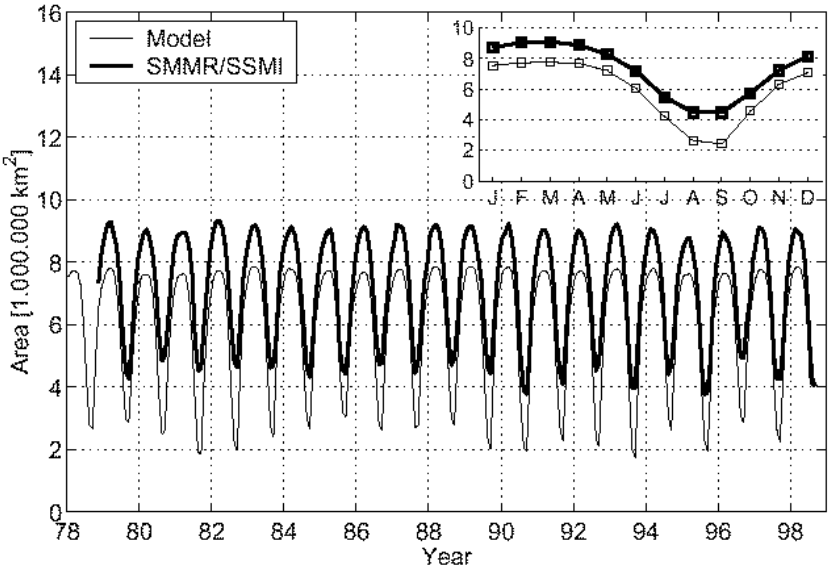

b)

Figure 24: Time series of (a)sea ice extent and (b) sea ice area from satellite sensors (thick line) and model (thin line). The inset shows the average seasonal cycles.

A time series of A_p, which is a psevdofraction between ice area and ice extent, is shown for model and satellite derived data in Figure 25 along with an inset showing the average seasonal cycles. From this figure we see that the model on average shows too low sea ice concentrations within the ice pack in summer, and to high concentrations in winter.

The miscalculation of sea ice concentrations in the model can create large errors in the heat fluxes between the ocean and atmosphere. In summer a too large open water area within the ice pack will receive short wave radiation. The actual lead parameterization the model uses will influence the error in A_p in summer through lateral melt, and the error in sea ice area will also be influenced by this. The too

high average model concentrations in winter occurs because the model shows no spatially smooth transition from 15% to 100% ice concentration, a feature that is present in the satellite-derived data. This could be caused by the larger grid cell size of the model as compared to the satellite data.

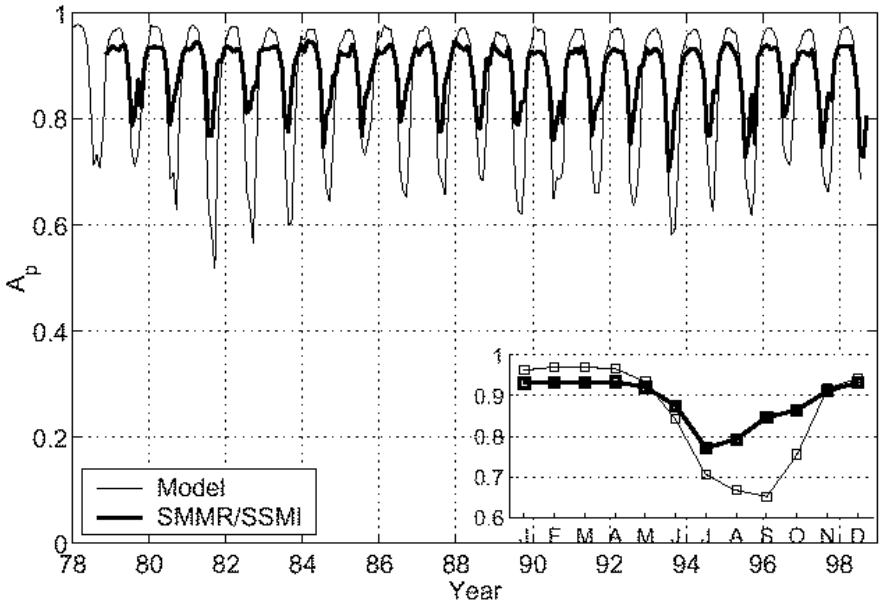

Figure 25: Time series of the pseudofraction (sea ice area/sea ice extent) from satellite sensors (thick line) and model (thin line). The inset shows the average seasonal cycles.

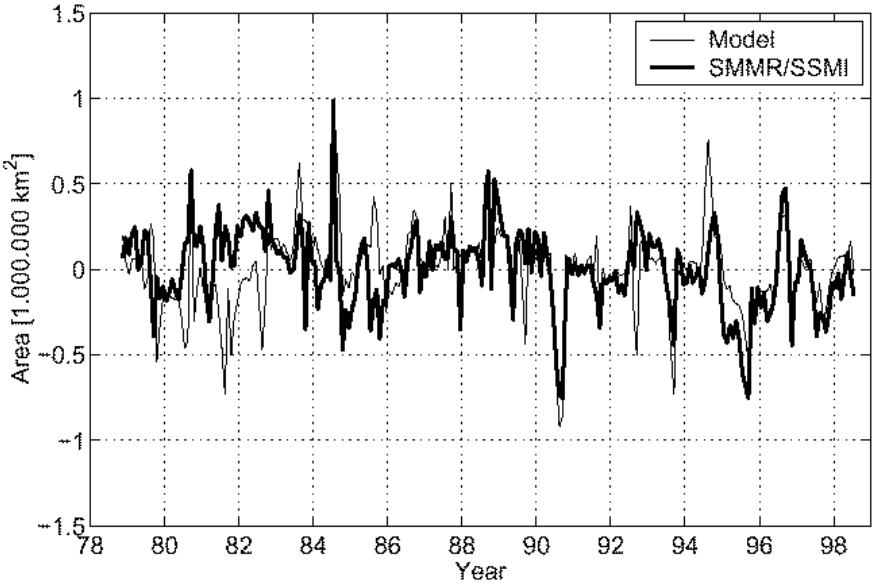

Figure 26: Time series of sea ice extent anomalies from model (thin line) and satellite data (thick line). The anomalies are based on the average seasonal cycle.

5.4.2 Trends from anomalies

The error in the model follow a similar pattern every year, both in sea ice area and extent (Figure 24). This suggests that long term trends present in the satellite data are present in the simulated sea ice field too. The anomalies in sea ice extent from model and satellite data are shown in Figure 26. The anomalies were calculated by subtracting the average seasonal cycle from the monthly means. On the

basis of these anomaly plots we can estimate trends in sea ice extent using linear least squares fit (LSF) analysis. We focus on sea ice extent because the sea ice area has a similar behaviour regarding the anomalies. The following results should not be directly compared to results from other studies of SMMR/SSMI-derived sea ice area and extent, e.g. Bjørgo et al. (1997), Parkinson et al. (1999), because here we consider these parameters over a region common to the model domain and the satellite coverage. As already mentioned this means excluding the area poleward of 84.6° N and some regions containing ice in the satellite data. For the entire time series November 1978 to July 1998, the LSF trends from the model and satellite sea ice extent are markedly different. The trend from the satellite data is -12.000 km^2/yr for the period November 1978 to July 1998. The negative trend is significant, as the hypothesis of a positive trend is rejected at the 99% confidence level. In the region considered and for this time period (1978-1998), this adds up to a decrease of 3% relative to a yearly mean value of sea ice extent. The trend from the model data is 200 km^2/yr, and the correlation coefficient between the model and satellite sea ice extent time series is 0.48.

A reason for the difference in trends is visible in the anomaly plot in Figure 26: In the period from 1981 to 1983 the anomaly curves differ considerably, while the period before and after show better agreement. That the model has large errors in this period is also visible in sea ice extent and area and in the pseudofraction A_p (Figure 25). The mismatch between model data and satellite data in 1981-1983 was studied by examining the applied forcing fields. Air temperature is an important factor for creation of sea ice for most regions in the Arctic, and examination of the NCEP temperature fields revealed high temperatures in regions along the coast of Siberia, Alaska and Canada in the winter of 79/80, 80/81 and 81/82. These regions are close to the Novosibirskiye islands, south of Novaja Zemlja, north of Point Barrow and close to Banks Island.

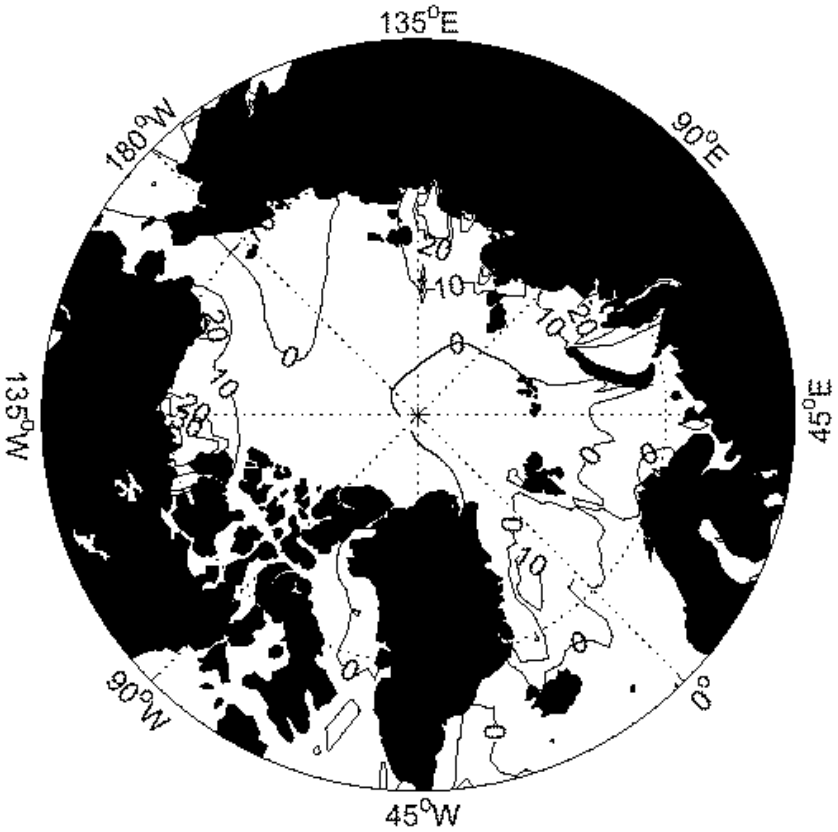

Figure 27: NCEP temperature anomaly field for January 1981. The field show unrealistic temperature anomalies (up to 30 K) along the Siberian and Canadian coasts.

A comparison of the NCEP temperature data with temperature data from the European Center for Medium-range Weather Forecasts (ECMWF) shows that the two fields are different in the Arctic for

the winters 79/80, 80/81 and 81/82. Figure 27 shows the mean monthly temperature anomalies for January 1981 from the NCEP data set. Along the coast of Siberia and Canada we see large anomalies in the NCEP temperature field, features which are nonexistent in the ECMWF temperature field. Ice production along the Siberian Coast is particularly important for the net Arctic ice production, because of the Transpolar Drift Stream (TPDS). The TPDS transports ice away from the Siberian Coast towards Fram Strait, and this divergence leads to high growth rates on the Siberian Coast. As a consequence, high surface air temperatures in this region could have a large impact upon the total Arctic ice production.

The high-temperature areas in the NCEP field do not cause a significant reduction in the winter sea ice extent of the model, but the reduced ice production due to high temperatures causes a more rapid decay of the ice cover and low values of summer sea ice extent. The situation is most dramatic in the winter 80/81, when the temperature anomalies not only cause a low sea ice extent in the model, but a significant reduction in total sea ice volume (Figure 28).

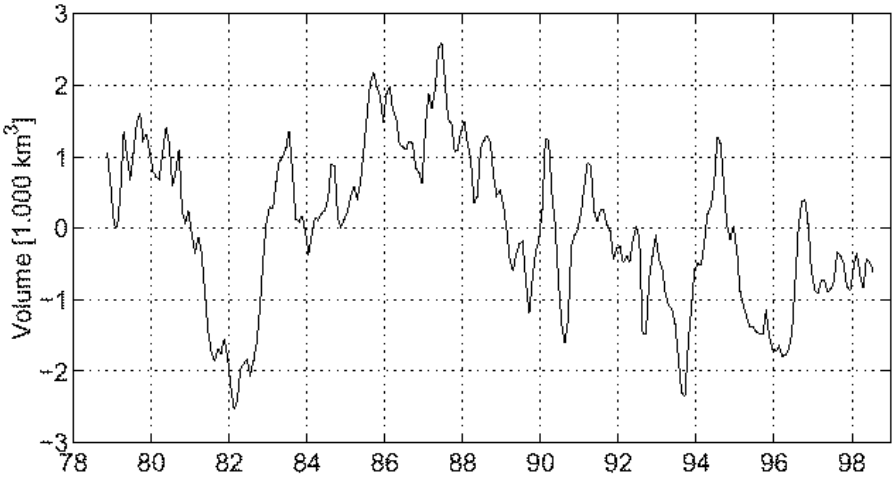

Figure 28: Anomalies in total sea ice volume from the model. The anomalies are based on the average seasonal cycle.

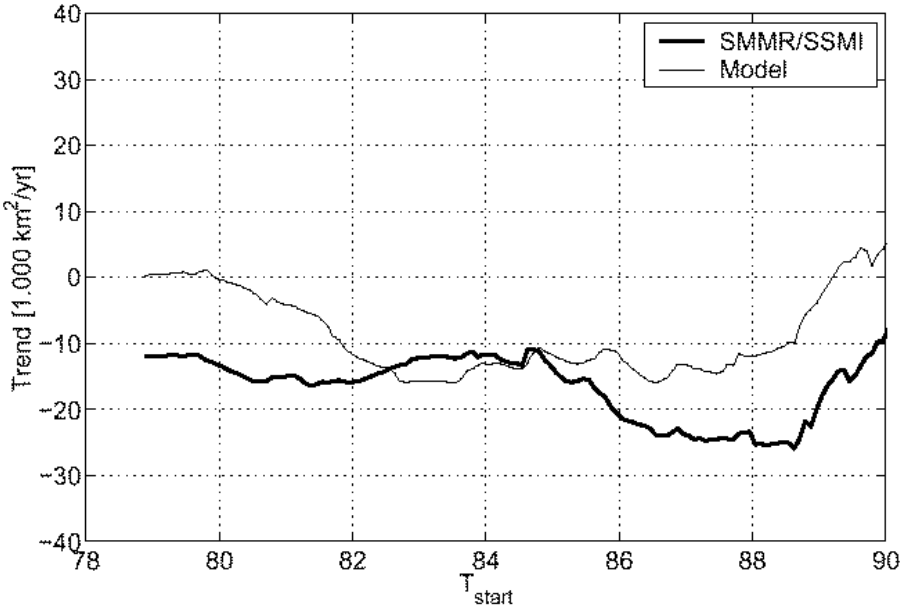

Figure 29: Estimated trend in linear least square fit of sea ice extent anomalies from model (thin line) and satellite (thick line) data. The trends are estimated over the time period T_{start}-July 1998, and the curves are created by varying T_{start}.

The discrepancy between sea ice concentrations from the NCEP-forced model and satellite data, and the discrepancy between NCEP and ECMWF temperature fields suggests that the winter time NCEP temperatures used in the period 1979-1982 are in error at the specified locations.

If we exclude the above mentioned period of disagreement, the satellite-derived and sim- ulated sea ice extent trends are closely matched. When we choose the period January 1984 to July 1998 the LSF trend from model and satellite sea ice extent is -12.000 km^2/yr and -11.000 km^2/yr, respectively. For both model and satellite data the hypothesis of a positive trend is rejected at the 99% confidence level, and the correlation coefficient between the model and satellite data sea ice extent time series is now 0.68. The close match of the trends is not entirely representative of the level of agreement between model and satellite sea ice extent, because the individual trends are dependent upon the time period considered. To examine this further we estimated the sea ice extent trends over the time interval T start to July 1998, and varied the starting time T_{start} . Figure 29 displays the results for model and satellite data sea ice extent, and shows that the close match between sea ice extent trends over the period January 84-July 98 was close to being the best one. However, the trends show reasonably good agreement for T start between 1982 and 1986, with both model and satellite data showing approximately the same negative trends. As T starts to get closer to July 1998, the 95% confidence intervals for each trend gets very large, and comparison of the slopes proves less. As the time series get shorter the trends become more dependent upon individual anomalies. From Figure 26 we see that some extreme anomalies in the 1990s are not properly captured by the model. This causes a tendency towards positive model trends for T start close to 1990. For the sea ice area we see similar results as for sea ice extent, and the trends from both sea ice area and extent are given in Table 5.1.

Table 5.1 Slopes from trend analysis of satellite and model data

Para-meter	Period	Model data			Satellite data		
		Slope ($x10^3 km^2$/yr)	Δ % per decade	Confidence level (%)	Slope ($x10^3 km^2$/yr)	Δ % per decade	Confidence level (%)
Ice area	Nov 1978 – July 1998	1 ± 3	0.1	-	- 18 ± 3	- 2.5	99
Ice area	Jan 1984 – July 1998	14 ± 3	2.9	99	17 ± 4	2.3	99
Ice Extent	Nov 1978 – July 1998	0 ± 4	0.0	-	12 ± 3	1.5	99
Ice Extent	Jan 1984 – July 1998	- 12 ± 4	- 1.5	99	- 11 ± 4	- 1.4	99

5.5 Temporal and spatial distribution of the model error in ice concentration

To obtain information on the spatial and temporal distribution of the model error in sea ice concentration, we used Principal Component (PC) analysis. The PC analysis splits our data set into orthogonal eigenvectors of the covariance matrix (EOFs) and time dependent parts (PCs). What separates this from many similar looking splittings is that the time dependent parts are uncorrelated and the EOFs are orthogonal, this makes it possible to sort the modes according to their contribution to the total variance of the data set. To examine the model error we created the following data set: For a given month we calculated the mean sea ice concentration from the satellite data for each model grid cell. This involves both temporal and spatial averaging as the model grid is coarser than the satellite grid. These values were subtracted from the monthly averaged model sea ice concentration for the respective grid cells, and the resulting data set describes the model deviation from the satellite data for each month in the period November 1978 to July 1998. The mean deviation of the model relative to the satellite data for the entire time interval is shown in Fig. 30 a.

.

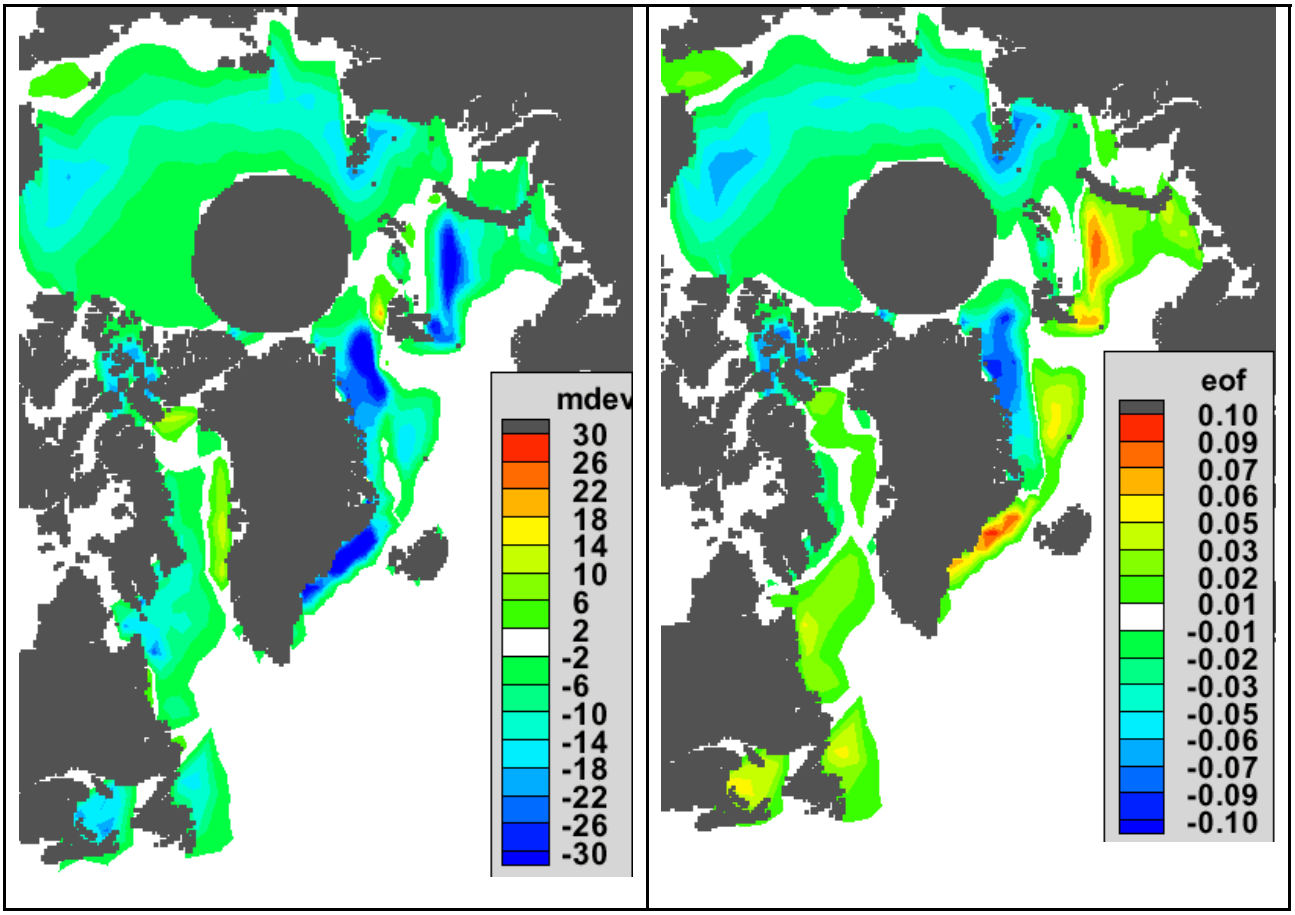

Figure 30: (a) Mean deviation of model sea ice concentration relative to satellite derived sea ice concentrations (model minus satellite). Concentration is measured in percentages (%); (b) First empirical orthogonal function in model deviation from satellite data (model minus satellite).

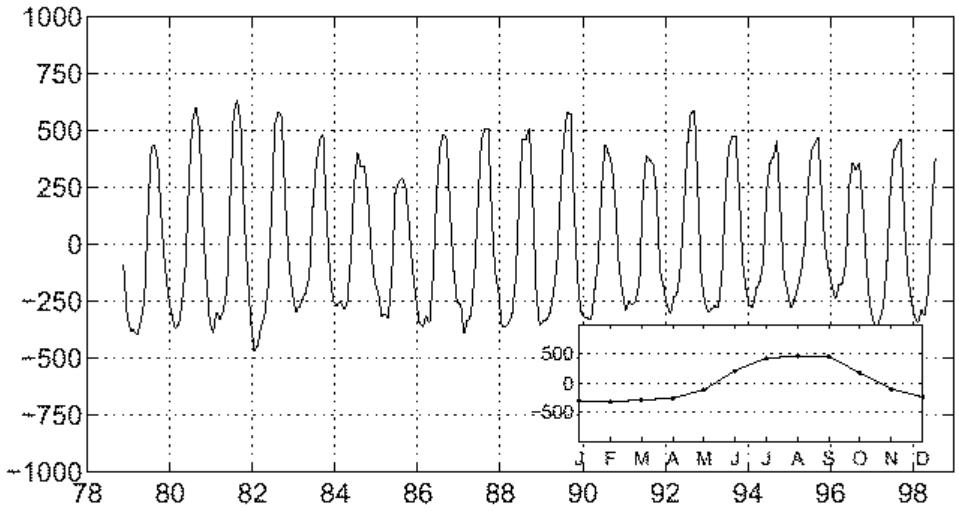

Figure 31: First principal component of model deviation from satellite data. First mode contributes 28% to the total variation of the model deviation. The inset shows the average seasonal cycle.

Figure 30 a shows the areas that have a bias towards too low or too high sea ice concentrations. It is evident, as it was from sea ice extent and sea ice area, that the model has generally too low sea ice concentrations. In the Barents Sea, the Fram Strait and along the coast of east Greenland the model shows, on average, an ice concentration deficit in excess of 30%. The mean model deviation is less pronounced (a deficit of 10-15%) in the Davis Strait, along the coast of Newfoundland, and in a sector from the Beaufort Sea along the Siberian Coast towards the Laptev Sea. There are also some regions with positive deviation, but these are small compared to the regions with negative values

The anomaly data set used in the PC analysis was created by subtracting the mean model deviation from the model-deviation data set. The resulting data set contains information on the seasonal variation in the model deviation. The first and strongest mode (measured as contribution to the variance of the data set) explains 28% of the model-deviation variance. The first EOF is shown in Figure 30 b, and the first PC is shown in Figure 31 with an inset of its average seasonal cycle. The first PC shows a similar pattern from year to year, and the first mode describes the seasonal variation of the model deviation. By using the mean deviation and the first PC analysis mode, a reconstruction of the model deviation is obtained. The mean value of the first PC has negative values in the period November-May (see inset in Figure 31). This means that the red/yellow areas in the first EOF in Fig. 30 b contribute negatively to the model deviation for this time of the year. Since the mean deviation in Fig. 30 a is mostly negative in the regions which are red/yellow in the first EOF, the red/yellow areas in Fig. 30 b indicate too low sea ice concentrations in the model during winter. The blue areas in the first EOF contribute positively in November-May, but since the mean deviation is negative in these areas the resulting approximation to the model deviation is close to zero.

From these observations we conclude that the model has to low winter time sea ice concentrations in the Barents Sea and the Southeast Coast of Greenland (up to 60% underestimate), on the coast of Newfoundland, in the Labrador Sea and in the Odden ice tongue between Iceland and Spitsbergen (up to 30% underestimate). A similar analysis for the period June - October show that the first PC multiplied with its EOF give values in the red/yellow regions in Fig. 30 b which more or less cancels with the values in the same regions in the model mean deviation, whereas the blue regions in Fig. 30 b will have too low sea ice concentrations in summer. This means that the model has too low summer time sea ice concentrations in the Fram Strait (up to 80% underestimate), and in the blue area stretching from the Beaufort Sea to the Kara Sea (up to 50% underestimate). From the PC analysis we see that the strongest model underestimate (in summer and winter) occurs along the sea ice margin. The regions with the strongest underestimate from the PC analysis indicate a receded ice edge as compared to satellite data. In addition the model show too low sea ice concentrations within the ice pack in summer.

5.6 Multi-year ice area

Ice thickness is a prognostic variable in the sea ice model, but ice thickness observations are not possible to obtain from the SMMR/SSMI sensors. To quantify changes in the composition of the ice cover using passive microwave data, the area of Multi-Year Ice (MYI) can be considered. With MYI we mean sea ice which has survived at least one melt season. We still consider sea ice in the region common to both satellite coverage and model domain as presented in the beginning of section 4.

To obtain an estimate of the MYI area from the model we consider two approaches: The first approach is based on the results of Johannessen et al. (1999), which propose that the minimum summer ice area is a good estimate of the MYI area. In this approach, the MYI area in the model is set equal to the area of sea ice with a thickness in excess of 0.5 m at the time of sea-ice area minimum. The minimum sea ice area may not be entirely descriptive of the area of ice that survives summer melt, since the ice still melts or freezes in different parts of the ice pack. This is the reason for choosing the 0.5 m cutoff thickness, as it ensures that we really have ice surviving the melt season in our calculations.

The second method for calculating MYI area calculates the time of the Local Temporal Minima (LTM) in each grid cell of the model. LTM is the time during summer when the local sea ice concentration starts to increase, and will be different for different locations in the ice pack. The total sea ice area from this approach is the sum of the model grid cell sea ice areas at LTM. The LTM approach gives a sea ice area that corresponds well with the MYI area (Gloersen et al., 1992).

In Figure 32 we have plotted the two model derived estimates of MYI area along with SMMR/SSMI MYI area, the latter taken from Johannessen et al. (1999). For the SMMR/SSMI MYI area, each of the five individual monthly means from November to March are plotted each winter, along with the average winter-MYI area estimated from these five monthly means. As we can see the two methods for the model (the bars in the figure) give approximately the same results and show the same variation, with the LTM area being slightly smaller. The satellite MYI area differs considerably from the model MYI area ($2x10^6$ km^2). This is to be expected because the largest errors and largest anomalies of the sea ice area occur during summer, and because the model MYI area is highly dependent upon the minimum sea ice area in summer.

Note the low values of MYI area in winter 81/82 and 82/83, corresponding with minimum in sea ice extent and volume in 1982 (see Figures 26 and 28). The model needs several years to rebuild the ice volume lost due to the high temperature anomalies in the NCEP forcing in 1979-1982, but in the period starting at about 1984 the model performs better. For the entire period November 1978.July 1998 the correlation between the model MYI area and winter- averaged satellite-derived MYI area is 0.48, while for the period 1984-1998 the correlation is 0.59.

The MYI area is related to the total volume of the sea ice. Since MYI is typically thicker than FYI, a reduction of MYI area could reflect changes in the mean thickness of the perennial ice (Johannessen et al., 1999). The trend in the simulated MYI area over the time period 1984-1998 is -30.000 km^2/yr, whereas the reduction in MYI area from satellite data over the same time period is -32.000 km^2/yr, which corresponds well with that of the model. To assess changes in the simulated ice thickness we start by considering two estimates of model MYI thickness. First, a mean spatial MYI thickness which is the MYI volume divided by MYI extent, this will include the zero thickness of open water areas when calculating the mean thickness. Secondly, we consider a mean intrinsic MYI thickness which we define as MYI volume divided by MYI area, an estimate of the average thickness of the MYI ice floes. The trend of the model in both mean spatial and intrinsic MYI thickness is -2cm/yr for the time period 1984-1998.

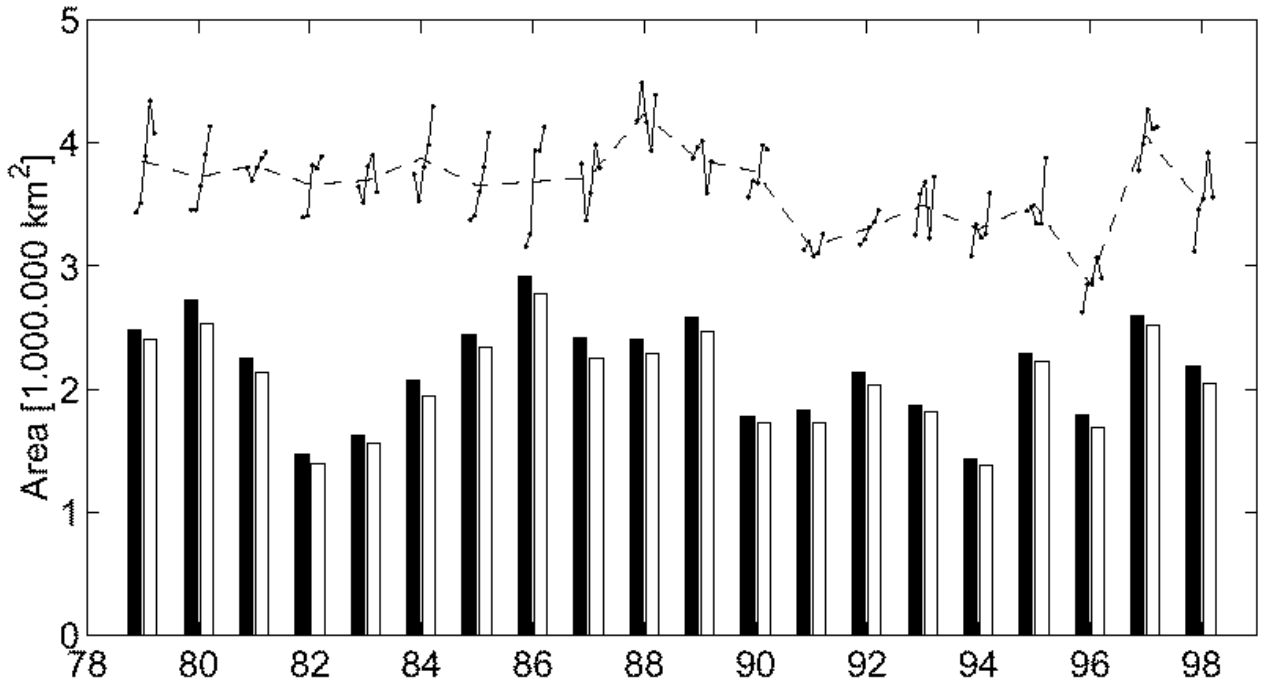

Figure 32: Estimated MYI area from model and satellite data. Bars are from model, where the white bar is from LTM procedure and the black bar is obtained with cutoff thickness of 0.5m at the time of minimum sea ice area. The broken lines are individual measurements of MYI area each winter from SMMR/SSMI sensors, whereas the dashed line is the mean value of the individual SMMR/SSMI MYI areas each winter.

In Rothrock et al. (1999) it is estimated that there has been an average reduction in ice thickness of approximately -4 cm/yr from the 1958-1976 period to the 1990s, a result based on sonar drafts obtained during submarine cruises. The data is mostly gathered in September months and data gathered in nearby months are extrapolated to September values by utilizing a modeled seasonal cycle of ice thickness. Ice thickness estimates are also available from the Russian "North Pole" drifting stations (Nagurnyi et al., 1994), for the time period 1970- 1991. The Russian data are based on surface measurements of elastic-gravity waves in the ice. Utilizing a dispersion relation one can find spatially-averaged estimates of ice thickness and the measurements indicate a reduction of the average ice thickness of - 0.5 cm/yr over the time period 1970-1991. We find that the simulated MYI thickness trends (- 2 cm/yr) is of the same sign and comparable magnitude as the two measured trends (- 4 cm/yr and - 0.5 cm/yr), but the different time periods considered for model and measurements restrict a more rigorous comparison.

A comparison between model and values from (Rothrock et al., 1999) for a common period can be done in the 1990s. The 1990s data from (Rothrock et al., 1999) are originally from the SCICEX cruises in 1993, 1996 and 1997 and show a mean thickness of 2.0 m (mean draft multiplied with 1.12). The mean spatial MYI thickness of the model has a value of 1.6 m, while the intrinsic MYI thickness has a value of 2.4 m, and consequently bracket the 2.0 m estimate of (Rothrock et al., 1999). The (Rothrock et al., 1999) ice thickness trend over the three years show a decrease in mean ice thickness of -10 cm/yr, whereas the model shows a slightly positive trend in MYI thickness over this period (mean spatial MYI thickness trend - 0.3 cm/yr, mean intrinsic MYI thickness trend - 1 cm/yr).

5.7 First results from assimilation of satellite data into the ice-ocean model

Assimilation of SSM/I data into the ice-ocean model has been prepared by the analyses described in sections 1 – 6, whereas the actual assimilation ice extent and ice area has not yet been implemented. This is part of K. A. Lisæters Dr. Sc. Thesis and will be done in 2002 – 03. However, assimilation of ice thickness data have been done, mainly as part of an ESA study (Sandven et al., 2001) which has been focussed on use of ice thickness data from CRYOSAT. The ESA project has developed simulated ice thickness data for the Arctic which are similar to the ice thickness products which CRYOSAT is expected to deliver.

In this study simulated sea ice thickness data were assimilated into a coupled sea ice/ocean model to investigate the sensitivity of using CRYOSAT-like data in sea ice modelling (Fig. 33). Several experiments were performed to assess the impact of this assimilation on the model state by varying the observation error variance as shown in Table 5.2. Example of error variance for the observations and the model run in the E11 experiment is shown in Fig. 34.

Table 5.2 List of assimilation experiments carried out

Experiment ID	Year	Observation variance	Additional comments
E10	1987	-	No assimilation
E11	1987	$\sigma^2_{h_{obs}} = 1 \times^* \sigma^2_{h_{obs}}$	
E12	1987	$\sigma^2_{h_{obs}} = 4 \times^* \sigma^2_{h_{obs}}$	
E13	1987	$\sigma^2_{h_{obs}} = .25 \times^* \sigma^2_{h_{obs}}$	
E14	1987	$\sigma^2_{h_{obs}} = 100 \times^* \sigma^2_{h_{obs}}$	
E20	1990	-	No assimilation
E21	1990	$\sigma^2_{h_{obs}} = 1 \times^* \sigma^2_{h_{obs}}$	
E22	1990	$\sigma^2_{h_{obs}} = 4 \times^* \sigma^2_{h_{obs}}$	
E23	1990	$\sigma^2_{h_{obs}} = .25 \times^* \sigma^2_{h_{obs}}$	

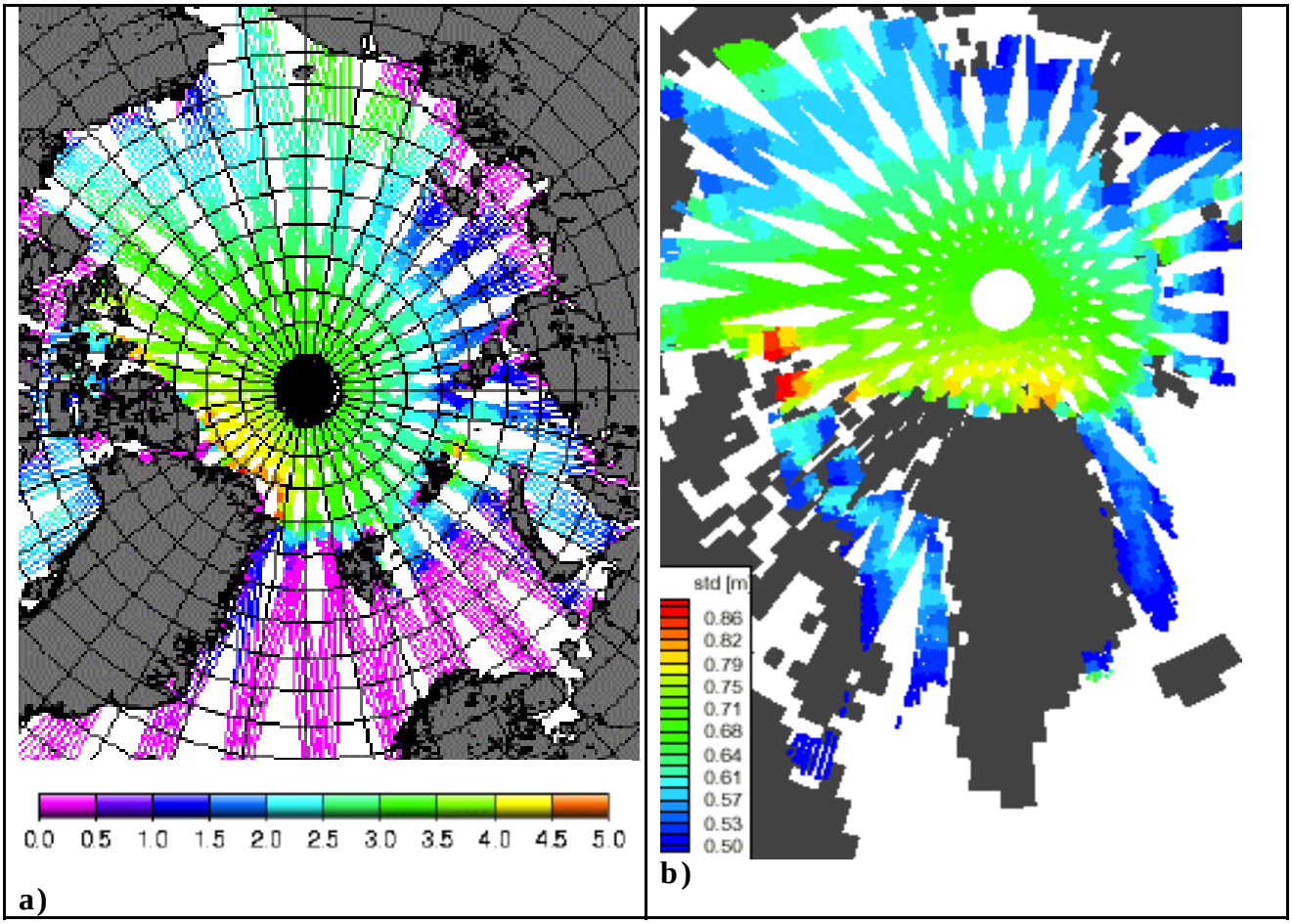

Figure 33. (a) Simulated CRYOSAT data based on climatological ice thickness for the Arctic for the two first weeks of May, resampled to the CRYOSAT orbits for the same period; (b) Standard deviation of the input data after processing with CRYOSAT algorithms including spatial averaging.

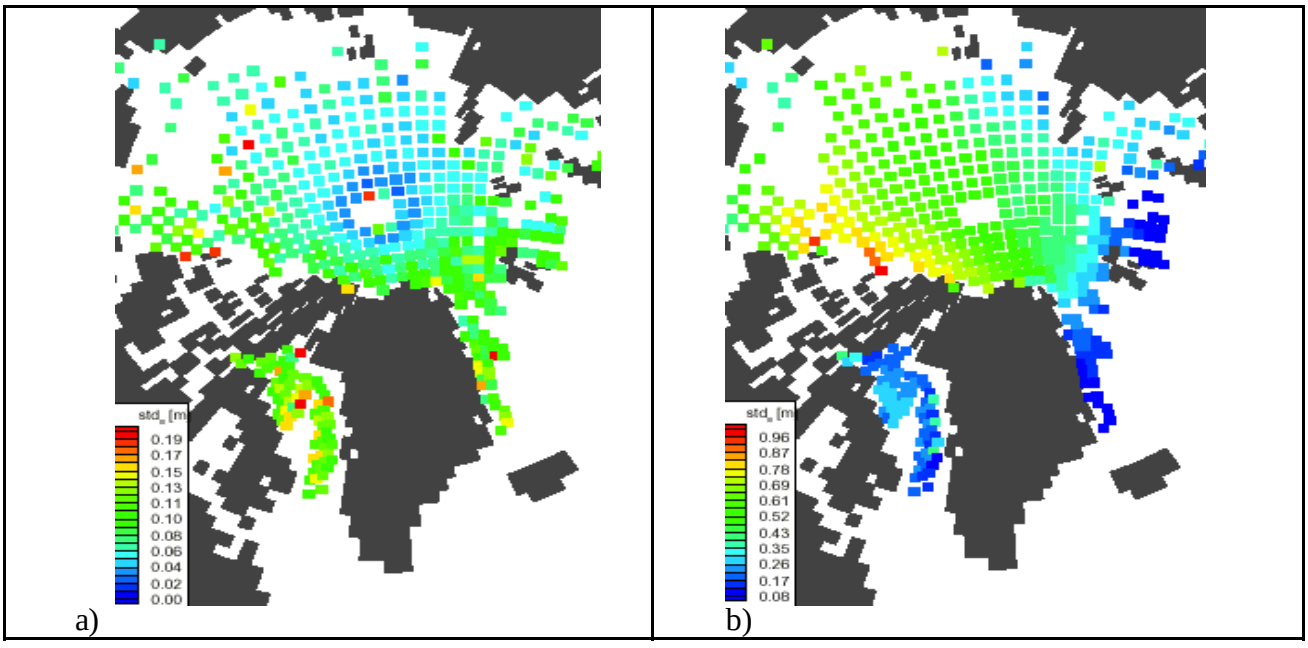

Figure 34. (a) Observed error variance for experiment E11; (b) Model error variance for the same experiment

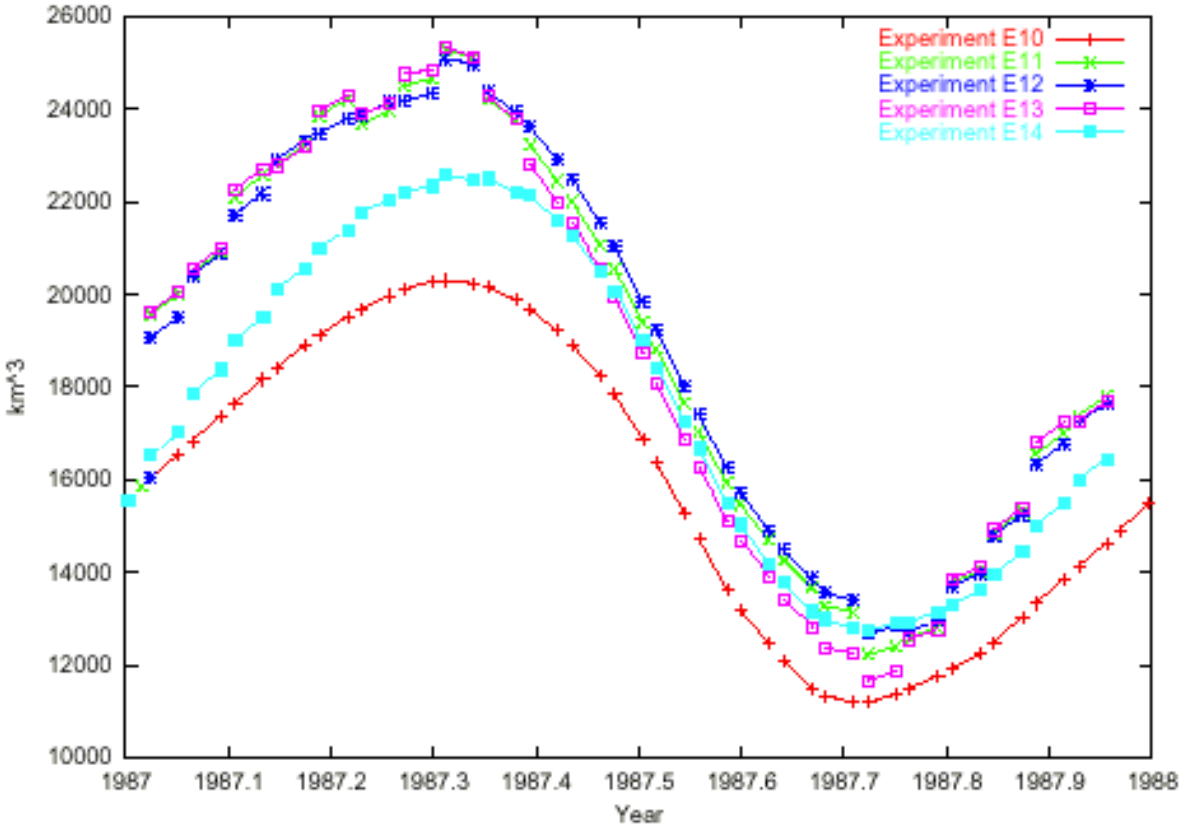

a)

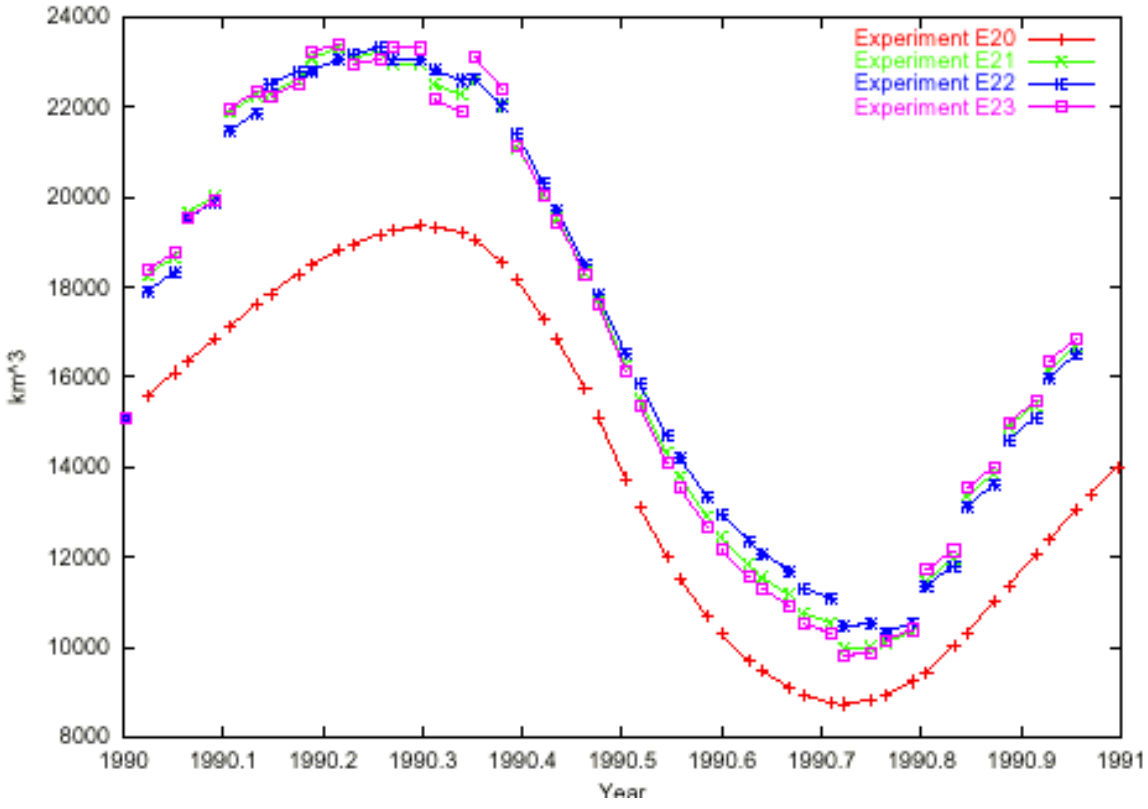

b)

Figure 35. Annual cycle of the total ice volume for 1987 (a) and 1990 (b) from the model simulations without assimilation (red lines) and for three assimilation experiments with different observation error variance (see Table 5.2)

The model experiments were performed for two years, 1987 (a year with relatively much ice – low NAO year) and 1990 (a year with relatively little ice – high NAO year). The ice volume growth and decay for the two years are shown in Fig. 35. Specifically we varied the observation error variance by multiplying it with factors in the range from 0.25 to 100 to examine the effect it had on the assimilation step. The assimilation scheme chosen for the experiment was the Optimal Interpolation (OI) scheme. The time step in the assimilation scheme was 15 days, except in the melt season when no data were available.

The experiments performed in this study have shown that the synthetic observations of ice thickness have an error variance which is low enough to have a strong impact on the analyzed ice thickness fields in the analysis scheme. The experiments showed that only a few assimilation steps were required to obtain e-folding of the RMS distance between the modeled and the observed ice thickness field, using the original error variance of the observations, which represent a typical measurement sample error of 0.5 m. In this case the experiments showed that the data had a strong "pull" on the model state. Similar results were obtained for the experiments where the error variance was multiplied by a factor of 0.25 and 4. However, when this factor was increased to 100 (corresponding to a typical measurement sample error of ≈ 5 m), the experiments showed that it would take at least 20 analysis updates to obtain an e-folding of the RMS distance. This translates into 1500 days of model run to obtain the e-folding, not taking into account the melt period when no observations are available, indicating that the data had much weaker "pull" on the model state.

The conclusion of the assimilation experiments for ice thickness, with the given assimilation method and data updated every 15 days, is that a data field with measurement error of ≈ 1 m will have significant effect on the analyzed fields.

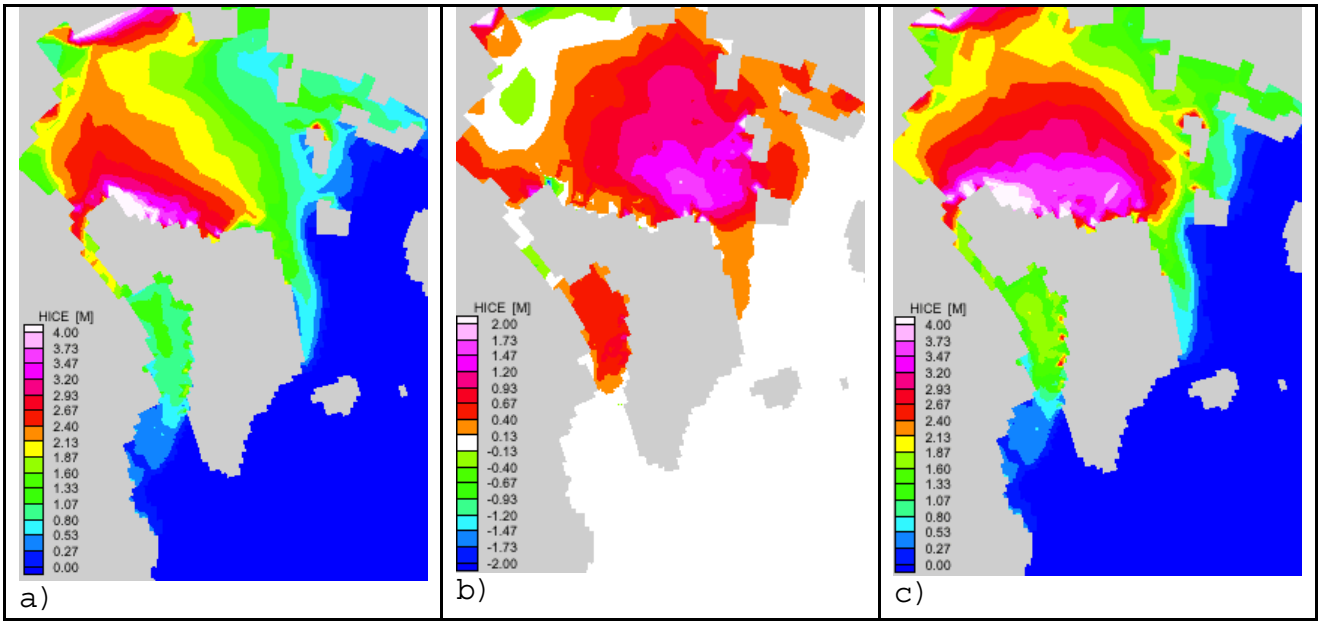

Figure 36. (a) Example of ice thickness forecasting based on the model alone; (b) the update ice thickness field from data, showing that most areas have increased ice thickness while a few places have decreased ice thickness, and (c) final result of data assimilation from experiment E11. Since the E11 experiment has much small error variance in the data than in the model estimates, the update strongly pulls the model ice thickness towards the observed ice thickness for all regions.

The assimilation experiments showed that also other variables were affected. For example when ice was introduced close to the marginal ice zone, SST was reduced and SSS was increased. Also ice concentration is updated, with higher values in the marginal ice zone and lower values in the interior of the Arctic, where ice thickness was increased. The OI method tries to estimate these error statistics by

using an ensemble which is fixed in time, and with samples from a seasonal cycle of the model. The real error statistics for Arctic regions should be expected to show strong spatial and temporal variations related among other things to the positioning of the ice edge. Such behaviour cannot be correctly portrayed by the OI method.

This type of multivariate data assimilation scheme has, to our knowledge, not been used with ice variables before. The results are encouraging, and the shortcomings of the scheme is mainly due to the choice of the ensemble members. Future work should try to utilise a more realistic ensemble of members to better be able to describe the error covariance matrix. This will give more realistic updates for model fields associated to ice thickness through covariances in this matrix.

5.8 Links to related projects

Most of the work on modelling, data analysis and data assimilation in task 3 has been done with funding from Norwegian Research Council through the Ph. D. Scholarship for Knut A. Lisæter. The first results of this work are given in a paper submitted to JGR (Lisæter et al., 2002). The ESA project related to CRYOSAT preparation, reported in 5.7, is relevant because it gives the first results of data assimilation of ice thickness data in a coupled ice-ocean model. This work is recently presented in a report by Sandven et al., 2001. The contribution from Norwegian Space centre to this task has been used in the analysis of satellite data (SSM/I ice concentration from 1978 to 2000) to assess and validate the ice-ocean model.

Relevant publications:

Lisæter, K. A., Johannessen, O. M., Drange, H., Evensen, G., and Sandven, S. (2000). Comparison of modeled and observed sea ice concentration and thickness fields in the Arctic. J. Geophys. Res. (Submitted).

Sandven, S. et al., 2001. The quantification of the importance of the sea ice budget in the climate system. ESA contract no. 13971/00/NL/DC, Final Report. NERSC Technical report no. 207, November 2001.

6. Subcontract to Vladimir N. Kudryavtsev

In order to build up improved SAR retrieval algorithms for the seas surface, Dr. Vladimir N. Kudryavtsev from Marine Hydrophysical Institute (Sebastopol)/ Nansen International Environmental and Remote Sensing Center (St. Petersburg), who has first class expertise on SAR modelling, has visited NERSC for about two weeks in 2001, giving several lectures on topics related to SAR imaging of the sea surface. Ths modelling expertise is necessary to establish algorithms to derive quantitative estimates of currents, fronts and other sea surface parameters which are not yet well retrieved from SAR images.

The abstract of two topics are presented below:

6.1 A semi-empirical model of the normalized radar cross section of the sea surface

Multi-scale composite models based on the Bragg theory are widely used to study the normalized radar cross-section (NRCS) over the sea surface. However, these models are not able to reproduce correctly the NRCS in all configurations and wind-wave conditions. Our improved model takes into account, not only the Bragg mechanism, but also the non-Bragg scattering mechanism associated with wave breaking. The NRCS is assumed to be the sum of a Bragg part (2-scale model) and of a non-Bragg part. The description of the sea surface is based on the short wind wave spectrum (wavelength from few millimeters to few meters) developed by Kudryavtsev et al. (1999), and wave breaking statistics proposed by Phillips (1985). We assume that non-Bragg scattering is supported by quasi-specular reflection from very rough wave breaking patterns and that the overall contribution is proportional to the white cap coverage of the surface. A comparison of the model NRCS with observations is presented. We show that neither pure Bragg nor composite Bragg model are able to reproduce observed feature of the sea surface NRCS in wide range of radar frequencies, wind speeds, and incidence and azimuth angles. The introduction of the non-Bragg part in the model gives an improved agreement with observations.

A single model was built to explain on the same physical basis, both the background behavior of the NRCS and its variations caused by the upper ocean phenomena. Some examples of application of developed model to interpret the sea surface radar signature are given.

6.2 Air-sea interaction: wind over wave coupling approach

Part 1: Spectrum and other statistical properties of the sea surface;
Part 2: Turbulent airflow and the sea surface drag;
Part 3: The impact of dominant surface waves.

This series of three lectures describes recent studies related to one of the intriguing aspect of the air-sea interaction, notably the wind over wave coupling. The general goal is to build a coupled model, which should self-consistently describe dynamical and aerodynamical properties of the sea surface and characteristics of turbulent airflow. In part 1: "Spectrum and other statistical properties of the sea surface" a physical model of the wind waves in the wavelength range from a few millimeters to a few meters is proposed. The shape of the spectrum is found as solution of the energy balance equation accounting for the main source/sink of wave energy. Model spectra are compared with available measurements in a wide range of wind speeds and fetches obtained in laboratory and real conditions.

On one hand, wind input is the main energy source governing the waves. On the other hand interaction of the air flow with wind waves determines the sea surface drag and momentum flux in the turbulent atmospheric boundary layer. In part 2: "Turbulent airflow and the sea surface drag" various mechanisms supporting sea surface drag and their relation to the surface statistical properties are discussed. Viscous surface stress, wave-induced momentum flux and momentum flux due to the airflow separations are the main components responsible for the sea surface drag. The significance of

each of these components at various wind/wave and environmental conditions is discussing. Model predictions of the sea surface drag compare with field data.

Impact of dominant surface waves (wave of the spectral peak and swell) on the shorter surface waves, turbulent airflow and the sea surface drag are discussed in the part 3. There are at least two aspects of this problem. First aspect relates to the modulation problem. Dominant waves disturb atmospheric boundary layer and modulate shorter wind waves affecting aerodynamical roughness of the wavy surface. It results in strong modification of the turbulent boundary layer, affecting both short waves and wind growth of dominant waves. The second aspect of the problem relating to the direct and indirect (via modulation of short waves and airflow) impact of dominant waves on the sea drag is also discussed

Vladimir N. Kudryavtsev has delivered material for a series of lectures on air-sea interaction and SAR modelling which will be prepared for use in new SAR retrieval algorithms and for education and training. This is planned to be done in 2002 – 2003.

7. Conclusions and recommendation for further work

7.1 The MARSAS system

The first part of this work has been focused on defining a concept for MARSAS as a SAR analysis system which should enable the user to ingest different types of SAR data, perform calibration and geolocation, apply SAR algorithms, integrate meteorological and oceanographical data, perform analysis with existing tools (i.e. Matlab) and combine SAR with other satellite data (optical and infrared images, scatterometer, altimeter data, etc.). The users should not only be scientists but also operational entities and other professional users with background in oceanography and/or meteorology who are active users of marine data. MARSAS should function as an overall coordinating tool where use of SAR algorithms is a central element. To use SAR algorithms it is often required to use temperature, wind, currents and other metocean data either as input to the algorithms or for validation of the algorithm output. With ENVISAT data it will be possible to observe the ocean surface with SAR, infrared radiometer and optical imager at the same time. This requires tools for synergetic use and analysis of data from several sensors. MARSAS will facilitate such synergetic analysis of ENVISAT data. MARSAS will have a user interface that makes it possible to access other tools (image processing software, GIS, statistical analysis packages) as well as ocean and ice simulation models. Thereby, MARSAS can be further developed into an operational monitoring and forecasting system.

An overall concept for operational monitoring and forecasting services have been defined which consists of three levels:

Level 1: Overall monitoring and forecasting system (the extended MARSAS system)
Level 2: From observations to geophysical parameters (the core MARSAS system)
Level 3: Algorithm level

The MARSAS system will consist of several modules:

A *Data Exchange Module* is needed for ingestion of new data sets from various data providers, and for exporting data in digital form to other information systems or project repositories. A *Data Storage & Retrieval Module*, including a *Marine DataBase*, will be the central module in MARSAS. Its main responsibility is to structure observations and estimates of marine environmental parameters in a way that facilitates integration of data from different sources. In addition, it must provide the other modules with capabilities for permanent storage and selection of data based on user-defined criteria.

The *Analysis Module* will contain a suite of algorithms and models that process, extract or forecast a marine parameter using data from the Marine DataBase. This module will include tools for format conversion, resampling, etc., that are needed to harmonise the legacy algorithms and models within the MARSAS data structure. Likewise, data tranformations tools will be needed in the *Presentation Module*, which will offer presentation and visualisation facilities needed to assist the operator in

interpreting and quality controlling observations and estimates. Finally, the *Monitoring and Forecasting Module* uses the other modules to run operational services.

The overall system on Level 1 will interact with the MARSAS core system (Level 2) which will provide data and information products needed for the delivering monitoring and forecasting to specific end-user groups.

Status of the MARSAS system implementation and remaining tasks to complete MARSAS are reviewed in Table 7.1.

Table 7.2 Status of MARSAS system implementation

Service levels and modules	MARSAS elements	Plan and Design	Implementation & Testing	Pre-operational demonstration	Operational system
Level 1[1]	***Overall monitoring and forecasting***				
	High level description of system	yes	-	-	-
	Links to all required elements	yes[1]	yes[1]	yes[1]	no
	Fully operational system	yes[1]	yes[1]	yes[1]	no
Level 2[2]	***Processing to geophysical parameters***	yes	yes	no	no
	Methodology to derive parameters from several types of data (EO and non-EO)	yes	yes	no	no
	Processing and interpretation of data	yes	yes	no	no
	Synergetic use of several data sources	yes	no	no	no
	Application examples: sea ice, wind, slick	yes	yes	no	no
Level 3 [3]	***Algorithm level***				
	CMOD wind algorithm	yes	yes	no	no
	Sea ice classification	yes	yes	yes	no
	Sea ice kinematics	yes	yes	yes	no
	Slick detection and classification	yes	yes	no	no
	Other SAR algorithms including ASAR	yes	yes	no	no
	Other algorithms from optical/IR images	yes	yes	no	no
Module 1	***Data Exchange Module***	yes	no	no	no
Module 2	***Data Storage and Retrieval Module***	yes	no	no	no
Module 3	***Analysis Module***	yes	yes	no	no
Module 4	***Presentation Module***	yes	no	no	no
Module 5	***Monitoring and forecasting module***	yes	no	no	no

[1] Level 1 is not addressed in this project, but it is developed and demonstrated in DIADEM and TOPAZ projects coordinated by G. Evensen, NERSC

[2] Level 2 is developed in this project for three SAR applications: sea ice monitoring, wind reteival and oil slick. Other applicaions for SAR and optical/IR sensors have not been included in this project.

[3] Level 3 is focussing on developing and testing each algorithm. This work is mainly done in the related projects funded by ESA, EU and Norwegian Research Council.

Table 7.1 shows which elements of MARSAS have been completed and to what extent. The other elements, indicated by "no" in the table, will be developed within the framework of ongoing (IWICOS and MARSAS) and new (DISMAR) EO-related projects at NERSC.

Most of the implementation work have been concentrated on the Analysis Module, which have been developed for Sea Ice applications, Wind retrieval applications, and partly for SAR oil spill. The underlying software tools are the ESA SAR Toolbox, IDL, Matlab and retrieval algorithms which can also be programmed in Fortran, C or other languages. Further development of MARSAS need to develop also the other modules, and to exploit Internet and Java technologies. It is recognised that most information services today are under restructuring and transformation to be able to use these technologies.

With regards to cooperation with other partners, we have had meetings with Kongsberg Spacetec to discuss how the SAR application modules of MARSAS can be integrated into the MEOS hardware/software system which Kongsberg Spacetec produces and exports. We have agreed to cooperate in joint proposals to build and demonstrate an integrated system. Further work is needed to stimulate this cooperation. A concrete project is necessary to implement in order to make process to develop an integrated system in conjunction with MEOS.

The SAR ice monitoring service has been more or less in idle mode in the last three years, mainly because use of SAR data is expensive whereas ice maps from other satellite data (SSM/I, NOAA AVHRR) are offered free-of-charge on Internet. We have had discussion with VNN to push the SAR ice monitoring activities further in Norway when ENVISAT starts to deliver ASAR data. Some SAR ice monitoring activities have been done in conjunction with EU and INTAS/INCO COPERNICUS projects with Russian partners.

SAR oils spill service also needs to be strengthened, and we have had discussions with TSS as well as SFT/Kystverket how to make progress in this direction. From 2002, NERSC will coordinate an new EU-project under GMES called DISMAR, where SAR oils spill monitoring is a central theme. This project will involve several Norwegian institutions: MI, NIVA, SFT/Kystverket and TSS as SAR data provider.

SAR wind applications have been well documented, but the exploitation of this method in services needs to be strengthened. We are in contact with energy companies who are building wind mills in coastal regions, especially NEG Micon in Denmark. It is clear that SAR images in coastal regions can deliver higher resolution wind fields which are useful for the industry, but the cost-benefit of SAR data is questionable. In the marginal ice zone SAR can also provide more accurate wind data, but the application of the method is not adopted in any services yet. With development of sea ice modelling and forecasting, the method is expected to be useful.

In the continuation project for the Norwegian Space Center we propose to incorporate some elements of MARSAS into the work packages which are focused on ENVISAT applications.

7.2 SeaWiFS monitoring of algael blooms

The current algae monitoring system (ALGEINFO – http://algeinfo.imr.no) in Norway is routinely based on a regular network of 29 observational stations along the entire Norwegian coastline and the expert knowledge of the executing organizations. The system has limited early warning capabilities for locations outside the regular observational network, however other field observations may be used from both Norwegian and surrounding countries. The observations used are based on both spices determination, quantitative estimates of the algae blooms (cell-counts) as well as determination of their potential harmfulness. EARLY warning of potential harmful algae blooms is of crucial importance for both the aquaculture industry and authorities in order to implement mitigation actions. Efficient planning and execution of field observational programmes are also necessary under identified HAB events. For both these aspects EO data have under past and current projects documented its usefulness. An international (trans-boundary) monitoring approach including EO-derived environmental information has been developed to achieve earlier warning of potential HAB, necessary for successful mitigation actions and efficient public control and management during emergency situations. Potential benefits of including EO based information is identified for:

- Potential earlier warning of algae blooms
- Better integration of the regional (international) dimension of HABs
- Improved planning and efficiency of *in situ* measurements and sampling
- Improvement of transboundary co-operation with neighbour countries, e.g., Sweden and Denmark, by providing regional information.

Furthermore, integration EO product with numerical forecast models have the potential to improve significantly quantitative assessment and predictions of the bloom transport, development and decay.

Combining EO data from similar sensors from different satellites (e.g., SeaWiFS and MODIS) may lead to improved, albeit irregular temporal/sensor sampling. Nonetheless, it is apparent that the present spaceborne sensor systems have spatio-temporal sampling capabilities that are adequate to meet the monitoring requirements for HAB. However, the dependency of cloud free conditions is a severe limiting factor with increasing importance at higher latitudes.

In this project we have identified, demonstrated and validated the benefit of using satellite Earth observation information in support of an existing decision making processes for disaster management operations, specifically the ALGEINFO HAB monitoring service. We have developed and implemented a pre-operational demonstration towards a sustainable service for harmful algae bloom monitoring and management decision support, related to the effective management of fisheries/aquaculture, public health, and ecosystem problems related to marine HABs. A limiting factor for full acceptance of EO data in the traditional "algae monitoring community" is the precession of the EO observations, i.e. the quantitative accuracy of the measurements, lack of data under cloud covered conditions, sub-surface blooms and the need for field observations in order to specie determine the actual blooms.

The HAB monitoring and warning system has been constructed around a web-page concept. All operations, except the interpretation, have been automated in order to ensure the provision of information within three hours after the acquisition of the satellite data by the receiving station. This automation includes data decoding, processing up to level 2 (bio-geophysical parameters), extraction and mapping, and generation and updating of web-pages. The interpretation and reporting can be performed online, using a number of image-processing and information extraction tools are implemented on HAB web-site.

The capability of the developed system was demonstrated through to effective provision of documented useful information during two HAB events in respectively May 2000 and March 2001. During these events, we were able to monitor the bloom, providing daily information on the extension, progression and movement of the blooms, and even predict the decay of the bloom in May 2000. Significantly, the 2000 bloom was first detected by EO. The Norwegian fisheries authorities have actively used and acknowledged the usefulness of the information provided by the DeciDe-HAB service and are interested in including the service in the future HAB monitoring activities, however this will require dedicated budget allocations, which yet not are confirmed.

Presently, the development of the system into an operational and commercial service is limited due to the costs of accessing and maintaining the only present ocean colour sensor having the level of reliability required for the activity, namely SeaWiFS. Accordingly the SeaWiFS data have strict limitations with respect to non-scientific (defined by OrbImage as commecial) use of the data in near real time. This is a hampering factor for a wider near real-time dissemination of the information gathered in the current project. In the future, other alternatives will be available such as the data from MERIS and MODIS. However, Terra-MODIS has not reached this level so far. A number of actions are foreseen in order to improve the current prototype toward an operational and commercial service. The main aspect of the proposed development is summarised in Table 7.2.

Table 7.2. Action plan for further development of the DeciDe-HAB service.

Service component	Actions
Products	
Information content	Digest-maps (risk assessment map) should be generated operationally and become the main information product in the future. Satellite-derived maps would still be accessible through links for advanced user and analysts.
Accuracy	The accuracy achieved so far for the SST products is sufficient for the application conducted. Chlorophyll-a products required a better accuracy in order to achieve a reliable identification and monitoring of HAB events. According to the specification and coastal zone specific algorithm, we may expect a breakthrough on this matter from the ENVISAT MERIS sensor products
Algorithms	We may be able in the future to use indifferently SST products from AVHRR or ATSR (AATSR) sensors. Although ATSR algorithm is much more complex than the split-window method used in the processing of AVHRR data, the capability offered by ENVISAT to provide simultaneous images from AATSR and MERIS may greatly ease the interpretation of surface ocean features, and thus help in performing better analysis of certain algal bloom events. New algorithms for processing case II water (PML bright pixel algorithm, and artificial neural network) should lead to improved estimates of chlorophyll-a in coastal waters as well as a number of new ocean colour products such as suspended sediment and yellow substances, which may greatly help to analyse the biogeochemical state of the water masses, with direct implications on the reduction of false alarm rate of algal bloom events.
Functioning	
Availability	SeaWiFS data are available free-of-charge for science and educational purpose to NASA authorised users. Near real-time access to SeaWiFS data has been granted to the DeciDe-HAB project through special agreement. More general utilisation of SeaWiFS derived products requires to pay a fee to sensor data owner - Orbimage Corp. It is not clear that near real-time provision might be provided by the data distributor. Therefore the DeciDe-Hab service can not been pursued on the basis of SeaWiFS ocean colour data. Other ocean colour data such as MODIS and OCM have shown problem while access liability and operational use if of concern. We expect ESA policy regarding ENVISAT data provision and distribution to allow the continuity of the service regarding specially the provision of ocean colour data.
Timeliness	Calibration and validation of MERIS data will be conducted during spring and summer 2002 in the context of DeciDe-HAB project follow-on.
Reliability	Improved reliability would come from algorithm development, new sensor capability and synergy between monitoring tools. One can expect discrimination of algal family from satellite data to be feasible in the near future (within 5 years), which should lead to better identification of algal bloom type and associated risk. Routinely use of satellite-derived information with ecosystem models should also lead to better monitoring and hopefully forecast of HAB events. These aspects will be integrated to the current service when validated.

Table 7.2 follow-on	
Service component	**Actions**
Supply chain	
Distribution performance	The current system has reached a high performance level, which is adequate for the pursued application. We would have to ensure for similar performance to be achieved with other satellite data sources and suppliers.
Automation level	According to the current level of automation, improvement can only be made on the data analysis part, as well as the production of information digest (e.g. regional risk map). Such development is nowadays limited by the accuracy of the information produced. The less accurate the information the more human input required in the analysis process.
Packaging of the information	Currently the information packaging is based on the data sources. In the future, it would be certainly recommended for the temporal aspect of the information to be the main classification criterion, while information might originate from many different sources including, *in situ* and satellite observation, and model simulation and forecasting.
Benefit	
Cost effectiveness	In the future, coast-effectiveness might only be guaranteed if remote sensing data is provided free-of-charge or at very low cost. Multiplying the number of monitoring area may increase the number of potential customer while extending the period of operation of the service
Competitiveness	An optimal service should focus on interpretation of algal bloom events, prediction of events and assessment of risk. This would require the integration of remote sensing, *in situ* and modelled data. Such an integrated service may result from the merging of different existing services. Merging services will result in decreasing possible competitiveness for the monitoring of a given region.
Customer readiness	
Awareness	It would be easy to improve awareness about the HAB service by conducting market prospecting and promotion. This has not been done in the frame of DeciDe-HAB because of the restricted aspect of a large part of the information provided.
Acceptance	Operational authorities has accepted and endorsed the service development through the project. The next step is toward the possible funding entities, e.g. government and ministries, insurance company, aquaculture co-operatives, etc.
Customers	We foresee that the main customers of the type of service implemented in this project would be national authorities in charge of environmental, health and food-consumption issues, as well as industries such as insurance company, fisheries and aquaculture groupments, possibly tourism industry.

7.3 Assimilation of sea ice data in a climate model

In this study we have validated a coupled sea ice-ocean model using data from satellite- borne passive microwave sensors. The sea ice model is similar to one of the models in the SIMIP project (Kreyscher et al., 2000), so our results should be of general interest for users of this type of sea ice model. The first conclusion is that the model underestimates sea ice concentration in the Arctic. This can be seen

through the too low values of sea ice extent and area. The underestimate of these values vary between 1.000.000 km^2 and 2.000.000 km^2, which is significant compared to the total values of sea ice area and extent which lie between 5.000.000 km^2 and 10.000.000 km^2 over the area studied. As a consequence, the model estimate of MYI area is too low by about 2.000.000 km^2, which is significant compared to the satellite derived MYI area of approximately 4.000.000 km^2.

Using principal component analysis the locations of the model errors in sea ice concentration in winter and summer are identified. In winter and summer we find that some of the error occur along the sea ice margin with a too receded ice edge. In summer we also see that there is too low sea ice concentrations within the ice pack, resulting in too much open water. The analysis of sea ice area and extent is carried out over the period 1984-1998 instead of the entire available period 1978-1998 due to apparent errors in the NCEP temperature fields for the period 1979-1982. The observed anomalies in sea ice area and extent are picked up by the model, with a correlation coefficient between model and satellite sea ice extent of 0.68 over the period 1984-1998. The model and satellite trends in sea ice extent are also very similar for this period with values of -12.000 km^2/yr and -11.000 km^2/yr, respectively. It is also shown that the model performs well in describing trends in MYI area for this period: The model predicts a MYI area trend of -30.000 km^2/yr, while the satellite data give a MYI area trend of -32.0000 km^2/yr.

Although the model underestimates the sea ice concentration, it is encouraging that the trends are so accurately represented by the model, and that there is a high correlation between model and satellite sea ice extent. We briefly considered the average thickness of MYI and compared this to measurements from submarine sonar data (Rothrock et al., 1999), and surface elastic-gravity waves (Nagurnyi et al., 1994). The simulated MYI thickness trend of 2 cm/yr over the period 1984-1998 is bracketed between the trend of Rothrock et al. (1999) (- 4 cm/yr, 1950s-1990s) and that of Nagurnyi et al. (1994) (- 0.5 cm/yr, 1970-1991). Although the considered time periods are different, this shows that the model thickness trend is of comparable magnitude and the same sign as the measured thickness trends.

There can be several reasons for the detected model error in sea ice extent and area. First of all the model is relatively coarse, which naturally restricts its comparison with the more well-resolved satellite data. The parameterization of leads might be improved by using lateral melting rates as in Maykut and Perovich (1987), which could correct the model error within the ice pack in summer. In addition the thermodynamic part of the sea ice model (see appendix) does not include the effect of thermal inertia. For smoothly varying atmospheric forcing, thermal inertia is less important, but for the forcing used in this study the lack of thermal inertia could explain some of the error. The rheology used in the sea ice model could also lead to errors, due to slow response in numerical implementations of the Viscous-Plastic rheology. The Elastic-Viscous-Plastic rheology of Hunke and Dukowicz (1997) could perhaps give some improvement here, although this is speculations at the present stage.

Aside from the inherent aspects of the sea ice model, one should not forget that the forcing fields of the ocean-sea ice model also can lead to errors. For instance, apparent errors in the temperature fields were detected for the winters 1979-1982. In addition, the downward short wave radiation from NCEP data seems to be too high (e.g. Maslowski et al. (2000)), which is of importance for the sea ice concentration in summer. The latter observation can be partly compensated by adjusting the snow and ice albedo values, but such an adjustment would most likely fail if other forcing fields are applied. Furthermore, errors in the sea ice field can also be introduced by the ocean component of the model system, through errors in the water mass characteristics.

We conclude that the coupled ice-ocean model gives a fairly good description of the sea ice variation and trends in the Arctic, with the main problem being an underestimate of the sea ice concentration. The presented model can be implemented in a fully coupled climate model with some performance tuning integrations, and possibly implementing some of the suggested modifications.

The assimilation experiments for ice thickness, using the Optimal Interpolation method with data updated every 15 days, showed that a thickness data field with measurement error of $\approx$ 1 m will have significant effect on the analysed fields. Experiments using measurement error of $\approx$ 0.5 m, only needed a few assimilation steps to obtain e-folding of the RMS distance between the modelled and the observed ice thickness field, indicating a strong "pull" of the model state towards the observation fields. There exist some uncertainty in the actual model error statistics for a data assimilation method such as Optimal Interpolation. Using a data assimilation scheme with an Ensemble Kalman Filter

could give more correct statistics for the model error. However, for the model described in this study, using the EnKF will have a high demand on computer resources.

In 2002 – 2005 the plan is to use results from the modelling and assimilation work fro 1999 – 2001 to buld up an integrated monitoring and forecasting system for the Fram Strait region. The system will combine satellite-derived ice parameters, in situ ocean and ice parameters from buoys and model simulations from the coupled ice-ocean model. A part of this plan is to run assimilation experiments in the Arctic and Nordic Seas with a coarse-resolution model (50 – 100 km grid cells) nested with a higher resolution model (10 – 20 km grid cells) for smaller areas such as in the Fram Strait and around Svalbard. Assimilated data will come from satellites (sea ice parameters) and from anchored oceanographical moorings with Upwrad-Looking Sonars providing data on ice thickness and ice drift. The high resolution model will be tested with use of ice drift and other ice parameters from ASAR. The results of the assimilation experiments will be evaluated and assessed with respect to forecasting and with respect to the usefulness of assimilating satellite-derived data. This work will be done in cooperation with the Norwegian Polar Institute which has responsibility for monitoring ice fluxes in the Fram Strait and other climate related parameters in the region. A joint proposal from NERSC, NPI and other Norwegian partners is in preparation to the Norwegian Research Council to develop an integrated monitoring system for the Fram Strait. It is also proposed to develop ice forcasting for the Svalbard area with input data from ASAR. This will be done in cooperation with MI. Specific tasks related to acquisition, processing and retrieval of ice parameters from ENVISAT / RADARSAT wide-swath SAR data will be included in the Norwegian Space Center prohect for 2002 – 2005.

7.4 Air-sea interaction and SAR modelling

The first year of cooperation with Dr. Vladimir N. Kudryavtsev in 2001 have been very useful in building up expertise and compentence in SAR ocean modelling which is very important for algorithm development of SAR ocean and ice applications. It has been a problem for many years that there is no solid theoretical fundament for the SAR retrieval algorithms, especially for surface currents, fronts and slicks. It is planned to continue this cooperation in the period from 2002 to 2005 with the objective to establish new and better SAR retrieval algorithms which can applied to ASAR data.

7.5 Development of satellite data products for operational oceanography

The development of ENVISAT applications for use in operational oceanography will be central theme in the coming years for the Nansen Center. This development will take place in the context of GMES and EuroGOOS. Within EuroGOOS the importance of space observations have been explicitly defined in a number of documents such as "*Operational Ocean Observations from Space*" (EuroGOOS, 2001), and conference proceedings by Johannessen et al., 1997 a, b, c; 2002). The Nansen Center is coordinator of two new EU-projects under GMES: MERSEA (Marine EnviRonment and Security for the European Area) and DISMAR (Data Integration System for Marine Pollution and Water Quality). NERSC will also participate actively in GODAE (Global Ocean Data Assimilation Experiment).

In addition to ENVISAT Europe will contribute significantly to space observations of the ocean in the next decade, through ESA's Earth Explorer Programme, the GMES initiative, etc. Important new satellites for ocean observation will be CryoSat, SMOS and GOCE. A review paper on Europe's emerging capabilities to observe the ocean from space is recently published by Johannessen et al., (2001). The paper which is attached in the Appendix, gives a background for planning activities to build up ocean observing systems.

8. Ackowledgement

In addition to the Norwegian Space Center, the work in this project has been supported by Norwegian Research Council, ESA and EU.

9. References

Aagaard, K., and Carmack, E. C. (1989). The role of sea ice and other fresh water in the arctic circulation. J. Geophys. Res., 94(C10), 14485-14498.

Aiken, J., Moore, G.F., Trees, C.C., Hooker, S.B. And Clark, D.K., 1995, The SeaWiFS CZCS-type pigment algorithm. NASA Technical Memorandum 104566, Vol. 29, Ed Hooker, S.B. and Firestone, E.R., NASA Goddard Space Flight Center, Greenbelt, Maryland, USA.

Aksnes, D. L., Ulvestad, K.B., Baliño, B., Berntsen, J., Egge, J. and Svendsen, E, 1995. Ecological modelling in coastal waters : Towards predictive Physical-Chemical-Biological simulation models. *Ophelia*, 41, 5-36.

Anderson, L., and Dyrssen, D. (1989). The arctic seas. Van Nostrand Reinhold Company.

Arbetter, T. E., Curry, J. A., and Maslanik, J. A. (1999). Effects of rheology and ice thickness distribution in a dynamic-thermodynamic sea ice model. J. Phys. Oceanogr., 29 (10), 2656-2670.

Aukrust, T., and Oberhuber, J. M. (1995). Modeling the greenland, iceland, and the Norwegian seas with a coupled sea-ice mixed-layer isopycnic ocean model. J. Geophys. Res., 100(C3), 4771-4789.

Bentsen, M., Evensen, G., Drange, H., and Jenkins, A. D. (1999). Coordinate transform on a sphere using conformal mapping. Mon. Wea. Rev., 127, 2733-2740.

Bishop C.M., "Neural networks for pattern recognition". Oxford: Clarendon Press, 1995, 481 p.

Bjørgo, E., Johannessen, O. M., and Miles, M. W. (1997). Analysis of merged SMMR-SSMI time series of Arctic and Antarctic sea-ice parameters 1978-1995. Geophys. Research Letters, 24 (4), 413-416.

Bleck, R., Rooth, C., Hu, D., and Smith, L. T. (1992). Salinity driven thermocline transients in a wind- and thermohaline-forced isopycnic coordinate model of the north atlantic. J. Phys. Oceanogr., 22, 1486-1505.

Bleck, R., and Smith, L. (1990). A wind-driven isopycnic coordinate model of the north and equatorial atlantic ocean. 1. model development and supporting experiments. J. Phys. Oceanogr., 95, 3273-3285.

Bogdanov, A.V., et al. Automatic Classification of RADARSAT SAR Images of the Northern Sea Route. In Proceedings of IGARSS'99, Hamburg, Germany, June-July 1999.

Broecker, W. S., Peteet, D. M., and Rind, D. (1985). Does the ocean-atmosphere system have more than one stable mode of operation? Nature, 315, 21-26.

Cattle, H., and Crossley, J. (1995). Modeling arctic climate-change. Phil. Trans. R. Soc. Lond. A, 352, 201-213.

Clarke, G.L., Ewing, G.C. & Lorenzen, C.J., 1970, Spectra of backscattered light from the sea obtained from aircraft as a measure of chlorophyll concentration. Science, 167, pp. 1119-1121.

Comiso, J. C. (1990). Arctic multiyear ice classification and summer ice cover using passive microwave satellite data. J. Geophys. Res., 95(C8), 13411.

Drange, H. (1999). Regclim ocean modelling at NERSC. In RegClim, regional climate development under global warming (pp. 93{102). Norwegian Institute for Air Research, Kjeller, Norway.

Drange, H., and Simonsen, K. (1996). Formulation of air-sea fluxes in ESOP2 version of MICOM (Tech. Rep. No. 125). Nansen Environmental and Remote Sensing Center, Bergen, Norway.

Dundas, I., Johannessen, O. M., Berge, G. and Heimdal, B. R., 1989. Toxic Algal Bloom in Scandinavian Waters, May-June 1988. Oceanography, 2(1): 9-14.

Durand, D., D. Pozdnyakov, S. Sandven, F. Cauneau, L. Wald, K. Kloster, M. Miles, 1999a. Characterisation of inland and coastal waters with space sensors. Final report of CEO study, NERSC Tech. Rep. No. 164, 175 p.

Durand, D. L.H. Pettersson, O.M. Johannessen, E. Svendsen, H. Søiland and M. Skogen, 1999b. Satellite observation and model prediction of toxic algae bloom. In the refereed book "*Operational Oceanography – Extending the limits of predictability*", proceedings of the Second International Conference on EuroGOOS", in press.

Espedal, H. A., O.M. Johannessen, J.A. Joahnnessen, E. Dano, D.R. Lyzenga and J.C. Knulst, COASTWATCH'95: ERS _ SAR detection of natural film on the ocean surface, *J. Geophys. Res.*, vol.103, no.C11, 1998.

Espedal, H.A., and Johannessen O.M., Detection of oil spills near offshore installations using synthetic aperture radar (SAR), *Int. J. of Remote Sensing*, vol.21, no.11, pp.2141-2144, 2000

EuroGOOS: The Science Base of EuroGOOS, publication no. 6, September 1998, 58 pp.

EuroGOOS: Operational Ocean Observations from Space, publication no. 16, May 2001, 131 pp

Evensen, G., 1997, Advanced data assimilation for strongly nonlinear dynamics. *Mon. Weather Rev*., 125:1342-1354.

Furevik, B. and E. Korsbakken. Wind field retrieval from Synthetic Aperture Radar compared to Scatterometer wind field during the ERS Tanem Phase. Proceedings of the 27th International Symposium on Remote Sensing of Environment, 8 - 12 June 1998, Tromsø, Norway, pp. 201 - 204.

Furevik, B. R., and Korsbakken, E. (2000). Comparison of derived wind speed from Synthetic Aperture Radar and Scatterometer during the ERS Tandem Phase, *IEEE Transactions on Geoscience and Remote Sensing*, Vol. 38, No. 2, pp. 1113-1121.

Furevik, B. R, O. M. Johannessen and A. D. Sandvik, 2001, "SAR-retrieved wind in polar regions – comparison with in situ data and atmospheric model output", accepted in *IEEE Transactions on Geoscience and Remote Sensing*.

Furevik, B. R and H. Espedal, Wind energy mapping using Synthetic Aperture Radar, Canadian Journal of Remote Sensing, in press (2002).

Gargett, A. E. (1984). Vertical eddy diffusivity in the ocean interior. J. Mar. Res., 42, 359{393.

Gaspar, P., Gregories, Y., and Lefevre, J.-M. (1990). A simple eddy kinetic energy model for simulations of the oceanic vertical mixing: Tests at station Papa and long-term upper ocean study site. J. Geophys. Res., 95(C3), 16179-16193.

Gloersen, P. (1995). Modulation of hemispheric ice cover by ENSO events. Nature, 373, 503-505.

Gloersen, P., Campbell, W. J., Cavalieri, D. J., Comiso, J. C., Parkinson, C. L., and Zwally, H. J. (1992). Arctic and Antarctic sea ice, 1978-1987: Satellite passive-microwave observations and analysis. National Aeronautics and Space Administration.

Hamre, T. et al. FET-ENVIS: Extraction and synthesis of environmental information from multi-source data. Final report on EU contract IST–1999-29005, 34 pp. NERSC Technical report no. xxx, 34 pp, December 2001..

Harder, M. (1996). Dynamik, rauhigkeit und alter des meereises in der arktis. Unpublished doctoral dissertation, Alfred-Wegner-Institut fur Polar- und Meereisforschung, Bremerhaven, Germany.

Hibler, W. D., III. (1979). A dynamic thermodynamic sea ice model. J. Geophys. Res., 84, 815-846.

Holland, D. M., Mysak, L. A., and Oberhuber, J. M. (1996). An investigation of the general circulation of the Arctic Ocean using an isopycnal model. Tellus, 48A, 138-157.

Hooker, S.B., Esaisas, W.E., Feldman, G.C., Gregg, W.W. and McClain, C.R., 1992. Volume 1: An Overview of SeaWiFS and Ocean Color. *SeaWiFS Technical Report Series*, National Aeronautics and Space Administration Technical Memorandum 104566, Washington.

Hunke, E. C., and Dukowicz, J. K. (1997). An elastic-viscous-plastic model for sea ice dynamics. J. Phys. Oceanogr., 27, 1849-1867.

Hurrell, J. (1995). Decadal trends in the North Atlantic oscillation. Science, 269, 676-679.

IOCCG Working Group, 1998, Minimum requirements for an operational ocean-colour sensor for the open ocean. Report of an IOCCG working group held in Villefranche-sur-Mer, France, October 6-7.

Johannessen, J. A. et al. Observing the Ocean from Space: Emerging Capabilities in Europe. In *Observing the Oceans in the 21st Century* (Eds. Koblinsky and Smith), pp. 198 – 208, 2001.

Johannessen, O. M., Miles, M. W., and Bj¯rgo, E. (1995). The arctic's shrinking sea ice. Nature, 376, 126-127.

Johannessen, O. M., L. H. Pettersson, E. Bjørgo, H. Espedal, G. Evensen, T. Hamre, A. Jenkins, E. Korsbakken, P. Samuel and S. Sandven. A review of possible applications of satellite earth observation data within EuroGOOS. In "Operational Oceanography. The Challenge for European Co-operation" (Editor in Chief: J. H. Stel). Proceeedings of the First International Conference on EuroGOOS, 7 -11 October 1996, The Hague, The Netherlands. Elsevier Oceanography Series, No. 62, 1997 a, pp. 192 - 205.

Johannessen, O. M., A. M. Volkov, V. D. Grischenko, L. P. Bobylev, S. Sandven**,** K. Kloster, T. Hamre, V. Asmus, V. G. Smirnov, V. V. Melentyev and L. Zaitsev. ICEWATCH - Ice SAR monitoring of the Northern Sea Route. In "Operational Oceanography. The Challenge for European Co-operation" (Editor in Chief: J. H. Stel). Proceeedings of the First International Conference on EuroGOOS, 7 -11 October 1996, The Hague, The Netherlands. Elsevier Oceanography Series, No. 62, 1997 b, pp. 224 - 233.

Johannessen, O. M., E. Korsbakken, P. Samuel, A. D. Jenkins and H. A. Espedal. COASTWATCH: Using SAR imagery in an operational system for monitoring coastal currents, wind, surfactants and oil spills. In "Operational Oceanography. The Challenge for European Co-operation" (Editor in Chief: J. H. Stel). Proceeedings of the First International Conference on EuroGOOS, 7 -11 October 1996, The Hague, The Netherlands. Elsevier Oceanography Series, No. 62, 1997 c, pp. 234 - 242.

Johannessen, O. M., Shalina, E. V., and Miles, M. W. (1999). Satellite evidence for an arctic sea ice cover in transformation. Science, 286 (5446), 1937-1939.

Johannessen, O. M., E. Bjørgo and H. Espedal (1999) SatWind Final Report, NERSC tech. report No. 171, European Commision, Joint Research Center, Contract no. 14427-1998-10 F1 PC ISP NO.

Johannessen, O. M. and E. Bjørgo. Wind energy mapping of coastal zones by synthetic aperture radar (SAR) for siting potential wind mill locations. Int. J. Remote Sensing, Vol 21. No. 9, pp. 1781 – 1786, June 2000.

Johannessen, O. M., and Miles, M. (2000). Arctic sea ice and climate change, will the ice disappear in this century ? Sc. Progr., 83 (3), 209-222.

Johannessen, O. M. and S. Sandven. Monitoring of the Arctic Ocean. In Proceedings from the EuroGOOS Conference in Rome 1999 (in press 2002).

Kalnay, E., Kanamitsu, M., Kistler, R., Collins, W., Deaven, D., Gandin, L., Iredell, M., Saha, S., White, G., Woollen, J., Zhu, Y., Chelliah, M., Ebisuzaki, W., Higgins, W., Janowiak, J., Mo, K. C., Ropelewski, C., Leetmaa, A., Reynolds, R., and Jenne, R. (1996). The NCEP/NCAR reanalysis project. Bull. Am. Met. Soc, 77, 437-471.

Korsbakken, E. J. A. Johannessen and O. M. Johannessen. Coastal wind field retrievals from ERS synthetic aperture radar images. J. Geophys. Res., Vol. 103, No. C4, p. 7857 - 7874, 1998.

Kloster, K., Flesche, H. and O. M. Johannessen (1992), "Ice motion from airborne SAR and satellite imagery". In Adv. Space Res., vol.12, no. 7, pp. 49-53.

Kreyscher, M., Harder, M., Lemke, P., and Flato, G. M. (2000). Results of the sea ice model intercomparison project: Evaluation of sea ice rheology schemes for use in climate simulations. J. Geophys. Res., 105(C5), 11299{11320.

Lekve, O., 1998. Oppsummering av algeinvasjonen i mai. Fiskets Gang 5: 4-6.

Lemke, P., Hibler, W. D., Flato, G., Harder, M., and Kreyscher, M. (1997). On the improvement of sea-ice models for climate simulations: the sea ice model intercomparison project. Ann. Glaciol., 25, 183-187.

Levitus, S., and Boyer, T. P. (1994). World ocean atlas 1994 volume 4: Temperature. NOAA Atlas NESDIS 4, Washington, D.C.

Levitus, S., Burgett, R., and Boyer, T. P. (1994). World ocean atlas 1994 volume 3: Salinity. NOAA Atlas NESDIS 3, Washington, D.C.

Manabe, S., Spelman, M. J., and Stouffer, R. J. (1992). Transient responses of a coupled ocean-atmosphere model to gradual changes of atmospheric CO 2, II, seasonal response. J. Clim., 5, 105-126.

MARSAIS Consortium: MARSAIS First Annual Consolidated Report – Scientific-technical Part, January 2002, 39 pp. (see http://www.nersc.no/~marsais/).

Maslowski, M., Newton, B., Schlosser, P., Semtner, A., and Martinson, D. (2000). Modeling recent climate variability in the Arctic ocean. Geophys. Research Letters, 27 (22), 3743-3746.

Maykut, G. A., and Perovich, D. K. (1987). The role of shortwave radiation in the summer decay of a sea ice cover. J. Geophys. Res., 92(C7), 7032-7044.

Midttun, L. (1985). Formation of dense bottom water in the Barents Sea. Deep Sea Res., 32, 1233-1241.

Mitchell, J., Johns, T., Gregory, J., and Tett, S. (1995). Climate response to increasing levels of greenhouse gases and sulphate aerosols. Nature, 376, 501-504.

Nagurnyi, A. P., Korostelev, V. G., and Abaza, P. A. (1999). Wave method for evaluating the effective ice thickness of sea ice in climate monitoring. Bull. Russian Acad. Sci. Phys. Supp. Phys. Vib., 58, 168-174.

Nagurnyi, A. P., Korostelev, V. G., and Ivanov, V. V. (1994). Multiyear variability of sea ice thickness in the Arctic basin measured by elastic-gravity waves on the ice surface. Meteor. Hydrol., 3, 72-78.

New, A., Bleck, R., Marsh, Y., Huddleston, M., and Barnard, S. (1995). An isopycnic model study of the north atlantic. part 1: Model experiment. J. Phys. Oceanogr., 25, 2667-2699.

Parkinson, C. L., Cavalieri, D. J., Gloersen, P., Zwally, H. J., and Comiso, J. C. (1999). Arctic sea ice extents, areas, and trends, 1978-1996. J. Geophys. Res., 104(C9), 20837-20856.

Pettersson, L.H., D. Durand, O.M. Johannessen, E. Svendsen, and H. Søiland, 2000. Satellite observations and model predictions of toxic algae bloom in coastal waters. In proceedings of the 6th Int. Conference on Remote Sensing of Marine and Coastal Environments, Charleston, South Carolina, 1-3 May 2000. In press.

Pettersson, L.H., D. Durand, O.M. Johannessen, E. Svendsen, H. Søiland, and P. Regner 2000. Satellite observations and model predictions of toxic algae bloom in coastal waters. In proceedings of the 28th Int. Symposium on Remote Sensing of Environment, Cape Town, South Africa, 27-31 March 2000. In press.

O'Reilly, J.E., Maritorena, S., Harding, L., Magnuson, A. And Zibordi, G., 1999, Ocean Chlorophyll 2 version 2. Presentation given at the SeaWiFS Post-launch Algorithm Mini-Workshop, NASA/GSFC, 28-29 July.

O'Reilly, J.E., Maritorena, S., Mitchell, B.G., Siegel, D.A., Carder, K.L., Garver, S.A., Kahru, M. and McClain, C., 1998, Ocean color chlorophyll algorithms for SeaWiFS. Journal of Geophysical Research, 103, C11, 24937-24953.

Pettersson, L.H., 1995, Remote Sensing of Coccolithophorid blooms: The European *Emiliania Huxleyi* programme - EHUX. Final report to CEC under contract MAST-CT92-0038, September 1995.

Pettersson, L.H., Kloster, K. and Johannessen, C.E., 1992: Promotion of remote sensing for identification of pollution. Test Case: "Monitoring of a toxic algae bloom." NERSC report for EOS Ltd. under ESA/ESTEC Contract no. 9678-91-NL-JG(SC). November, 1992.

Pettersson, Lasse H., Dominique D. Durand, Einar Svendsen, Thomas Noji, Henrik Søiland, Steve Groom and Samantha Lavender: DECIDE for near-real-time use of ocean colour data in management of toxic algae blooms - Definition and Design document. NERSC Technical report No. 186 to European Space Agency, September, 2000.

Pettersson, L. H., et al., DeciDe for near real time use of ocean colour data in management of harmful algael blooms. ESA Contract no. 13662/99/I-DC, Final Report. NERSC Technical Report no. 200, September 2001, 79 pp.

Preisendorfer, R. W. (1988). Principal component analysis in meteorology and oceanography. Elsevier Science Publishing Company, New York.

Quilfen, Y., ERS-1 off-line wind scatterometer products, IFREMER Technical report C1-EX-MUT-CD0000-03-IF, 1995

Rothrock, D. A., Yu, Y., and Maykut, G. A. (1999). Thinning of the Arctic sea-ice cover. Geophys. Research Letters, 23, 3469-3472.

Ruddick, K.G., Ovidio, F. and Rijkeboer, M., 2000. Atmospheric correction of SeaWiFS imagery for turbid coastal and inland waters. *Applied Optic*s, 29(6): 897 – 912.

Sandven, S, O. M. Johannessen, Martin Miles, Lasse H. Pettersson and K. Kloster. Barents Sea seasonal ice zone features and processes from ERS-1 SAR. J. Geophys. Res. Vol 104, No. C7, p. 15843 – 15857, July 15, 1999.

Sandven, S, O. M. Johannessen and H. Drange. The Arctic test case: Use of satellites and models in ice monitoring and forecasting. In *Operational Ocean Observations from Space*, p. 108 – 117. Report from EuroGOOS Conference 5 – 6 October 2000 at EUMETSAT, Darmstadt, Germany. EuroGOOS Publication no. 16, 131 pp, May 2001.

Sandven, S, T. Hamre, et al., Integrated Weather, Sea Ice and Ocean Service System (IWICOS). Baseline System Report, NERSC Technical Report no. 204, 67 pp, December 2001. (see http://www.nrsc.no/~iwicos)

Sandven, S. et al., 2001. The quantification of the importance of the sea ice budget in the climate system. ESA contract no. 13971/00/NL/DC, Final Report. NERSC Technical report no. 207, November 2001.

Skogen, M. and Søiland, H., 1998. *A user's guide to NORWECOM v2.0, the NORWegian ECOlogical Model system*. Tech. rep. Fisken og Havet, 18. Institute of Marine Research, Norway.

Skogen, M. D., Svendsen E., Berntsen J., Aksnes D. and Ulvestad K., 1995. Modelling the Primary Production in the North Sea using a Coupled Three-dimensional Physical-Chemical-Biological Ocean Model. Estuarine, *Coastal and Shelf Science*, 41, 545-565

Smolarkiewicz, P. K., A Fully Multidimensional Positive Definite Advection Transport Algorithm with Small Implicit Diffusion, J. Comp. Phys., 54,325-362, 1984

Svendsen, E., Kloster, K., Farrelly, B., Johannessen, O. M., Johannessen, J. A., Campbell, W. J., Gloersen, P., Cavalieri, D., and Matzler, C. (1983). Norwegian remote sensing experiment: Evaluation of the nimbus 7 scanning multichannel microwave radiometer for sea ice research. J. Geophys. Res., 88(C5), 2781-2791.

Thompson, D. W. J., and Wallace, J. M. (1998). The arctic oscillation signature in wintertime geopotential heights and temperature fields. Geophys. Research Letters, 25, 1297-1300.

Vinnikov, K. Y., Robock, A., Stouffer, R. J., Walsh, J. E., Parkinson, C. L., Cavalieri, D. J., Mitchell, J. F. B., Garrett, D., and Zakharov, F. (1999). Global warming and northern hemisphere sea ice extent. Science, 286 (5446), 1934-1937.

Wackerman, C. and D. L. Miller (1996), "An Automated Algorithm For Sea Ice Classification in the Marginal Ice Zone Using ERS-1 Synthetic Aperture Radar Imagery". ERIM Technical Report.

WEMSAR Consortium: WEMSAR Second Annual report - Scientific-technical Part, March 2002, 31 pp (see http://www.nrsc.no/~wemsar)

Yang, J., and Neelin, J. D. (1993). Sea-ice interaction with the thermohaline circulation. Geophys. Research Letters, 20, 217-220.

Appendix

Reprint of

Johannessen, J. A. et al.

Observing the Ocean from Space: Emerging Capabilities in Europe.

Article published in *Observing the Oceans in the 21st Century* (Eds. Koblinsky and Smith), pp. 198 – 208, 2001

2.7

Observing the Ocean from Space: Emerging Capabilities in Europe

Johnny Johannessen,[1,2] Christian Le Provost,[3] Helge Drange,[1] Meric Srokosz,[4] PhilipWoodworth,[5] Peter Sclüssel,[6] Pascal Le Grand,[7] Yann Kerr,[8] Duncan Wingham,[9] and Helge Rebhan[10]

[1]Nansen Environmental and Remote Sensing Center, Bergen, Norway, [2]Geophysical Institute, University of Bergen, Norway, [3]LEGOS, Toulouse, France, [4]Southampton Oceanographic Centre, UK, [5]Proudman Oceanographic Laboratory, UK, [6]EUMETSAT, Darmstadt, Germany, [7]Ifremer, Brest, France, [8]CESBIO, Toulouse, France, [9]University College London, UK, [10]ESA-ESTEC, Noordwijk, The Netherlands.

Abstract – *During the first decade of the 21st century Earth observation from satellites will be faced with two major demands: provision of continuity missions and launch of new exploratory missions. This paper addresses European plans for new Earth observations in the context of Ocean Observing System for Climate at the onset of this new millennium. It highlights three quantities: ice mass fluctuations, sea surface salinity and fine resolution marine geoid. Their relevance and importance for climate are briefly reviewed in connection with important processes such as, for example, thermohaline circulation, sea level change, and evolution of large scale salinity events. The associated satellite mission concepts approved by ESA are then presented in light of their objectives, scientific observation requirements and degree of complementarity and synergy with other relevant missions.*

Introduction

During the first decade of this millennium, relatively long time series (in some cases almost 30 years) of satellite-derived quantities (including sea surface temperature, ocean wave field, near-surface wind, ocean colour, sea surface topography and sea ice extent, types and concentration) will become available. As an essential element of integrated ocean observing systems (in combination with an *in situ* data collection system and model tools), the need for continuous access to calibrated and corrected satellite data is indisputable. The challenge is, however, to ensure the continuity of existing Earth observation data while at the same time developing new observation techniques.

Three geophysical quantities that in different ways are relevant for important processes within the fields of cryosphere and oceanography will be highlighted in this paper, namely:

- the ice mass fluctuations;
- sea surface salinity; and
- the marine geoid (and steady-state ocean circulation).

So far none of these quantities has been adequately observed from satellite. It is generally agreed that the lack of these observations inhibits the development of scientific interpretation and understanding of basic processes that contribute to the ocean circulation and the effects of the ocean on climate at seasonal to multi-decadal timescales.

In this paper some of the major scientific questions at stake will be reviewed regarding these three quantities followed by a consideration of the associated candidate satellite mission concepts.

Scientific questions

In Table 1 some of the important processes and interactions occurring in the ocean are listed in the context of the three quantities mentioned above.

By gaining new and advanced understanding of these quantities and their associated contribution to the processes listed in Table 1, opportunities for improved seasonal to interannual climate predictions are created. This is further elaborated in the next three sections.

Observing the Oceans in the 21st Century, C.J. Koblinsky and N.R. Smith (Eds), GODAE Project Office and Bureau of Meteorology, Melbourne.

Table 1. Connection between the three geophysical quantities and oceanic processes that in different ways are contributing to the climate

Processes	**Parameters**		
	Ice mass	**Ocean salinity**	**Marine geoid***
Thermohaline circulation	X	X	X
Sea level change	X	(X)	X
Air–sea–ice interaction (+ albedo effect)	X		
Evaporation minus precipitation		X	
Mass and heat transport		X	X
Large-scale frontal dynamics		X	X
Evolution of large-scale salinity event	X	X	

*Note: We are mostly considering the marine geoid in support of radar altimetry.

Sea ice mass fluctuations

The cryosphere has a central role in the Earth's radiation budget imposed by the large albedo due to the presence of ice and snow. In the context of the greenhouse effect, loss of sea ice is predicted to cause a larger warming in the Arctic than elsewhere on the Earth, whereas uncertainty in ice sheet and glacier mass balances are the largest error sources on present sea level change (Wingham, et al., 1999). Moreover, thermohaline circulation and deepwater formation are likely affected by changes in sea ice and ice sheet masses.

Trends in the supply of fresh water from the cryosphere may profoundly affect the characteristics and strength of the thermohaline circulation. Recent analyses have established reductions in the total Arctic sea ice extent of about 3% per decade since 1978 (Bjørgo et al., 1997) while Østerhus et al., (1999) have reported a decreasing trend in overflow of cold (less than 3°C) water from the Greenland–Iceland–Norwegian seas to the North Atlantic over the last 50 years. In cases when the surface water at high latitudes is replaced by fresher water supplied through sea ice and ice sheet melting, the deep-water formation can be reduced or prevented (Aagaard, 1994). Moreover, coupled ocean–atmosphere models show a decline in the Northern Hemisphere poleward transport in response to increased freshwater supply (Manabe and Stouffer, 1988) and/or greatly increased latitudinal variability (Weaver and Sarachik, 1991). Such changes in the present state of the thermohaline circulation pattern are expected to have the greatest impact on areas in northwestern Europe. However, as the current trends in ice mass changes are far from accurately known, the corresponding freshwater fluxes and their quantitative importance on the thermohaline circulation cannot be properly estimated and accounted for in climate models.

Episodical changes in the freshwater and heat fluxes in the Southern Hemisphere are also known to take place. The formation of the Weddell Sea Polyna in the mid-seventies (Zwally et al., 1983) and the collapses of the Antarctic Peninsula ice shelves (Rott et al., 1996) are recent examples. Little is known of the variability and frequency of occurrence of these episodic events, and their consequences on the thermohaline circulation is far from entirely understood.

It is also a challenge to come up with a full explanation for the changes that have taken place in sea level rise in the 20th century as a number of competing geophysical processes, each of which is a complex process in itself, are contributing. Among these are interior Earth tectonics, the redistribution of water from ice sheet and glacier retreat, the rebound of the lithosphere and mantle and the effect of these on the Earth's gravity field, the thermal expansion of the oceans, the extraction of ground water, and changes in coastal sedimentation and erosion. The largest potential source is, nonetheless, the cryosphere. The sea level rise in the 20th century corresponds to approximately 0.2% of the Antarctic Ice Sheet mass. However, little is known about the magnitudes of fluctuations in the ice sheets on this timescale. In comparison, it appears that glacier retreat in Europe and North America may explain 4 cm of the present rise (Meier, 1984), whereas the thermal expansion of the ocean associated with global warming is also estimated to have contributed perhaps 4 cm last century.

Predicting future sea level change depends on better knowledge of fluctuations in marine and land ice mass fluxes. Present observations are

deficient in time and space. Satellite observations are the unique source of these measurements at large space and time scales.

Sea surface salinity

The distribution of salt in the global ocean and its annual as well as interannual variability are crucial in understanding the role of the ocean in the climate system. *In situ* salinity measurements are only sparsely distributed over the oceans. In fact, 1° x 1° boxes distributed over the global oceans show that for only about 70% of them do salinity measurements exist at all (Levitus and Boyer, 1994). A far smaller fraction of such areas has been monitored more than once. This means that the average structures of the ocean salinity field are known to some extent, but details about its variability even on seasonal and interannual scales remain hidden. Consequently the scientific design plan for the Global Ocean Observing System states:

> *The improvement of the ocean salinity data base must have high priority since it is an important constraint in ocean models, an indicator of freshwater capping, and may have predictive uses in the tracking of high latitude salinity anomalies that could affect the thermohaline circulation and the regional climate.*

The joint Argo profiling float program (see Argo Science Team, this volume) and sea surface salinity satellite mission are focused on this priority.

Knowledge of salinity distribution is also necessary to determine the equation of state. For the calculation of dynamic height anomalies the salinity distribution must be known. For instance, when calculating geostrophic currents using satellite altimetric measurements, better knowledge of the ocean salinity structure would improve the accuracy of the estimates (e.g. a 0.5 psu error in sea surface salinity (SSS) accounts for 3.8 cm/s error in geostrophic velocity at 1 km depth calculated from the corresponding surface value).

The need, importance and requirements for SSS observations can be further substantiated (Delcroix and Hénin, 1991; Donguy, 1994; Drange et al., 1999; and Lagerloef and Delcroix, this volume). The SSS varies as a result of exchange of water between the ocean and the atmosphere, via sea ice freezing and melting, and from continental runoff. Salt affects the thermohaline circulation and therefore the distribution of mass and heat. Salinity may control the formation of water masses, which allows its use for tracer studies. Salinity is also thermodynamically important as salinity stratification can influence the penetration depth of convection at high latitudes and may determine the mixed layer depth in equatorial regions.

Positive surface temperature anomalies in the North Atlantic are suggested to be associated with anomalously strong thermohaline circulation (Timmermann et al., 1998). It is possible that the atmospheric response to this is an enhanced North Atlantic Oscillation (NAO). Occasionally a strong NAO, in turn, leads to anomalous freshwater fluxes off Newfoundland and in the Greenland Sea. The resulting surface salinity anomalies are advected by the sub-polar gyre and finally reach the convectively active region south of Greenland (Belkin et al., 1998). The weakening in deepwater formation and subsequent change in thermohaline circulation may reduce the poleward oceanic transport which, in turn, forms negative surface temperature anomalies. The duration of this cycle is roughly 35 years. Whether such a cyclic process was associated with the formation of the observed great salinity anomalies in the North Atlantic during the 1970s is not yet clear.

In tropical areas salinity is useful as an indicator of precipitation and evaporation, thus it plays an important role in studies of surface freshwater fluxes. For example, during heavy rainfall, freshwater lenses are produced on the ocean surface, which are stable features. They mix slowly with the bulk sea water and can persist from hours to weeks depending on the wind speed conditions. Heavy rainfall such as typically encountered in the tropics can cause a drop in surface salinity of 7 psu for short periods and still be 4 psu in hourly averages (Paulson and Lagerloef, 1993). The area coverage of single freshwater lenses is of the order 50–100 km, depending on the size and lifetime of the convective rain cell as well as their horizontal displacement with time. Their role in the formation and maintenance of barrier layers and mixed layer thermodynamics is far from fully understood. The role of salinity and its change by freshwater fluxes at the atmosphere–ocean interface have also to be included for a full understanding of the entire ENSO process (Lukas and Lindstrom, 1991).

Sea surface salinity has not been observed from space so far (except for the very short duration of the *Skylab* experiment in the early 1970s). Such space observations would be very welcome as the current knowledge of SSS is rather poor and insufficient to account for the role of salinity in the ocean climate system.

Marine geoid and steady-state ocean circulation

In the current climate state, the ocean circulation is responsible for half of the poleward heat transport, the other half being contributed by the atmosphere (Peixoto et al., 1992). By the time the warm water from the Gulf Stream has reached northern Europe and the Nordic Seas, the surface water has given up much of its heat to the atmosphere and can subsequently become dense enough to sink through convective overturning and thus maintain the thermohaline circulation pattern. This process takes place during the winter season. However, quantitative knowledge and estimates are incomplete, and predictions of how poleward heat transport and fluxes through the air–sea interface would be modified by enhanced greenhouse forcing are even coarser.

While variations of the sea level and thus of the ocean currents can be derived directly from satellite altimeter data, the absolute value of the ocean dynamic topography, and hence the absolute surface circulation, requires the independent determination of what would be the elevation of an ocean at rest, that is the geoid. The latter is not known at present with sufficient precision. The typical elevation scale of the dynamic topography is of the order of 0.1–1 m, while the precision of present geoid models is on the scale of many ocean circulation features.

With current altimetric missions (such as TOPEX/POSEIDON, ERS-1 and ERS-2) providing such effective measurements of ocean circulation variability, and with future missions (JASON, ENVISAT) likely to continue the measurements well into this century, it is reasonable to ask why oceanographers need to know the mean circulation itself to such spatial detail. There are several reasons, as thoroughly discussed in ESA (1999).

First, modelled and real oceans undoubtedly contain short spatial-scale components of mean flows. It is important to be able to measure the locations and magnitudes of such short-scale features by means of altimetry and gravity, to compare them to information from conventional hydrography, to understand their relationships to bathymetry and other controlling factors, and to assess their importance for oceanic mass and heat flux estimation. It is known that it is through mean flows as well as variabilities (e.g. eddies) that the ocean transports its heat, fresh water and dissolved species and through which it controls climate, and the aggregated short-scale mean flows could prove to be of importance to climate.

Second, it is through instabilities in the mean flows that the ocean generates eddies and that it is possible to generate different degrees of variability in different numerical models depending on the mean flows programmed into them, and on the way in which the factors controlling the means are parameterized (e.g. interactions with bathymetry). Consequently, in dealing with non-linear processes, and in studying transient perturbations of the system, it is essential to start from as good a description as possible. This was essentially the motivation for the WOCE 'decadal snapshot' of the ocean, to provide a dataset on which models might be based with potential for predictive capability.

Third, it is clear that data assimilation schemes for 'ocean forecasting' have reached a stage of development wherein optimal use of altimetric variability information can be achieved as long as the mean ocean state (i.e. the absolute ocean circulation) can be simulated. In this case, the dynamic topography obtained from the mean sea surface height minus the geoid acts as a powerful model constraint on the assimilation of inevitably noisy altimeter variability information, providing a window on ocean processes at depth.

Fourth, knowledge of the short spatial-scale geoid will be essential to computations of fluxes through basin-size oceanic sections, again by providing model constraints to the assimilation of other information (altimetry, hydrography), which will contain measurement uncertainties.

Therefore, it is clear that understanding the mean and the variability of the ocean circulation must go hand-in-hand, particularly with regard to the construction of a next generation of numerical ocean models with the potential for a better description of the role of the ocean in the global climate system. Dedicated satellite gravity field missions will be essential elements in the establishment of such improved understanding.

Satellite mission concepts

The present technology, including use of remote sensing by satellites and a large array of *in situ* measurements (many of which are expendable) as well as the existence of models for climate change prediction and analysis, makes the implementation of a truly global ocean observing system feasible now. But further development is necessary and this relies heavily on more complete and more accurate data sets.

The need to explore new Earth observation capabilities aimed at bringing new scientific data has been elaborated in ESA's Earth Explorer Programme (ESA, 1998) composed of the Opportunity Mission and the Core Mission elements. This program has been drawn up following extensive consultation with the Earth Observation community. It is intended to reflect not only their ideas and aspirations but also to be a response to concerns about climate change and our impact on it. Likewise, the US Earth Observing System (EOS) Science Plan (EOS, 1999) draws the attention to major scientific issues of concern in the context of climate change derived from several years of discussion and debate among the EOS scientific investigators. Additional and complementary views and plans for Earth observations regarding global climate change are implemented among other space agencies including CNES, NASDA, ISRO and EUMETSAT, and are also addressed in the Ocean Theme for the IGOS Partnership (IGOS, 2000).

The geophysical quantities highlighted above are considered by three candidate mission of ESA's Earth Explorer Programme.

- The Opportunity Mission CryoSat will observe fluctuations of ice masses on land and in the ocean.
- The Opportunity Mission SMOS (Soil Moisture and Ocean Salinity) will provide for the first time spaceborne observations of the sea surface salinity (as well as soil moisture over land).
- The Core Mission GOCE (Gravity Field and Steady-State Ocean Circulation) will give new knowledge of the marine geoid with high accuracy and fine spatial resolution.

The objectives and mission concepts for each of these missions are briefly summarized below. (On the website http://www.estec.esa.nl/explorer/ it is possible to obtain regular updates about the evolution of these three missions.) They are complemented by NASA's plans for the Ice, Clouds and Land Elevation Satellite (ICESat) mission, the joint NASA/DLR Gravity Recovery and Climate Experiment (GRACE) mission and also to some extent by the ongoing joint NASA/NASDA Tropical Rainfall-Measuring Mission (TRMM) and its planned follow-on Global Precipitation Mission (GPM).

Sea ice mass fluctuations

The primary goal of the CryoSat mission is to estimate trends in the ice masses of the Earth. This will be achieved by measuring the change in sea ice and ice sheet thickness with a radar altimeter using interferometric and synthetic aperture techniques for resolution enhancement. Of principal importance is the need to determine:

- the regional and basin-scale trends in perennial Arctic sea ice thickness and mass due to global warming; and
- the regional and total contributions to global sea level of the Antarctic and Greenland Ice Sheets.

These objectives are relevant and important to the Climate Variability and Predictability Program (CLIVAR) and the Arctic Climate System Study (ACSYS).

Three operating modes of CryoSat are foreseen: synthetic aperture operation for sea ice with an along-track sampling interval of 300 m, conventional pulse-limited operation for ice sheet interior (and ocean if desired), and dual-channel synthetic aperture/interferometric operation for ice sheet margins (interferometer baseline of 1 m). An illustration of the satellite is shown in Fig. 1.

The CryoSat mission (Wingham et al., 1999) will determine trends in ice mass through repeated measurements of ice thickness during its mission lifetime of about 3 years. A residual uncertainty in the mass and thickness trends of sea ice and land ice will remain at the end of the mission. The scientific requirements of the mission specify the magnitude of this residual uncertainty. It cannot be smaller than the natural variability in thickness. The task is to characterize the natural variability of thickness followed by determination of the measurement accuracy, which makes the residual uncertainty close to the natural variability. This is the required measurement accuracy. These considerations have led to the following science and measurement requirements (specified in Table 2).

Table 2. The Cryosat science and measurements requirements specified for different characteristics spatial scales over sea ice and ice sheets

Requirement	**Arctic sea ice 10^5 km²**	**Ice sheets 10^4 km²**	**Ice sheets 13.8 x 10^6 km²**
Residual uncertainty	3.5 cm/year	8.3 cm/year	1 cm/year (i.e 130 Gt/year)
Measurement accuracy	1.6 cm/year	3.3 cm/year	0.7 cm/year

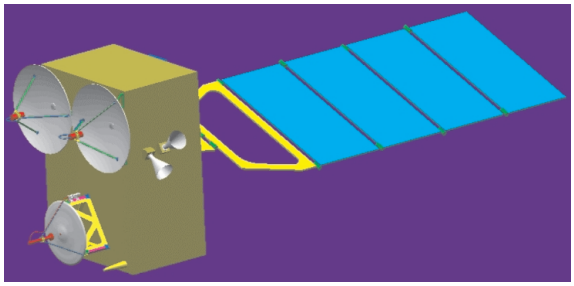

Figure 1. CryoSat satellite configuration.

The CryoSat technical development passed the system design review in February 2001 and is proceeding in compliance with a launch in 2004. CryoSat will provide nearly complete and continuous coverage of the cryosphere, but is limited in its resolution. The US ICESat mission planned for launch in 2002 is of particular complementary importance to CryoSat. ICESat aims to provide details of the sea ice and land ice roughness spectrum by using a fine resolution (100 m scale) laser altimeter technique. The limits imposed by cloud cover (in the Polar regions typically ranging from 50% to 90%) will reduce sea ice thickness measurements and change measurements at fixed ice sheet locations. With a launch date in 2004, combination of the CryoSat radar altimeter and the ICESat laser altimeter data is foreseen.

Sea surface salinity

The primary scientific objectives of the ocean salinity observations provided by the SMOS opportunity mission are, *inter alia*, to:

- improve seasonal to interannual climate predictions by effective use of SSS data to initialize and improve the coupled climate forecast models;
- improve oceanic rainfall estimates and global hydrologic budgets via the new and improved knowledge of the SSS variability;
- monitor large-scale salinity events.

These objectives are particularly relevant for the major international ocean programs and their observing system and experiments planned for the

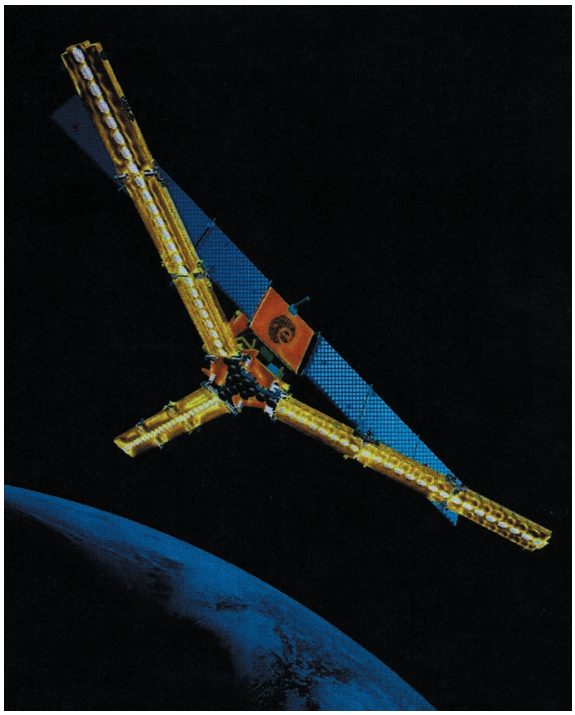

Figure 2. Artistic view of the SMOS satellite with the three-legged (4.5 m) passive microwave L-band antenna (Kerr et al., 1999)

next 5–7 years including the Global Ocean Observing System (GOOS), CLIVAR, the Global Ocean Data Assimilation Experiment (GODAE), and the Global Climate Observing System (GCOS), which is established to coordinate the provision of data for climate monitoring, climate change detection and response monitoring. Moreover, the provision of SSS nicely complements the thermohaline structure observed with the Argo profiling floats (Argo Science Team, this volume). Additional value of SSS data from remote sensing is realized by obtaining better information on the spatial gradients, particularly along-track, and by better space–time resolution over and above that obtained by *in situ* systems such as Argo.

The spatial resolution requirements for spaceborne passive microwave imaging of ocean salinity (and soil moisture) at L-band (= 21 cm)

lead to large antenna apertures such as proposed by the two dimensional interferometric approach for the Microwave Imaging Radiometer Aperture Synthesis (MIRAS) instrument (Martin-Neira and Goutoule, 1997; Kerr et al., 1999). This approach uses a Y-shaped antenna (each arm about 4.5 m long) with equally spaced antenna elements for redundant spacing calibration (Fig. 2). The structure exhibits many advantages in terms of ground resolution and can be accommodated on board a satellite. This instrument will be tilted by 20°–30° with respect to nadir ensuring an incidence angle range from 0° to 50°. The spatial resolution will be 35 km within the central part of field of view with a swath of about 1000 km.

The sensitivity of L-band (1.4 GHz) passive microwave radiometer measurements of oceanic brightness temperature to SSS is well established (Lagerloef et al., 1995). However, the sensitivity is a function of the sea surface temperature (SST) decreasing from 0.5 K/psu in 20°C water to 0.25 K/psu for an SST of 0°C (Skou, 1995; Lagerloef et al., 1995). Hence, strong demands are put on the SSS retrievals from space in polar and sub-polar regions where the water masses are very sensitive to small changes in SSS (below 0.1 psu). Other oceanic factors which will influence the brightness temperature retrievals at L-band are surface roughness (wind speed and direction) and foam. Precise estimates for the uncertainties associated with these features are required in order to obtain sufficiently accurate SSS retrievals from SMOS, in particular since this opportunity mission will not carry a second, higher frequency, antenna.

The characteristics of the surface salinity variability and its effects on the ocean show large regional differences from the equatorial and tropical region via the mid-latitudes to the high latitudes. An overview of these characteristics in terms of required retrieval accuracy and corresponding resolution for the sea surface salinity measurements is given in Table 3.

In general, temporal and spatial averaging improves the retrieval accuracy as long as excellent stability and calibration of the radiometer is ensured (Kerr et al., 1999). From Table 3 it follows that an accuracy of 0.1–0.2 psu over a distance of 100–200 km for an averaged sampling time of about a week to a month is adequate for description and quantification of many central ocean processes. As such it will satisfy the requirement given for SSS measurements in the context of the Global Ocean Data Assimilation Experiment (GODAE; http://www.bom.gov.au/GODAE/). Further scientific support studies initiated by ESA are currently underway. These studies explore the salinity variability indicated in Table 3 in the context of more refined observation requirements.

The technical developments related to SMOS are progressing as planned, and system definitions support studies and end-to-end performance simulation studies have recently been initiated. The mission duration is planned for a minimum of 3 years in order to cover two complete seasonal cycles, with a candidate launch date in 2005. Complementarity and synergy with other operating passive and active microwave systems are foreseen and in particular it will provide extremely valuable data for constraining the evaporation minus precipitation budget over the tropical oceans provided a TRMM follow-on such as GPM is flown simultaneously.

Marine geoid and steady-state ocean circulation

The scientific objectives of the GOCE Mission are based on the unique measurements by the gravity gradiometer to provide an accurate and detailed global model of the Earth's gravity field and geoid (ESA, 1999). This model will, in turn, serve the following multi-disciplinary scientific objectives:

- to provide new understanding of the physics of the Earth's interior including geodynamics associated with the lithosphere, mantle composition and rheology, uplifting and subduction processes;
- to provide, for the first time, a precise estimate of the marine geoid, needed for the quantitative determination, in combination with satellite altimetry, of absolute ocean currents and their transport of heat and other properties;
- to provide estimates of the thickness of the polar ice sheets through combination of bedrock topography derived from space gravity and ice sheet surface topography;
- to provide a better global height reference system for datum connection which can serve as a reference surface for the study of topographic processes, including the evolution of ice sheets and land surface topography.

Table 3. Overview of sea surface salinity variability for given areas and processes together with the characteristic temporal and spatial scales as well as retrieval accuracy (Drange et al., 1999)

Area and process	Accuracy	Horizontal resolution	Temporal resolution
Coastal processes	1 psu	20 km	1–10 days
ENSO	0.1 psu	100 km	1 month
Tropical Circulation (buoyancy driven)	0.3 psu	50 km	1–3 days
High latitude fronts/eddies	0.2 psu	50–100 km	10 days
Freshwater lenses	0.1–1.0 psu	50 km	1–10 days
Great salinity anomalies	0.1 psu	100 km	1–6 months

The oceanic objective fits well within the goals of CLIVAR under the World Climate Research Programme, GCOS and GOOS under the joint Intergovernmental Oceanographic Commission (IOC) and World Meteorological Organization (WMO). In addition the implementation and execution of the Argo array of profiling floats will provide a significant complement to the GOCE mission in combination with altimetric missions.

The GOCE mission has been conceived and designed taking into account scientific requirements and technological solutions, to provide the most accurate, global and high resolution map of the gravity field and its corresponding geoid surface. It will combine the satellite gradiometry and satellite-to-satellite high–low tracking (SST-hl) techniques (Fig. 3), which have been found to be optimal for providing the required high-quality, high-resolution static gravity field. To ensure the global completeness of the derived gravity model, which also impacts on its accuracy, a quasi-polar orbit must be chosen. The mission duration is planned for about 20 months with candidate launch date in 2005.

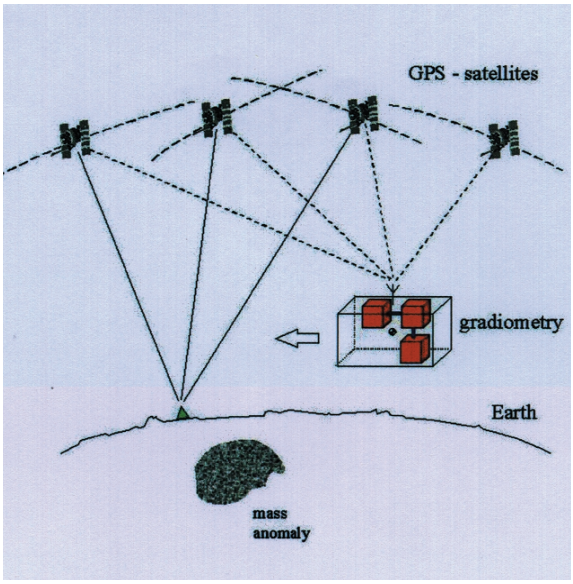

Figure 3. Schematic illustration of the principles of combined satellite gradiometry and satellite-to-satellite tracking in high–low configuration (ESA, 1999).

The quantitative requirements for the different scientific goals are derived in terms of geoid height and gravity anomaly accuracies and linked to the corresponding spatial resolution to which they apply (expressed in half wavelength). Specifically, in the context of meeting the scientific objectives addressed under oceanography, notably absolute ocean circulation, the key requirements are to:

- determine (from the measured gravity anomaly field) the geoid with an accuracy better than 1 cm radially; and
- achieve these measurements at a length scale of 100 km or less.

These requirements are also relevant to studies of sea level change as explained in ESA (1999). The technical development of the space segment is proceeding well, and the recent outcome of a comprehensive end-to-end performance study (Sünkel et al., 2000) shows encouraging results with regards to the scientific observation requirements.

Recent simulation studies (LeGrand and Minster, 1999; Le Provost et al., 1999) demonstrate that the accurate knowledge of the marine geoid provided by GOCE can lead to significant reduction in ocean transport uncertainties, notably in the upper ocean. Using the present day EGM96 gravity model to produce the

reference geoid error variance, they report reductions being as large as 30–50% for selected sections in the South and North Atlantic, and reaching up to 60% in narrow and intense current paths. In absolute terms, this is typically in the range of 1–4 Sv with maximum exceeding 10 Sv.

GOCE does not need data from other missions to achieve its primary goals. However, its complementarity with GRACE has been evaluated by Balmino et al. (1998). GRACE will be the first gravity field mission using the principle of satellite-to-satellite low-low tracking (SST-ll). It will improve the accuracy of the spherical harmonic coefficients at the long and medium spatial scales (≥500 km) by up to three orders of magnitude. This will allow measurement of the temporal variations in the gravity field to be recovered at a 30–90 day interval over a period of about 5 years (planned to begin in late 2001). Over the ocean this means that bottom pressure variations can be derived at a typical horizontal scale of 1000 km, whereas changes in the ice masses can be studied over the Antarctica and Greenland Ice Sheets. The aim (and challenge) is then to convert these sea floor pressure variations to changes in global ocean circulation.

Conclusion

During this decade, Earth observation from satellites, as an integral part of the global ocean observing system for climate, will be faced with two major requirements, namely, operation of 'continuity' (operational) missions, and launch of new exploratory missions. In this paper we have briefly addressed the latter type of missions, which are research driven, in regards to three geophysical quantities, i.e. ice mass fluctuations, sea surface salinity, and fine resolution and accurate marine geoid, which so far have not been adequately observed from space. The recommendations for these three mission concepts have been derived in close cooperation with the scientific user communities, and the level of complementarity is also quite good as shown in Table 4.

However, it must be emphasized that the overall long-term design criteria of the ocean observing system for climate, as expressed by the Oceans Observation System Development Panel (OOSDP) is:

> *to monitor, describe and understand the physical and biogeochemical processes that determine ocean circulation and the effects of the ocean on seasonal to decadal climate change, and to provide the observations necessary for climate predictions.*

A critical factor in this sense is the requirement for long-term measurements, both *in situ* and from satellite. No space agency by itself can ensure to meet such a continuity requirement. International cooperation in implementation and operation of key missions is therefore highly necessary. This will also avoid duplication and ensure complementarity, and should lead to significant reductions in the costs of each agency in addressing the objectives of the ocean observing system for climate.

We think it would be useful to distinguish the nature of geoid measurements. GOCE is an example of an exploratory remote-sensing mission

Table 4. Connection between the three geophysical quantities, the oceanic processes and the candidate satellite missions

Processes	**Parameters**		
	Ice mass	**Ocean salinity**	**Marine geoid***
Thermohaline circulation	ICESat, CryoSat	SMOS	GOCE, (GRACE)
Sea level change	ICESat, CryoSat, GRACE, GOCE		GOCE
Air-sea-ice interaction (+ albedo effect)	ICESat, CryoSat		
Evaporation minus precipitation		SMOS, + TRMM follow-on	
Mass and heat transport		(SMOS)	GOCE, (GRACE)
Large-scale frontal dynamics		SMOS	GOCE
Evolution of large-scale salinity event	(ICESat, CryoSat)	SMOS, +TRMM follow-on	

*Note: We are mostly considering the marine geoid in support of radar altimetry.

with a fixed lifetime, but with potential lasting benefits for the long-term observing system (topography measurements have a similar role).

Future plans and implementation of new Earth observation satellite missions must also maintain a degree of flexibility to ensure optimum adjustment and complementarity with development and improvements of models and their subsequent need for data. The same is valid vis-à-vis technology development for *in situ* instruments, for which there have been significant advances in autonomous expendable systems and unmanned observing vehicles that return data via telemetry. The deployment of up to 3000 profiling Argo floats within the timeframe of 2005 is one such example of a new and powerful element of a comprehensive international system for observing the global ocean. In 'A Consensus Statement' it is argued that these data, in combination with complementary ocean topography observations derived from satellite radar altimetry and new improved spaceborne estimates of the marine geoid and ocean surface salinity, will be very important for ocean prediction and seasonal-to-interannual climate applications.

Acknowledgement

We are grateful for the valuable and stimulating discussion and exchange of views with the technical experts at the European Space Agency's Science and Technology Center (ESTEC) in The Netherlands. The paper was outlined and drafted when J.A. Johannessen was with ESA-ESTEC, Earth Sciences Division.

References

Aagaard, K. 1994, The Arctic Ocean and climate: A perspective, *Geophysical Monograph* **85**, 5–20, AGU.

Balmino G. et al., 1998, European Views on Dedicated Gravity Field Missions: GRACE and GOCE, ESA-ESTEC Earth Sciences Division Report No. 1, Noordwijk, The Netherlands.

Belkin, I.M., S. Levitus, J. Antonov, and S.-A. Malmberg, 1998, Great salinity anomalies in the North Atlantic, *Prog. Oceanography*, **41**, 1–68.

Bjørgo, E., O.M. Johannessen, and M. Miles, 1997, Analyses of merged SMMR-SSMI time series of Arctic and Antarctic sea ice parameters 1978–1995, *Geophys. Res. Lett*., **24**(4), 413–416.

Delcroix T., and C. Hénin, 1991, Seasonal and interannual variations of sea surface salinity in the tropical Pacific Ocean, *J. Geophys. Res*., **96**, 22 135–22 150.

Donguy, J.-R., 1994, Surface and sub-surface salinity in the tropical Pacific Ocean. Relations with Climate, *Prog. Oceanography*, **34**, 45–78.

Drange, H., P. Schlüssel, and M. Srokosz, 1999, Study of critical requirements for ocean salinity retrieval using a low frequency microwave radiometer, Final Report, ESA Contract No. 13224/NL/M, Earth Sciences Division, ESA-ESTEC, Noordwijk, The Netherlands.

ESA, 1998, *The Science and Research Elements of ESA's Living Planet Program*, ESA Publication Division, SP-1227, Noordwijk, The Netherlands.

ESA, 1999, *Report for Mission Selection, Gravity Field and Steady-State Ocean Circulation Mission*, ESA Publication Division, SP-1233, Noordwijk, The Netherlands [http://www.estec.esa.nl/explorer/].

EOS, 1999, *The US EOS Science Plan: The State of Science in the EOS Program*, NASA NP-1998-12-069-GSFC.

IGOS, 2000, An Ocean Theme for the IGOS Partnership: Final report from the Ocean Theme Team, (E. Lindstrom, J.-L. Fellous, M. Drinkwater, R. Navalgund, J. Marra, T. Tanaka, J.A. Johannessen, C. Summerhayes), L.B. Charles (Ed.). [http://www.unep.ch/earthw/IGOS-Oceans-Final-0101.pdf]

Kerr, Y. et al., 1999, SMOS: Soil moisture and ocean salinity, Proposal selected under the ESA Living Planet Program: Earth Explorer Opportunity Mission [http://www.estec.esa.nl/explorer/].

Lagerloef, G.S.E., C.T. Swift, and D.M. Le Vine, 1995, Sea surface salinity: The next remote sensing challenge, *Oceanography*, **8**, 44–50.

LeGrand, P., and J.-F. Minster, 1999, Impact of GOCE gravity mission on ocean circulation estimates, *Geophy. Res. Lett*., **26**(13), 1881–1884.

Le Provost, C. et al., 1999, Impact of GOCE mission for ocean circulation study, ESA-ESTEC Contract No. 13175/98/NL/GD, Final Report. Earth Sciences Division, ESA-ESTEC, Noordwijk, The Netherlands.

Levitus, S., and T.P. Boyer, 1994, *World Ocean Atlas 1994, Volume 4: Temperature*, NOAA Atlas NESDIS 4, NOAA, 117 pp.

Lukas R., and E. Lindstrom, 1991, The mixed layer of the western equatorial Pacific ocean, *J. Geophys. Res*., **96**, 3343–3357.

Manabe, S., and R.J. Stouffer, 1988, Two stable equilibria of a coupled ocean–atmosphere model, *J. Climate*, **1**, 841–866.

Martin-Neira, M., and J.M. Goutoule, 1997, MIRAS-A two-dimensional aperture synthesis radiometer for soil moisture and ocean salinity observations, *ESA Bulletin 92*, ESA Publication Division, Noordwijk, The Netherlands.

Meier, M.F., 1984, Contribution of small glaciers to global sea level, *Nature*, **343**, 115–116.

Østerhus, S., B. Hansen, and R. Kristiansen, 1999, The overflow through the Faroe Bank Channel, *International Woce Newsletter*, Number 35.

Paulson, C.F., and G.S.E. Lagerloef, 1993, Fresh surface lenses caused by heavy rain over the western pacific warm pool during TOGA COARE, *Eos, Trans. Amer. Geophys. Union*, **74**, Suppl. to No. 43, 125.

Piexoto, J.P., and A.H. Oort, 1992, *The Physics of Climate*, American Institute of Physics, New York.

Rott, H., P. Shvarka, and T. Nagler, 1996, Rapid collapse of Northern Larsen Ice Shelf, Antarctica, *Science*, **271**, 788–792.

Skou, N., 1995, An overview of requirements and passive microwave radiometer options. In *Proceedings of consultative meeting on soil moisture and ocean salinity measurement requirements and radiometer techniques, ESA WPP-87*, pp. 41–48, Noordwijk, The Netherlands.

Sünkel, H. et al., 2000, From Eotvos to MilliGal, ESA/ESTEC Contract No. 13392/98/NL/GD, Final Report. Earth Sciences Division, ESA-ESTEC, Noordwijk, The Netherlands.

Timmermann, A., M. Latif, R. Voss, and A. Grötzner, 1998, North Atlantic Variability: A coupled air–sea mode, *J. Climate*, **11**, 1906–1931.

Weaver, A.J., and E.S. Sarachik, 1991, Evidence for decadal variability in an ocean atmosphere circulation model: An advective mechanism, *Atmos.–Ocean*, **29**, 197–231.

Wingham, D., et al., 1999, CRYOSAT, A mission to determine fluctuations in the mass of the Earth's land and marine ice fields, Proposal selected under the ESA Living Planet Program: Earth Explorer Opportunity Mission [http://www.estec.esa.nl/explorer/].

Zwally, H.J., A.C. Brenner, J.A. Major, R.A. Bindschadler, and J.G. Marsh, 1983, Greenland Ice Sheet: Is it growing or shrinking?, *Science*, **248**, 288–289.

Question and Answer Session

Roemmich: I am just wondering about the sea surface salinity error specification of 0.2 psu, which is relatively crude. Does this come from the practical aspects of what can be done technically or is it based on the signals that will be observed?

Johannessen: This comes from simple model simulations. It is what can be retrieved provided that we do not have too nasty an impact from sea surface winds. Sea surface temperature changes can be removed and corrected, they do not pose a problem. Surface roughness or winds is the most difficult to model and limits the accuracy and precision in the simulations. There will be several studies to improve this issue that will be initiated next year.

Roemmich: With that capability do you mostly observe coastal type signals, where salinity contrasts are large, or do you think there are useful climate signals in the open ocean that can be observed?

Johannessen: No, we think there will be useful climate signals that can be observed, such as in the tropical oceans. Observations at this precision in that region would provide a better handle on evaporation minus precipitation. At mid-latitudes it will absolutely be possible to look for large scale salinity anomalies, such as were observed in the mid-70s. At high latitudes, it is more difficult because there is a reduction in radiometric sensitivity in cold waters. We are not sure if we can measure the conditioning of waters that might identify active convection in these regions.